Deflections of Composite, Partially Prestressed Beams

By

Stephen Darby

B.E.(Hons)

A THESIS SUBMITTED FOR THE DEGREE OF MASTER OF ENGINEERING SCIENCE

Department of Civil Engineering

The University of Adelaide

Australia

March 1989

Contents

List of Figures

List of Tables

List of Plates

Abstract

Prestressed planks with a composite concrete deck poured over the top are becoming a popular form of bridge construction in Australia. The use of fully prestressed planks often leads to excessive camber during the life of the bridge, as a result of creep occurring under the high level of prestress. This problem can be avoided if the planks are partially prestressed, and designed with deflection control as a primary design aim, rather than the prevention of tensile stresses under bending.

For a design method which emphasises deflection control to be effective, good predictions of both short and long term deflections are required. A method for the predicting of deflections in composite, partially prestressed beams was developed and incorporated into a computer program. The method employs a step-by-step analysis procedure to allow for the effects of creep and shrinkage.

Two sets of planks were monitored to obtain information on long-term deflections. The data, along with data obtained previously, were used to check the accuracy of the method of prediction. Good agreement was found between predicted deflections and those determined by experiment.

Live load behaviour was examined in a load test performed on a road bridge built from composite, partially prestressed planks. A discussion of the results is presented, however a detailed analysis allowing for the lateral distribution of load was not performed.

After determining a method for predicting the deflections of composite, partially prestressed beams, the method was incorporated into a simple design procedure. Using this procedure, a series of designs were prepared for spans ranging from ten to twenty metres. The aim being to produce designs which exhibit good deflection control, avoiding the problems of excessive camber.

Statement of Originality

This thesis contains no material which has been accepted for the award of any other degree or diploma in any University and that, to my knowledge and belief, the thesis contains no material previously published or written by another person, except where due reference is made in the text. I consent to the thesis being made available for photocopying and loan if accepted for the award of the degree.

Stephen Darby

ACKNOWLEDGEMENTS

Professor Warner lectured me on reinforced and prestressed concrete during my undergraduate degree, in addition to being my supervisor for this project. It is as a result of his teaching that this thesis has been written and I am grateful for the excellent assistance he has always provided.

Funding for this work was provided by the Department of Main Roads in New South Wales. In addition, a great deal of help was provided by members of their staff, especially during work involving the partially prestressed bridge at Moama.

Experimental work on the Gawler Bridge could not have been conducted without the generous support and assistance of the Highways Department of South Australia, and in particular that of Peter Tymukas and John Clisby. David Robertson, the Production Manager at Hy-Stress Pty. Ltd. where the planks for the Gawler Bridge were cast, also provided a great deal of assistance. Without the help given in levelling the planks, both at Hy-Stress and at the Gawler Bridge site, it would have been impossible to collect the deflection readings required.

Help in setting up experimental work was given by the lab. staff and, in particular, by Stuart Mundey and Barry Dormer. Assistance with instrumentation was provided by Bruce Lucas and Stan Woithe.

All these people, and any others who helped are thanked for the contribution they made to this project.

I am extremely grateful to my family and friends who provided encouragement throughout the year.

Finally, I wish to thank Jo, whose support and friendship made this possible.

Principal Notation

$A11, A12, A13, A21, A22, A23$ See Appendix C,

A_{pk} = the area of the k^{th} layer of prestressing steel,

A_{sj} = the area of the j^{th} layer of reinforcing steel,

b_{ci} = the width of the i^{th} layer of concrete,

d = Parameter from ACI-209 creep function,

d_{ci} = depth to the i^{th} layer of concrete,

d_{sj} = depth to the j^{th} layer of reinforcing steel,

d_{pk} = depth to the k^{th} layer of prestressing steel,

D = overall depth of the section,

$E_c(t)$ = Young's modulus of the concrete at age t,

E_p = Young's modulus of the prestressing steel,

E_s = Young's modulus of the reinforcing steel,

E_t = Tensile strain softening modulus,

f = Parameter from the ACI-209 shrinkage function,

f_{py} = Yield stress of the reinforcing steel,

f_{sy} = Yield stress of the prestressing steel,

f'_t = Peak value of the direct tensile stress,

$F = \kappa_p/\kappa_y$ = ductility factor,

F_{ci} = Force produced by the i^{th} layer of concrete,

F_{pk} = Force produced by the k^{th} layer of prestressing steel,

F_{sj} = Force produced by the j^{th} layer of reinforcing steel,

k_u = neutral axis parameter, used as a measure of ductility,

$M_{applied}$ = the moment being applied to the section,

t_{ci} = the thickness of the i^{th} layer of concrete,

α = Parameter in the ACI-209 shrinkage function,

δ = Deflection of the beam,

$\epsilon(t)$ = Total strain at a point in the beam at time t,

$\epsilon_b(t)$ = Total strain at the bottom of the beam at time t,

ϵ_c = Uniaxial elastic strain in the concrete,

$\bar{\epsilon_c}$ = non-dimensional concrete strain, used in the non-linear stress-strain curve,

ϵ'_c = Strain at which the peak compressive stress is reached,

$\epsilon_{ci}(t)$ = Total strain in the i^{th} layer of plank concrete at time t,

ϵ_{py} = Strain at which the prestressing steel yields,

$\epsilon_{refc.i}$ = Offset to the strain in the topping concrete,

ϵ_{sy} = Strain at which the reinforcing steel yields,

ϵ_{tf} = Strain at which the tensile stress in the concrete reduces to zero,

ϵ_{tp} = Strain in the concrete at peak tensile stress,

$\epsilon_0(t)$ = Total strain in the top fibre at time t,

γ_1 = Non-dimensional stiffness used in the non-linear stress-strain curve,

γ_2 = Strain at which the non-linear concrete curve reduces to zero stress,

κ = Curvature of the beam, at a section,

κ_p = Curvature at which the peak moment is reached,

κ_y = See definition in Chapter 7,

ψ = Parameter from the ACI-209 creep function,

$\phi(t,\tau)$ = Creep coefficient at time t, for a loading at time τ,

$\phi^*(\tau)$ = Ultimate creep coefficient for a loading at time τ,

σ_c = Uniaxial stress in the concrete,

$\bar{\sigma_c}$ = Non-dimensional concrete stress, used in the non-linear stress-strain curve,

σ_{ci} = Stress in the i^{th} layer of concrete,

σ_{p0} = Initial stress in the prestressing tendons,

σ_u = Ultimate value of concrete stress in the non-linear stress-strain curve.

Chapter 1

Introduction

Composite, prestressed planks are becoming a popular method of construction for small single-span and multi-span bridges in Australia. The planks are precast before being transported to the bridge site, where they are placed side by side across the span. A layer of topping concrete is then poured over the top of the planks to complete the bridge deck. This process is illustrated in Plate 1.1.

At present these planks are commonly designed as fully prestressed beams, meaning that tensile stresses are not allowed to form in the beam under service loads. To achieve this, a high level of prestress is required, causing the plank to exhibit large cambers. Under the effect of creep and shrinkage, the long term camber often becomes excessive.

One solution to this problem is to use partial prestressing. Within this thesis the term partial prestressing is taken to mean that cracks are allowed to form in the beam under service loads. This form of construction allows a lower level of prestress in the beam, with a corresponding decrease in camber under dead load. A rational, performance based approach to design can then be used,

Plate 1.1: Composite bridge during the pour of the topping slab

Plate 1.2: Composite bridge prior to placement of asphalt

whereby deflections are controlled at various critical stages of construction and service.

In addition to improving the serviceability behaviour of the bridge, a decrease in camber produces economies, by reducing the amount of topping concrete required to form a flat surface on the bridge. It also eliminates the need for practices such as preloading, where the planks are loaded during storage to reduce deflections caused by creep and shrinkage.

Although composite, prestressed concrete planks form a simple and effective method of construction, they display a relatively complex pattern of behaviour which necessitates the development of sophisticated methods of analysis. Creep and shrinkage can lead to a redistribution of stresses within a section affecting the curvatures measured. The presence of two different concretes, poured at different times, means that creep and shrinkage effects will be developing at different rates. Steel will be compressed resulting in a drop in the level of prestress in the concrete.

In analysing the service load behaviour of composite, partially prestressed beams, account must also be made for the possibility of cracking in the beam under service loads.

The work described in this thesis forms part of a general investigation of composite, partially prestressed, concrete bridge planks. The overall aims of the investigation are to develop reliable methods of predicting their behaviour at service load and overload, and to recommend simple and effective design procedures which will result in planks with good deflection control.

The investigation commenced in 1986 with the manufacture of six prototype, partially prestressed planks of ten metre span, which were subsequently tested in the Chapman Laboratory at the University of Adelaide [Leong et.al. (1987)]. Information collected includes long term strains and deflections, as well as

behaviour under short term loading.

A computer based method of analysis is presented in this thesis which allows the behaviour of composite, pretensioned planks to be predicted during manufacture, construction and service. The analysis takes account of creep and shrinkage effects in both the plank concrete and the topping concrete, and allows for cracking to occur in either the plank or the topping. Experimental data from the previous plank tests were used to determine the accuracy of the methods of analysis.

The thesis also reports two further sets of test data which were obtained from experimental programs and used to further verify the methods of analysis. One program obtained data from four fully prestressed beams which were placed into a bridge over the Gawler River. Deflections were recorded for these planks during manufacture and construction of the bridge. Monitoring of the bridge is continuing during 1989. The other results come from a bridge built at Moama (New South Wales) out of planks to the same design as the prototype planks tested in 1986. Although little information was collected on long-term deflections, a load test was conducted on this bridge which provided information on the short term response of the real structure and in particular on the effects of continuity on the design.

Design procedures are also proposed in the thesis and a set of preliminary designs for partially prestressed planks are presented for spans ranging from ten to twenty metres.

1.1 Layout and Contents of thesis

Chapter 2 contains a review of the available literature, which was conducted to determine methods for predicting short term and long term deflections of

PPC and composite PPC members. Methods of design are also discussed in the literature survey. Chapter 3 gives details of the analysis used in the prediction of deflections and describes the methods used to implement it as a computer program.

Comparisons with the experimental data collected from the prototype planks are presented in Chapter 4. Several different analysis procedures were used to determine which factors are important in obtaining accurate predictions. The results from the live load tests of the prototype planks are also presented in this chapter and comparisons made with the predicted results. The results of the Moama bridge load test are in Chapter 6, while Chapter 5 contains details of the results of the deflection readings taken from the Gawler Bridge. Some additional details about the experimental work are included in Appendix B.

The design procedure used and an example of one of the designs which resulted are shown in Chapter 7. Full details of the preliminary designs are given in Appendix D. Conclusions and recommendations for further work are placed in Chapter 8.

Appendix A contains the User Manual for the program developed to predict long term deflections.

Chapter 2

Literature Review

Designing partially prestressed planks with the aim of providing a good degree of deflection control, requires both an appropriate design procedure and an accurate method of predicting the long term deflections of these planks. This chapter reviews methods available for predicting deflections and then looks at the details of several design methods, to allow a suitable approach to the problem to be determined. In addition, a short historical background is included.

A brief introduction to some of the basic concepts involved in the analysis of creep and shrinkage has been placed in Appendix C for those readers unfamiliar with the area.

2.1 Historical

Proposals for the use of prestressed concrete were first made in the nineteenth century by Jackson in the United States (1886) and Döhring in Germany (1888). However, it was Freysinnet's recognition of the importance of creep

and shrinkage effects and his subsequent patenting of a process in 1928 that opened the way for the practical application of prestressing concepts [Walley (1984); Bennett (1984)].

Partial prestressing appears to have originated with the proposal by Emperger, in 1939, to increase the service load of reinforced members by adding a number of pretensioned high strength steel wires and thus reducing the the effective stress in the reinforcement.

Freyssinet strongly opposed the idea of partially prestressed concrete where cracks would be allowed to open under service loadings. He considered it to suffer from the problems of both fully prestressed concrete and reinforced concrete. This opposition restricted the use of partially prestressed concrete for many years.

However, Abeles, who had been a student of Emperger, promoted the use of partially prestressed concrete during the 1940's. He carried out research into partial prestressing to prove its usefulness and designed several structures for British Railways [Abeles (1952)]. During this period he was possibly its major proponent.

By 1962 at the Fourth FIP Congress, when partial prestressing was first put on a conference agenda, there were several reports which indicated a growing acceptance of partial prestressing [Bay (1962); Hill (1962); Verna (1962)]. A general trend was noted by these authors, particularly in building construction, away from full prestressing because of problems with excessive camber causing serviceability failure.

Acceptance of partial prestressing as an alternative to fully prestressed construction required the development of methods of analysis and design which could take advantage of the full range of possibilities, ranging from reinforced concrete, through partially prestressed concrete to fully prestressed concrete.

While research into the behaviour of partially prestressed concrete probably peaked during the 1970s, there is still a great deal of work being carried out. [Naaman (1985)]

2.2 Design Procedures

Structural design requirements are commonly divided into two categories: strength and serviceability. Strength covers such things as strength in bending and shear and other factors which might cause a structural failure, while serviceability covers aspects such as deflections and crack control, which could cause a structure to become unserviceable. Codes provide guidelines on checking these limits. However, they do not normally indicate how a design can be found which satisfies these constraints.

One approach to the design of a structure, or an element within it, is to use mathematical optimisation. With this approach, the design requirements are expressed as a set of constraints which are written in terms of the design variables. An objective function is formed which states the overall aim, commonly minimum cost, and the problem is then solved to find the "optimum" solution. One difficulty with this approach is in formulating an objective function which takes into account all of the factors involved. Kirsch (1973), Cohn and MacRae (1984a, 1984b), Jones (1985) and others have reported various approaches to the particular problem of the optimal design of prestressed concrete beams.

As these methods have yet to result in an effective and practical procedure for the design of reinforced or prestressed concrete, they are not considered further in this thesis.

Apart from optimisation procedures, most design techniques can be thought

to consist of two stages, a preliminary design stage and a detailed design stage. The aim in the preliminary design is to determine design details which are reasonably close to the optimum. Detailed design procedures then systematically check all of the relevant constraints, adjusting the beam details when necessary. Most of the published procedures are concerned with the preliminary design phase, because if this is done well, the detailed design phase will only require minor changes to be made to the design details, as the various limit states are checked.

The choice of cross-section shape is dependent upon factors such as the construction method used and the loads which are applied to the beam. While guidelines to the choice of PPC sections are given in several text-books (See for example Warner and Faulkes (1988)), the experience of the designer is important in making an appropriate choice. Overall dimensions are generally chosen by considering the strength in shear and bending. Methods for this are given in most text books.

Having determined the concrete section and cover, the problem then becomes one of choosing the amounts of prestressing and reinforcing steel, and the prestressing force on the section.

One approach involves using the ultimate limit state of bending to produce the preliminary design and subsequently checking the serviceability limit states. This can be done by choosing a value of the partial prestressing ratio (PPR) before performing any calculations. Values of PPR are chosen on the basis of past experience or from values recommended for particular circumstances. PPR can be defined as:

$$PPR = \frac{A_p f_{pu}}{A_p f_{pu} + A_s f_{sy}} \tag{2.1}$$

where $A_p =$ the area of prestressing steel,

$f_{pu} =$ the ultimate strength of the prestressing steel,

A_s = the area of reinforcing steel, and

f_{sy} = the yield strength of the reinforcing steel.

Reinforcement details are then obtained from a consideration of the conditions in the beam at the ultimate state. Serviceability requirements are checked and the design adjusted as required.

Authors who have discussed this method include Naaman and Siriaksorn (1979a, 1979b), Peterson and Tadros (1985) and Bruggeling (1985). Thürlimann (1971) mentions the use of a prestressing ratio, but advocates the use of a serviceability based approach to preliminary design, where the dead load moments are counterbalanced by the moments due to prestress.

Serviceability based approaches are performance oriented and clearly relate each design decision to a required level of performance. Methods which give prior values to one of the prestressing indices can results in good preliminary designs, but the reason why they do so is not always obvious to the designer.

Lin (1963) presented a serviceability based design method termed load balancing which aims to provide zero initial deflection under a chosen portion of the design loads. The basis of this method involves replacing the effect of the cable with a set of equivalent loads, which produce identical stresses, strains and hence deflections in the section. For a straight cable, as is being used in this work, a pair of eccentric forces, or two force and moment pairs are all that is required (See Fig. 2.1).

A choice is then made as to the load at which the beam will exhibit zero deflections. As it is often desired to limit long-term deflections, the load chosen will generally be the dead load alone, or the dead load plus a small percentage of the live load. If the deflection under the sustained load is small, then the long-term deflections should also be small.

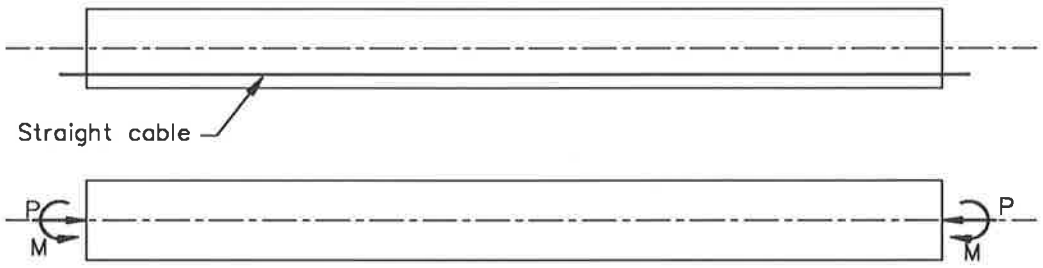

Figure 2.1: Equivalent loads replacing a straight prestressing cable (After Lin (1963)).

Once the choice is made, these loads are applied to the beam and the force which the prestress must apply to produce a zero deflection is calculated.

A similar approach which often has almost the same effect is to produce a constant stress distribution at the midspan, under some applied load.

These methods only give the prestressing force required. To determine the amount of prestressing steel required, it is necessary to choose what level of prestress is to be used in the tendons. **Thürlimann (1971)** argued that to use the full capacity of both the prestressing and the reinforcing steel, it is desirable to have them yield at the same time. To do this, it is necessary, when using Australian steels, to have the prestressing steel tensioned to almost its maximum value. However, as both steels yield eventually, this is probably an unnecessary constraint.

This does mean that to supply a given prestressing force, the smallest area of prestressing steel will be used. The increased amount of reinforcing steel should provide advantages in increased ductility and smaller crack widths [Bachmann (1984)].

Once the area of prestressed steel is known, the amount of reinforcing steel required is calculated from the moment strength required in the section.

The basis of this method was presented by **Warner and Faulkes (1979)** and later by **Bachmann (1984)** although the initial step was not restricted to load balancing. Rather a section along the beam is selected and the prestressing moment to be applied to this section is chosen. The choice depends upon the engineer's judgement in a particular situation and will be influenced by factors such as durability, economic conditions, deflections and fatigue.

Bruggeling (1985) suggested a similar design method and gives several examples of its use.

Wyche (1987) gives a "deflection controlled" design procedure which chooses a prestressing force for a number of sections along a beam. As no reinforcing steel is used in these designs, the area of prestressing steel is calculated from the ultimate moment requirements at midspan. The level of prestress required to give the section a slight upwards curvature is then calculated. At the other sections along the beam, strands are debonded to maintain the slight upwards curvature, while checks are made that adequate strength is available. Once incorporated into a computer program, as is done by Wyche, this method appears to provide a quick, simple solution technique.

By using only prestressed steel, a decrease in ductility may well occur. Under some conditions this disadvantage will be outweighed by economic advantages and the final decision will depend upon the particular situation when the design is undertaken.

Wyche also lists a number of other factors which he considers important in the design of these beams. These include the sensitivity of deflections to changes in the dead load, the debonding method and the development length for tendons, shear, handling stresses and detailing to account for longitudinal temperature

movements. All of these can be important and need to be considered in the detailed design calculations.

Wyche and Uren (1988) describe a slightly different approach, where as much prestressing steel as can be practically be fitted into the tensile section of a beam is placed into the midspan section. To help achieve this Wyche and Uren use the largest readily available strand (15.2mm diameter). Compression steel is then added to improve ductility and a span chosen which provides the design moment the section can resist.

Obviously all of these methods only provide preliminary design details and the design criteria need to be checked accurately in the detailed design. Most of the methods provide details which will be reasonably close to the final design. Iterations with adjustments to design details then lead to an acceptable design.

Once the detailed design stage has been reached, accurate predictions of deflections are required for the design of deflection controlled beams. The next section describes the methods available for predicting the deflections of prestressed beams.

2.3 Methods of Calculating Deflections

While there are a fairly large number of methods for calculating the long term deflections of composite, prestressed beams presented in the literature, only one procedure was found for the analysis of composite, partially PPC beams. Nevertheless, it is of interest to consider a range of methods for predicting the deflections of fully prestressed, composite planks. Where relevant, methods for plain, prestressed beams are also included.

The methods presented generally use either the step-by-step method or the

age adjusted effective modulus method for creep analysis. So to simplify the presentation, the prediction procedures using these methods are grouped under those headings. The remaining procedures are termed simplified methods of analysis, although that is perhaps not strictly accurate.

Techniques which use non-linear methods of creep analysis were not investigated, as it is thought that the small increase in accuracy that these methods might offer would be offset by inaccuracies in predicting material properties. The major value in attempting such an approach, would be the insight that it might give into the processes affecting the beam.

2.3.1 Simplified Methods

Branson and Ozell (1961) tested a number of both composite and non-composite, prestressed concrete beams and developed equations to predict the long term deflections of these planks. The equations developed include most long term effects, although the additional deflection caused by shrinkage in the plank was ignored.

A formula for the deflections of non-composite beams was obtained by integrating the formula for the curvature of a prestressed concrete beam. For a prestressed beam under the action of dead load and prestress, the curvature is given by:

$$\frac{d^2y}{dx^2} = \frac{1}{E_c(\tau_0)I}(M_G - P_i e) \qquad (2.2)$$

where $E_c(t) =$ the Young's Modulus of the concrete at age t,

$I =$ the moment of inertia of the beam,

$M_G =$ the applied dead load moment,

$e =$ eccentricity of the prestressing force,

P_i = the initial prestressing force, and

τ_0 = the time at which the prestressing force is transferred to the beam.

If it is assumed that the prestressing force was constant, then the effect of creep on long term curvature can be obtained from the following equation:

$$\frac{d^2y}{dx^2} = \frac{1 + \phi(t, \tau_0)}{E_c(\tau_0)I}(M_x - P_i e) \tag{2.3}$$

where $\phi(t_i, t_j)$ = the creep coefficient corresponding to a stress applied at time t_j which has been applied for a time of t_i. The creep coefficient is an experimentally determined property of concrete, defined as:

$$\phi(t_i, t_j) = \frac{\epsilon_c(t_i)}{\epsilon_e} \tag{2.4}$$

where $\epsilon_c(t_i)$ = the creep strain which has developed over time t_i, and

ϵ_e = the instantaneous elastic strain.

Further details about this are given in Appendix C.

Equation 2.3 comes from the definition of the creep coefficient, once it is assumed that total strain in the beam is linear across the section and that concrete has a linear stress-strain relation.

Long term curvature is affected by the decline in the prestressing force, so the initial prestressing force P_i and the prestressing force at time t, P_t, are used to write a prestress loss coefficient:

$$k_t = \frac{(P_i - P_t)}{P_i} \tag{2.5}$$

The long term curvature of the beam is then written as:

$$\frac{d^2y}{dx^2} = \frac{1}{E_c(\tau_0)I}[(1 + \phi(t, \tau_0))M_G - (1 + S_t)P_i e] \tag{2.6}$$

where

$$S_t = -\sum_{n=0}^{t} \frac{k_{t_n} - k_{t_{n-1}}}{E_c(t_n)/E_c(\tau_0)} + \sum_{n=0}^{t}(1 - k_{t_n})(\phi(t - t_n, t_n) - \phi(t - t_{n-1}, t_{n-1})) \quad (2.7)$$

For straight prestressing cables, Branson and Ozell solved this to obtain:

$$y = \frac{1}{E_c(\tau_0)I}\left[\frac{(1 + S_t)P_i L^2 e}{8} - (1 + \phi(t, \tau_0))\frac{5\omega_{G1}L^4}{384}\right] \quad (2.8)$$

where $L =$ the length of the beam, and

$w_{G1} =$ the plank dead load per unit length.

Branson and Ozell suggest that values of S_t obtained from experiments conducted under similar conditions to those being designed for, would be required if the equations were to be used in a design situation.

As shrinkage deflections are not included in the analysis, obtaining S_t from experiments could well cause the effect of shrinkage to get hidden in this term. While shrinkage effects are generally small, this effect can cause significant inaccuracies under some conditions.

Stress redistribution caused by the presence of non-reinforced steel is also not directly included in the analysis.

An equation for composite beams is developed by Branson and Ozell in a similar manner. The additional effects included in the analysis are the deflections due to the dead load of the topping and differential shrinkage between the topping and the plank concretes, as well as the resistance the slab provides to deflections.

Ignoring differential shrinkage, the curvature may be written as:

$$\frac{d^2y}{dx^2} = \left[\frac{1}{E_1(\tau_0)I_1}(1 + \phi(\tau_2, \tau_0))M_{G1} - \frac{1}{E_1(\tau_0)I_1}(1 + S_{\tau_2})P_i e + \frac{1}{E_1(\tau_2)I_1}M_{G2}\right]$$
$$+ \left[\frac{(\phi(t, \tau_0) - \phi(\tau_2, \tau_0))}{E_1(\tau_0)I_1}M_{G1} - \frac{(S_t - S_{\tau_2})}{E_1(\tau_0)I_1}P_i e + \frac{\phi((t - \tau_2, \tau_2)}{E_1(\tau_2)I_1}M_{G2}\right] \times$$

$$\left[\frac{E_1 I_1}{E_1 I_1 + E_2 I_2}\right] \tag{2.9}$$

where $I_1 =$ the moment of inertia of the topping concrete,

$I_2 =$ the moment of inertia of the slab concrete,

$E_1 =$ the Young's modulus of the topping concrete,

$E_2 =$ the Young's modulus of the plank concrete, and

$\tau_2 =$ the time at which the topping is added.

If the force due to differential shrinkage is then given a value F and assumed to act at a distance c_{2T} from the centroid of the section, the additional deflection caused by this force may be written as:

$$\left[\frac{1+\phi(t,\tau_2)}{E_1(\tau_2)I_1} g F c_{2T}\right]\left[\frac{E_1 I_1}{E_1 I_1 + E_2 I_2}\right] \tag{2.10}$$

As the force F builds up over the time period $t - \tau_2$, differential shrinkage being zero when the slab is cast, the factor g is included in the equation. The build up is approximately parabolic, so a factor of $g = 2/3$ is reasonable. The equation is then solved to give:

$$\begin{aligned} y = \Bigg[& \frac{1}{E_c(\tau_0)I_1}(1+S_{\tau_2})\frac{P_i L^2}{48}(e_0+5e_m) - \frac{1}{E_c(\tau_0)I_1}(1+\phi(\tau_2,\tau_0))\frac{5\omega_{G1}L^4}{384} \\ & - \frac{1}{E_c(\tau_2)I_1}\frac{5\omega_{G2}L^4}{384}\Bigg] + \Bigg[\frac{(S_t - S_{\tau_2})}{E_c(\tau_0)I_1}\frac{P_i L^2}{48}(e_0+5e_m) - \frac{(\phi(t,\tau_0)-\phi(\tau_2,\tau_0))}{E_c(\tau_0)I_1}\frac{5\omega_{G1}L^4}{384} \\ & - \frac{\phi(t-\tau_2,\tau_2)}{E_c(\tau_2)I_1}\frac{5\omega_{G2}L^4}{384} - \frac{(1+\phi(t-\tau_2,\tau_2))}{E_c(\tau_2)I_1}\frac{2}{3}F c_{2T}\frac{L^2}{8}\Bigg]\left[\frac{E_1 I_1}{E_1 I_1 + E_2 I_2}\right] \end{aligned} \tag{2.11}$$

where $e_0 =$ the cable eccentricity at the beam end, and

$e_m =$ the cable eccentricity at the midspan.

Branson and Ozell say in conclusion "These two equations are not practical for design purposes. However, any simpler method is not recommended since it

would require the use of approximations that may lead to erroneous results." The complexity of the equations, the requirement that S_t is obtained from experimental data, and the ignoring of shrinkage deflections other than differential shrinkage, all make it difficult to make practical use of these equations.

Branson and Kripanarayanan (1970, 1971) developed the equations of Branson and Ozell further, producing equations which, while still complex, are much simpler to use. Grossly approximate equations are also presented which could cause serious errors as some important effects are neglected.

The camber for non-composite beams is given as:

$$\Delta_t = (\Delta_i)_{F_0} - (\Delta_i)_{G1} + \left[-\frac{\Delta F_t}{F_0} + \left(1 - \frac{\Delta F_t}{2F_0}\right)\phi(t,\tau_0)\right](\Delta_i)_{F_0} - \phi(t,\tau_0)(\Delta_i)_{G1} - \Delta_Q \tag{2.12}$$

where $(\Delta_i)_{F_0}$ = initial camber due to the initial prestress after elastic losses,

$(\Delta_i)_{G1}$ = initial dead load deflection of the beam,

F_0 = prestress force at transfer (after elastic loss),

ΔF_t = total loss of prestress at time t minus the initial elastic loss, and

Δ_Q = the live load deflection.

For unshored, composite beams, the deflection is given as:

$$\begin{aligned}\Delta_t = {} & (\Delta_i)_{F_0} - (\Delta_i)_{G1} + \left[-\frac{\Delta F_s}{F_0} + \left(1 - \frac{\Delta F_s}{2F_0}\right)\phi(\tau_2,\tau_0)\right](\Delta_i)_{F_0} \\ & + \left[-\frac{\Delta F_t - \Delta F_s}{F_0} + \left(1 - \frac{\Delta F_s + \Delta F_t}{2F_0}\right)(\phi(t,\tau_0) - \phi(\tau_2,\tau_0))\right](\Delta_i)_{F_0}\frac{I_1}{I_c} \\ & - \phi(\tau_2,\tau_0)(\Delta_i)_{G1} - (\phi(t,\tau_0) - \phi(\tau_2,\tau_0))(\Delta_i)_{G1}\frac{I_1}{I_c} - (\Delta_i)_{G2} - \\ & (\Delta_i)_{G2}\phi(t,\tau_0)\frac{I_1}{I_c} - \Delta_{DS} - \Delta_Q \end{aligned} \tag{2.13}$$

where $(\Delta_i)_{G2}$ = the initial deflection of the precast beam under the slab dead load,

Δ_{DS} = the additional deflection due to differential shrinkage,

I_1 = the moment of inertia of the precast beam,

I_c = the moment of inertia of the composite section, and

ΔF_s = the total loss of prestress at the time of the slab casting.

While these equations are somewhat simpler than those given by Branson and Ozell, they are still fairly complex and require an estimation of the loss of prestress that has occurred. This can be estimated with moderate accuracy, but it adds an extra level of approximation to the problem.

Another problem is that partially prestressed beams cannot be modelled if cracks form in them under the action of dead load. An allowance can be made for the presence of non-prestressed tension steel through the use of a reduction factor developed by Shaikh and Branson (1970). Based on an energy requirement they give the reduction factor as:

$$k_r = \frac{1}{1 + A'_s/A_s} \tag{2.14}$$

where k_r = the reduction factor,

A'_s = the area of non-prestressed tension steel, and

A_s = the area of prestressing steel.

The reduction factor is applied by multiplying the creep coefficient and the shrinkage strain by k_r wherever they occur in the equation. Live load deflections are calculated using Branson's I-effective equation [Branson (1982b)]. Comparisons with experimental data prove this to be fairly accurate.

Experimental data is also used to provide a check on the long term deflections. (The data came from a series of test beams as well as four other studies.) Predictions of camber were generally found to be within ±15% when experimental values of creep and shrinkage were used and ±30% when general material parameters were substituted.

While these equations account in a fairly accurate manner for most major influences, they are probably too complex for routine use. A far simpler method is that presented by **Martin (1977)**, who attempted to produce a simplified method of calculating the long-term deflections of prestressed composite and non-composite concrete beams. To do this, he started with the ACI 318-71 equation (Section 9.5.2.3) for estimating the additional deflection of nonprestressed reinforced concrete members:

$$\mu_b = \left[2 - 1.2\left(\frac{A'_s}{A_s}\right)\right] \geq 0.6 \qquad (2.15)$$

where $A'_s =$ compressive reinforcement, and

$A_s =$ tensile reinforcement.

Using ratios of Young's modulus at various ages to account for times of loading, and the ratio of the final prestress force to the initial force to estimate the effect of the loss of prestress, a set of multipliers are obtained, which can be used to estimate the long term deflection. The method cannot be applied to beams which are cracked under dead load, but the effect of non-prestressed tension steel can be accounted for using the equation given by Shaikh and Branson (1970) (Eqn. 2.14). The factor obtained from the equation is then used to reduce the predicted increment in deflection.

Composite beams are allowed for by multiplying the difference between the non-composite long-time factors at the time of the topping pour and at the final time, by the ratio of non-composite to composite moments of inertia.

This provides a crude allowance for the effect of the slab on the long term deflections. Differential shrinkage effects are ignored.

While this approach is simple, it could easily lead to serious errors when used to predict deflections. Although Martin correctly argues that there is no point in the method of analysis being overly accurate when the data being used in the design is only known approximately, the methods used should reflect the design aims. Where deflection control is important, deflections should be calculated as accurately as possible.

This method ignores the fact that different concretes will have different values of creep and shrinkage, as the multiplier is only dependent on the relative amounts of tension and compression steel.

While this work is mostly concerned with long term deflections, short term deflections under live load also need to be calculated. Branson's I-effective method [Branson (1968)] is one of the few ways in which the effects of tension stiffening can be included into the hand calculation of deflections with a cracked section. The formulae were originally developed using the results of tests on reinforced concrete beams. A partially prestressed beam has an axial force applied to it by the prestress, which makes it difficult to directly apply the formulae.

Branson and Trost (1982a,1982b) suggested that the formulae could be adapted for use with partially prestressed beams in the following manner. In order to calculate the curvature of a section they give the effective moment of inertia as:

$$I_{eff} = \left(\frac{M'_{cr}}{M_{L2}}\right)^4 I_g + \left[1 - \left(\frac{M'_{cr}}{M_{L2}}\right)^4\right] I_{cr} \leq I_g \qquad (2.16)$$

While to calculate the average effective moment of inertia for a simply sup-

ported beam, the equation given is:

$$I_{eff} = \left(\frac{M'_{cr}}{M_{L2}}\right)^3 I_g + \left[1 - \left(\frac{M'_{cr}}{M_{L2}}\right)^3\right] I_{cr} \leq I_g \tag{2.17}$$

where I_{eff} = the effective moment of inertia used to calculate deflections or curvatures,

M'_{cr} = increment in moment which takes the beam from zero curvature to the point where the bottom fibre just cracks,

$M_{L2} = M_L - M_{L1}$,

M_L = the total live load moment,

M_{L1} = live load needed to produce zero deflection of the beam,

I_g = gross second moment of inertia of the cross-section, and

I_{cr} = the cracked second moment of inertia of the cross-section.

The procedure interpolates between two limiting values of second moment of inertia for the section. The gross second moment of inertia is simply calculated using the transformed cross-section, or alternately, with a slight loss of accuracy, using the concrete cross-section. To calculate the cracked second moment of inertia, Branson and Tros suggest that an equivalent area of prestressing and reinforcing steel can be used, while ignoring the effect of axial force. Tadros (1983), criticises this, stating that by ignoring axial compression, the cracked moment of inertia can be significantly underestimated.

M'_{cr} and M_{L2} are also difficult to define as, in most cases, zero deflection of the beam does not correspond to zero curvature. Indeed, curvature will often vary along the length of the beam. The definitions given by Branson and Trost seem reasonable.

Branson and Trost (1982b) also suggest coefficients which can be used to calculate long-term deflections from the initial deflection. They are as follows:

$$\text{Time Dependent } \Delta_{L2} = k_r \phi(t, \tau_0)(\text{ Initial}\Delta_{L2}) \tag{2.18}$$

$$k_r = \frac{1.0}{1 + 50\varrho'} \text{ ; for short term creep} \tag{2.19}$$

$$k_r = \frac{0.85}{1 + 50\varrho'} \text{ ; for long-term creep} \tag{2.20}$$

where ϱ' = the compression steel ratio = Area of compression steel / Area of concrete.

This method, while very simple, ignores shrinkage effects and relaxation of the prestressing tendons. Creep effects are treated empirically, so no comment can be made on its likely accuracy without comparison with experimental results.

2.3.2 Age Adjusted Effective Modulus Method

The Age Adjusted Effective Modulus Method (AAEMM) for analysing creep effects in concrete structures, was first developed by Trost, and later refined by Bažant (1972). The method assumes that the total strain in a concrete element due to a stress increment σ_0 applied at time τ_0 in combination with a stress varying from zero at time τ_0 to $\Delta\sigma(t)$ at time t can be written as:

$$\epsilon(t) = \frac{\sigma_0}{E_c(\tau_0)}(1 + \phi(t, \tau_0)) + \frac{\Delta\sigma(t)}{E_c(\tau_0)}(1 + \chi\phi(t, \tau_0)) + \epsilon_{sh}(t) \tag{2.21}$$

where $\epsilon(t)$ = the total strain in a concrete element at time t,

$\epsilon_{sh}(t)$ = the shrinkage strain, and

χ = the ageing coefficient. This is also a function of t and τ_0, but these are often not written when it is placed beside the creep coefficient, as it shares the same variables.

The method is theoretically exact for any problem in which strain varies proportionally with the creep coefficient. This is a reasonable assumption for structures where the load changes at a decaying rate [Bažant (1982)]. By using this equation the effect of time varying stresses can be included fairly accurately.

Methods for deriving values of the ageing coefficient are given by Bažant (1972). Graphs of the ageing coefficient are also available.

Dilger and Neville (1969) use this principle to write a series of equations which can be solved simultaneously to obtain an estimate of the stresses and hence the strain distribution in a composite, fully prestressed beam. Once the strain distribution is known at several sections along the beam, integration of curvatures gives the deflection of the beam.

Six equations are used, consisting of four equations of compatibility, in addition to the equations of force and moment equilibrium. Only six variables are required, these being the change in force in the topping and plank concretes, the change in moment resisted by the topping and plank concretes and the change in force in the prestressing and reinforcing steel. Equations of force and moment equilibrium are then written in terms of the changes in force and moment. Initial conditions must be found for the beam after the topping concrete is added. The time at which the topping concrete is added is thus taken into account by the initial conditions chosen for this section of the analysis. Obviously, by making appropriate simplifications, this method may be used to obtain the conditions in the plank when the topping is added.

Changes in strain are included by writing the change in a strain caused by a force, $\Delta c_N(t)$, as:

$$\Delta\epsilon_N(t) = \frac{N_{c0}}{E_c(\tau_0)A_c}\phi(t,\tau_0) + \frac{\Delta N_c(t)}{E_c(\tau_0)A_c}[1+\chi\phi(t,\tau_0)] \qquad (2.22)$$

and the change in a strain caused by a moment, $\Delta\epsilon_M(t)$, as:

$$\Delta\epsilon_M(t) = \frac{M_{c0}y}{E_c(\tau_0)I_c}\phi(t,\tau_0) + \frac{\Delta M_c(t)y}{E_c(\tau_0)I_c}[1+\chi\phi(t,\tau_0)] \qquad (2.23)$$

where N_{c0} = the initial force in the concrete,

ΔN_c = the change in force in the concrete,

M_{c0} = the initial moment in the concrete, and

ΔM_c = the change in moment on the section.

By writing the four equations of compatibility in terms of the changes in strain, it becomes a simple matter to write the six equations in six unknowns. The problem then becomes one of solving six simultaneous equations.

No allowance is made in this method for the effect of relaxation of the pre-stressing tendons, or for the formation of cracks in the beam under dead loads.

A simpler procedure was later presented by **Dilger (1982)** who developed a method utilising "creep transformed" section properties. The method is applicable to uncracked, composite sections.

To allow the calculation of time-dependent stresses and deformations, the forces produced in the steel by unrestrained creep (the restraint caused by the steel is ignored), free shrinkage and the "reduced" relaxation of the pre-stressing steel are applied to the creep transformed section. The properties of the creep transformed section are obtained using a modular ratio given by:

$$n^* = \frac{E_s}{E_c^*} = n_0[1+\chi\phi(t,\tau_0)] \qquad (2.24)$$

where $n_0 = E_s/E_c$ is the usual modular ratio.

Concrete stresses resulting from this analysis are due to the time dependent effects. While the corresponding time-dependent steel stresses are obtained

by adding the stresses due to unrestrained creep, free shrinkage and reduced relaxation, to those taken from the creep transformed section.

To apply the method, the change in stress caused by time effects, $\sigma_s^*(t)$, is calculated at the level of the steel. This can be written as:

$$\sigma_s^*(t) = n_0\sigma_{c1}\phi(t,\tau_0) + \epsilon_{sh}(t,\tau_0)E_s + f_r'(t) \tag{2.25}$$

where $f_r'(t)$ is the strain produced by the reduced relaxation of the steel, and

σ_{c1} is the initial stress in the concrete at this level.

The force applied to the section, N_s^*, is then:

$$N_s^* = A_s\sigma_s^*(t) \tag{2.26}$$

This force, which is applied at the centroid of the steel, can be used to calculate stresses in the concrete by applying it to the creep transformed section. The stresses in the steel are obtained by calculating the stress at the level of the steel in the creep-transformed section, multiplying by the modular ratio and adding this stress to $\sigma_s^*(t)$.

Composite sections are analysed by including the moment and force produced by the difference in time dependent free strains between the girder and deck, in the calculation of stresses in the creep transformed section.

This method is general and rigorous if it is assumed that shrinkage develops at the same rate as creep. It has the advantage of simplicity, however it would be difficult to make an allowance for cracking under dead loads using this method.

The "pressure line method" presented by **Naaman (1983a)** is another fairly simple method based on Bažant's ageing coefficient. Its name comes from the way it considers the beam to be subjected to a prestressing force following

the pressure line. The pressure line being the line of action of the concrete compressive stress resultant at each section. An example of this is shown in Figure 2.2. As presented in the paper, the method could only be applied to uncracked, non-composite beams. Additionally, deflections caused by shrinkage strains and the stress redistribution caused by non-prestressed reinforcing steel are ignored by this method.

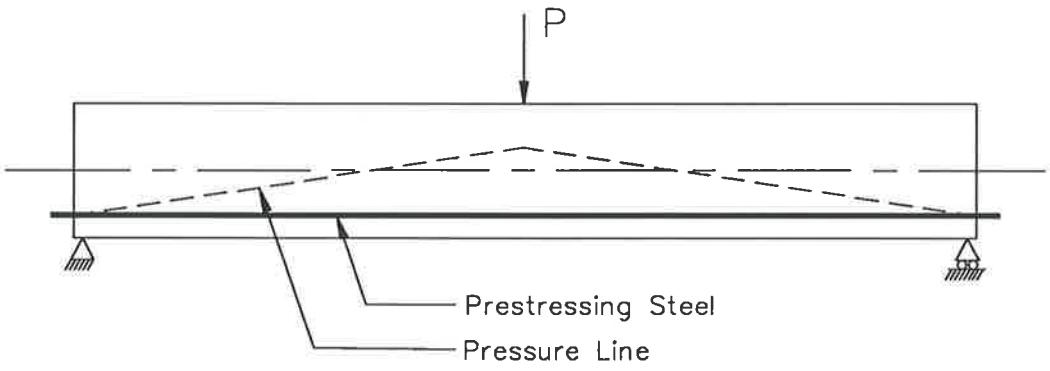

Figure 2.2: Pressure line produce by a straight cable with a point load (After Naaman (1983a)).

At any section along the beam, the eccentricity of the resulting compressive force at any time t is given by:

$$e_c(t) = e_0 - \frac{M}{F(t)} \tag{2.27}$$

where e_0 is the cable eccentricity,

M is the externally applied moment, and

$F(t)$ is the prestressing force.

The prestressing force, $F(t)$, varies with time as a result of the loss of prestress. Values of the top and bottom strain can be written in terms of the prestressing force as:

$$\epsilon_{ct} = \frac{F(t)}{E_{ce}(t)A_c}\left(1 - e_c(t)\frac{A_c}{Z_t}\right) \tag{2.28}$$

$$\epsilon_{cb} = \frac{F(t)}{E_{ce}(t)A_c}\left(1 - e_c(t)\frac{A_c}{Z_b}\right) \tag{2.29}$$

$$\tag{2.30}$$

where Z_t and Z_b are the section moduli for the top and bottom fibres respectively, A_c is the area of concrete and $E_{ce}(t)$ is given by:

$$E_{ce}(t) = \frac{E_c(\tau_0)}{1 + \chi\phi(t, \tau_0)} \tag{2.31}$$

This method is simple, but limited, and is mostly interesting as a different approach to the problem. Shrinkage effects are not included, but the paper states that attempts are being made to extend the applicability of the method to prestressed continuous beams, to cracked, partially prestressed beams and to generalise the solution to account for a variable loading history. If this could be done without enormously complicating the solution, then this method would become far more significant.

Ghali and Tadros (1985) also present a procedure which uses Bažant's ageing coefficient to calculate the long term deflections of partially prestressed concrete girders.

At the time t_i when the prestress is applied, the stress and strain distributions are calculated using conventional equations and a transformed cross section containing concrete and n times the steel area, where $n = E_s/E_c(t_i)$.

If the strain distribution across the section is assumed to be linear, it can be described by the strain at a reference point and the curvature across the section, allowing the following equations to be written:

$$\epsilon_i = \epsilon_0 + \kappa y \tag{2.32}$$

$$\sigma = E_c(\epsilon_0 + \kappa y) \tag{2.33}$$

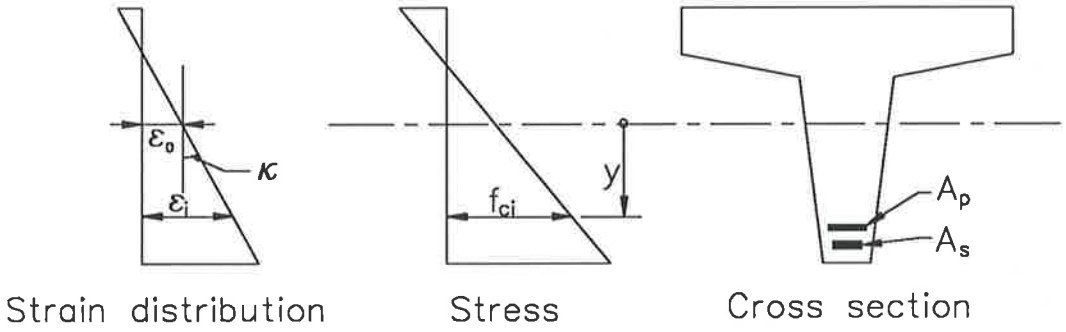

Figure 2.3: Variables used to describe the stress and strain distribution (After Ghali and Tadros (1985)).

and

$$E_c \begin{bmatrix} A & B \\ B & I \end{bmatrix} \begin{Bmatrix} \epsilon_0 \\ \kappa \end{Bmatrix} = \begin{Bmatrix} N \\ M \end{Bmatrix} \tag{2.34}$$

where $A = \int dA$ = cross-sectional area,

$B = \int y dA$ = first moment of area about an axis through the reference point,

$I = \int y^2 dA$ = second moment of area,

$N =$ force on the section, and

$M =$ moment applied to the section.

This equation can easily be solved to give values of ϵ_0 and κ.

To maintain force equilibrium, the sum of the changes in forces at a section must be zero. From this, Ghali and Tadros derived an equation for the change in resultant force in the concrete, P_c, between the times t_i and t_j:

$$(\Delta P_c)_{ji} = -\frac{\phi(t_i,t_j) f_{cei} n A_s + \epsilon_{sh} E_s A_s + \psi L_r A_p}{1 + \frac{\alpha n A_s}{A_c}(1 + \chi\phi(t_i,t_j))} \tag{2.35}$$

where f_{cei} = the instantaneous stress at the centroid of the total reinforcement area,

L_r = the intrinsic relaxation of the prestressing strand,

ψ = a relaxation reduction factor, to account for the change in length of the prestressing strand.

The change in force over a time interval is then calculated and the effects of creep and shrinkage accounted for. Superposition allows the stresses due to several loadings to be added, giving the stress distribution at the desired time.

As the stress distributions are to be superimposed, the beam must be uncracked under long term loads. Live loads which cause cracking can be included by calculating the stress distribution immediately before the load is applied. Values of curvature are calculated firstly by assuming that no cracking occurs, and secondly by assuming that the beam is fully cracked. Empirical equations such as those given by Branson (1982a, 1982b) can then be used to interpolate between these limits, allowing tension stiffening effects to be included.

A similar method is described by Ghali (1986).

2.3.3 Step-by-step Methods

The step-by-step method is potentially the most accurate of the linear methods of analysis for creep and shrinkage as it incorporates the fewest assumptions. Although it is tedious to use in hand calculations, it is well suited for implementation in a computer program as it consists of repetitive, easily programmable steps.

McHenry (1943) was possibly the first person to propose the use of the step-by-step method when he proposed the use of superposition in calculating the

effect of creep recovery on concrete.

In the step-by-step method (SSM), time is divided up into a number of intervals. If, at the beginning of the first interval, a uniaxial stress increment is applied to the concrete then creep will occur from this time. Strain caused by this can be calculated in terms of the creep coefficient. A stress applied at a later date can be treated similarly and the corresponding creep strain calculated. Superposition of strains allows the total strain to be obtained by adding the increments of strain together.

The situation in a beam is more complex with a stress distribution existing across the beam. At either the end, or the middle of a time interval, a stress distribution is applied to the section, to ensure that compatibility and equilibrium are satisfied at these times. Between these times, creep and shrinkage are assumed to occur, unrestrained by the beam. The principle of superposition allows the effect of each stress increment to be added to the effects of all the others, giving the final result. A more detailed description of the method is given in Chapter 3.

Warner and Lambert (1974) developed a computer based procedure which involves partitioning the section into elemental areas of steel or concrete. Stress on an elemental area can be assumed constant, allowing equilibrium equations to be written as a simple summation. One advantage of this is that the procedure can then be applied to a section of arbitrary shape under biaxial bending.

Creep effects are included in the formulation by writing the creep equations in difference form. During the time interval Δt_n, the increment in creep strain in the $(i,j)^{th}$ element is:

$$\Delta E^c_{ij}(t_n) = (\Delta E^d_{ij}(t_n) + \Delta E^v_{ij}(t_n))H(\sigma_{ij}(t_{n-1})) \tag{2.36}$$

where $\Delta E^d_{ij}(t_n) = E^e_{ij}(t_{n-1})\Delta\phi^d(t_n)$,

$\Delta\phi^d(t_n) =$ $\phi(t_n, \tau_0) - \phi(t_{n-1}, \tau_0)$,

$\Delta E^v_{ij}(t_n) =$ $(E^e_{ij}(t_{n-1})\phi^v_* - E^v_{ij}(t_{n-1}))\frac{\Delta t_n}{T_v}$,

$E^e_{ij}(t_{n-1}) =$ the normalised, elastic stress in the $(i,j)^{th}$ element at time t_{n-1},

$\Delta E^d_{ij}(t_n) =$ a component of the normalised creep strain given by Dischinger creep theory,

$\Delta E^v_{ij}(t_n) =$ the linear, viscoelastic component of the normalised creep strain,

ϕ^v_*, T_v are constant material properties,

$\Delta\phi^d(t_n) =$ the change in the Dischinger component of creep, and

$H(\sigma_{ij}(t_{n-1})) =$ an allowance for non-linear creep. For stresses in the service range, $H(\sigma_{ij}(t_{n-1})) = 1.0$.

Normalised strains are defined as:

$$E = \frac{\epsilon}{\epsilon'_c} \tag{2.37}$$

where $E =$ the normalised strain,

$\epsilon =$ the strain, and

$\epsilon'_c =$ the instantaneous strain associated with the peak stress of the concrete loaded at a particular age.

Shrinkage strains are also written in a normalised, differential form as:

$$\Delta E^s_{ij}(t_n) = E^s_* \Delta g(t_n) \tag{2.38}$$

$$\Delta g(t_n) = g(t_n) - g(t_{n-1}) \tag{2.39}$$

where $g(t) =$ an experimentally determined function which varies from 0 to 1, and

E^s_* = the normalised, final shrinkage strain.

At the end of each time interval, the total creep and shrinkage strains can be written as follows:

$$E^c_{ij}(t_n) = E^c_{ij}(t_{n-1}) + \Delta E^c_{ij}(t_n) \tag{2.40}$$

$$E^s_{ij}(t_n) = E^s_{ij}(t_{n-1}) + \Delta E^s_{ij}(t_n) \tag{2.41}$$

Warner and Lambert assume that the total strain is linearly distributed over the section and that strain in a steel element is the same as in surrounding concrete. Knowing this, the strain distribution at any time can be calculated and from this the deflection of a beam.

The method is developed for use with a non-composite beam, however it would not be difficult to extend it to the case of a composite beam. Cracking is accounted for, indeed a non-linear stress-strain relation is used for the concrete.

Rao and Dilger (1974b) developed a method for predicting the deflections of composite, fully prestressed concrete beams which they termed the "varying stiffness" method. The method assumes that changes in forces and the moduli of elasticity occur at the middle of a time interval. Changes in strain are evaluated at the ends of each interval.

The equations of equilibrium are written in the form:

$$[S]_k\{\Delta D\}_k = \{\Delta F\}_k \tag{2.42}$$

where $[S]_k$ = varying stiffness matrix of the composite section in the i^{th} interval,

$\{\Delta D\}_k$ = the strain vector, and

$\{\Delta F\}_k$ = the force vector.

Force strain relations are written in terms of the elastic stiffness coefficients by assuming that plane sections remain plane. Substituting these equations into the equations of equilibrium allows the solution of the elastic strains. The strain distribution is described in terms of the strain at the elastic centroid (or some suitable reference point) and the curvature of the section.

Time dependent strains are incorporated by writing iterative equations for the curvature and the strain at the centroid. The equation for the total strain at the centroid is given as:

$$\epsilon(t_k) = \epsilon(t_{k-1}) + \Delta\epsilon_c^p(t_k) + \Delta\epsilon_c(t_k) + \Delta\epsilon_{sh}(k) \tag{2.43}$$

where $\epsilon(t_k) =$ the total strain in concrete at the age t_k,

$\Delta\epsilon_c^p(t_k) = \sum_{i=2}^{k-1}\{P_c(i)/(E_c(t_i)A_c)\}\{\phi(t_k,t_i) - \phi(t_{k-1},t_i)\}$ = the change of total strain during the k^{th} interval, due to the forces acting during previous intervals,

$P_c(i) =$ the axial force applied to the concrete during the i^{th} time interval,

$\Delta\epsilon_c(t_k) = \frac{\Delta P_c(k)}{E_c(t_k)A_c}(1 + \phi(t_k,t_k))$ = elastic plus creep strain in interval k,

$\Delta P_c(k) =$ the change in axial force on the concrete during the k^{th} time interval, and

$\Delta\epsilon_{sh}(k) = \epsilon_{sh}(t_k) - \epsilon_{sh}(t_{k-1})$.

A similar equation is developed for curvature, allowing a set of time dependent force-strain relations to be written. The effect of the addition of topping concrete is included using a similar set of equations. The first set is then used to step through time until one day after the topping is poured when composite

action is assumed to begin. This method gives a closed form solution to the problem of finding the strain distribution. In order to write these equations, the assumption is made that concrete has a linear stress-strain relation. This makes it difficult to use these equations when cracks form, as is the case for partially prestressed sections.

Although the equations, as presented, ignore both the effect of relaxation in the prestressing strand and cracking in the concrete, this is still a reasonable solution to the problem. Relaxation could be included into the problem fairly easily, but cracking would be more difficult.

The matrices can be inverted giving a closed form solution for the strain distribution at each step, which should allow fairly quick solution times.

Tadros, Ghali and Dilger (1977b) described a way in which the step-by-step method of analysis can be used to calculate the deflections of composite frames. The method is general in that two or more concrete parts, with different properties, can be used along with reinforcing steel and prestressing strand to make a frame structure. Material and geometric non-linearities are ignored in the analysis.

Once it is assumed that plane sections remain plane, the axial strain ϵ and curvature κ can be written in terms of the axial force N and the bending moment M. This allows the incremental strain $\Delta\epsilon(i)$ and the incremental curvature $\Delta\kappa(i)$, during an interval i to be written as:

$$\Delta\epsilon(t_i) = \frac{\Delta N(t_i)}{AE(t_i)}[1+\phi(t_{i+1/2},t_i)] + \left\{\sum_{j=1}^{i-1}\frac{\Delta N(t_j)}{AE(t_j)}[\phi(t_{i+1/2},t_j)-\phi(t_{i-1/2},t_j)]+\epsilon_{sh}(t_i)\right\} \tag{2.44}$$

$$\Delta\kappa(t_i) = \frac{\Delta M(t_i)}{IE(t_i)}[1+\phi(t_{i+1/2},t_i)] + \left\{\sum_{j=1}^{i-1}\frac{\Delta M(t_j)}{IE(t_j)}[\phi(t_{i+1/2},t_j)-\phi(t_{i-1/2},t_j)]\right\} \tag{2.45}$$

If the effective modulus is defined as:

$$E_e = \frac{E(t_i)}{1 + \phi(t_{i+1/2}, t_i)} \tag{2.46}$$

Then the incremental strain and curvature can be written as a set of linear relations. Introducing $\Delta\bar{\epsilon}(t_i)$ and $\Delta\bar{\kappa}(t_i)$ as the "initial" strain and curvature at the start of an interval, they wrote:

$$\Delta\epsilon(t_i) = \frac{\Delta N(t_i)}{AE_e(t_i)} + \Delta\bar{\epsilon}(t_i) \tag{2.47}$$

$$\Delta\kappa(t_i) = \frac{\Delta M(t_i)}{IE_e(t_i)} + \Delta\bar{\kappa}(t_i) \tag{2.48}$$

$\Delta\bar{\epsilon}(t_i)$ and $\Delta\bar{\kappa}(t_i)$ are calculated from the results of the preceding intervals.

The effects of reinforcing and prestressing steel are included in the analysis using incremental equations of the form:

$$\Delta\epsilon_{ps}(t_i) = \frac{\Delta N_{ps}(t_i)}{A_{ps}E_{ps}} + \Delta\bar{\epsilon_{ps}}(t_i) \tag{2.49}$$

To solve for the strains in a frame, they suggest that the displacement method may be used, with $\bar{\epsilon}$ and $\bar{\kappa}$ being obtained using the same method used to model a temperature change.

It should be noted that the equation given for curvature requires the concrete to be exhibiting a linear stress-strain relation, preventing the modelling of the effect of cracking. The method can solve both statically determinate and indeterminate composite plane frames.

Al-Zaid, Naaman and Nowak (1986,1988b) were the only authors found who describe a method for calculating the long-term deflections of beams which may be cracked under dead loads. The method they describe can be used for

I, T and rectangular sections in the elastic range of behaviour. Cyclic creep can be accounted for and the topping concrete added when the beam is either propped or unpropped.

Short-term analysis

They made the following assumptions in the analysis of both cracked and uncracked sections:

1. Steel and concrete are linear elastic in the range of stresses considered;
2. Plane sections remain plane under bending;
3. Perfect bond exists between steel and concrete;
4. Full interaction between the precast beam and the cast-in-place slab is ensured.

These assumptions are normal in the analysis of composite concrete beams. A further four assumptions were made for the cracked section analysis:

1. Concrete does not withstand tensile stress;
2. The prestressed girder does not crack under the effect of its own weight and prestress;
3. The crack will not propagate into the cast-in-place slab under service loading;
4. Any external load applied after composite action leads to the same change in curvature in the precast beam and the cast-in-place slab.

The first assumption means that tension stiffening is being ignored, which, especially for the case of long-term loading, is unlikely to lead to significant

error. Assumptions two and four are also unlikely to lead to any serious error. However, while a crack is unlikely to penetrate from the bottom fibre into the topping, the topping slab can sometimes crack due to differential shrinkage between the plank and the topping concrete. It appears from the equations presented in the paper that this effect could be allowed for, but the paper is not clear on this point. If, as this assumption suggests, the effect is not accounted for, a serious error may be introduced on some occasions.

These assumptions, along with the equations of compatibility and equilibrium, were used by Al-Zaid and Naaman to write a cubic equation, from which the depth to the neutral axis may be found. Any other information desired can then be found by back substitution.

The equations given were derived for the case of an I-beam which allowed solutions to be obtained for T and rectangular sections by setting the top and bottom flange widths to the width of the web. While this covers many common sections and others can be included by appropriate approximations, many sections can not be analysed using the method as presented. This would only affect the part of the analysis involved with calculating the strain distribution on the section, so the extension would be quite possible.

Long term analysis

To allow this analysis to be extended to cover long term effects, a further four assumptions are required. These are:

1. Elastic and creep strains in concrete are linearly proportional to the applied stresses;
2. Elastic, creep and shrinkage strains in concrete are additive properties;
3. Shrinkage is uniform over the depth of the cross section;

4. The change in elastic curvature of the precast beam section after composite action is assumed equal to the change in elastic curvature of the cast-in-place slab.

Strains due to static creep and shrinkage are calculated using the formulae presented by ACI-209 (1978). Cyclic creep is included using the formula suggested by Balaguru [cited by Al-Zaid (1988b)].

$$\epsilon_{cc} = 129 S_{cm} t^{\frac{1}{3}} + 17.8 S_{cm} \Delta S_c N_t^{\frac{1}{3}} \tag{2.50}$$

where S_{cm} = the mean stress in the concrete, expressed as a fraction of the compressive strength,

ΔS_c = stress range in concrete expressed as a fraction of the compressive strength, and

N_t = the number of load cycles applied in the time interval (0,t).

Cyclic deterioration of concrete in tension is also included using a model developed by Saito and Imai (1983):

$$\frac{f_{t.max}}{f_t} = 98.73 - 4.12 \log N_f \tag{2.51}$$

where $f_{t.max}$ = maximum tensile stress, and

f_t = direct tensile stress.

Relaxation losses within the prestressing strand are given by a formula suggested by the PCI Committee on Prestress Losses (1975):

$$\Delta\epsilon_{rel}(t_i, t_j) = \frac{f_{ps}(t_i)}{10 E_p} \left(\frac{f_{ps}(t_i)}{f_{py}} - 0.55 \right) \log \left(\frac{t_j}{t_i} \right) \tag{2.52}$$

A step-by-step method and the cubic equation described above are then used to obtain the long term deflection history of the beam.

The method presented by Al-Zaid, Naaman and Nowak appears to provide a good solution to the problem of calculating long term deflections in partially prestressed beams. While one of the assumptions made might cause an error in some situations, these assumptions allowed strains across the section to be calculated using a cubic equation. This has the advantage of a relatively quick solution time.

2.3.4 Summary

Deflection Prediction

In reviewing the methods available for predicting deflections, the aim was to find a method which, at the least, satisfied the following requirements:

- Capable of analysing any type of cross-section,
- Cracks can develop under dead load,
- Topping concrete can crack independently of the plank,
- Creep and shrinkage effects are accounted for, including the effects of differential shrinkage and stress redistribution within the section,
- Ability to account for relaxation of the prestressing steel, although this was not required for the present stage of the work.

Out of the methods reviewed, those using the step-by-step method came closest to fulfilling the requirements listed. Those requirements not satisfied by any of

the procedures utilising the step-by-step method can all be satisfied by making appropriate alterations. A method which does this is presented in Chapter 3.

"Simplified" methods are not chosen for use, as they are either too crude to accurately model deflections, or too complex to routinely apply. All involve assumptions which make it impossible for them to satisfy the requirements given above.

The methods which use Trost-Bažant's ageing coefficient offer methods of solution which are often quick and fairly simple, but none of them are completely suitable for the prediction of long term deflections of composite, partially prestressed beams.

The main problem is that none of them allow cracks to form in the plank under the effect of dead load. Use of AAEMM makes it difficult to do this when long term loadings are applied at different times, as each loading will require a different value of the age adjusted effective modulus. If the concrete is assumed to have a linear stress-strain relation, stresses from each loading can be calculated and superimposed to give the solution. Once a crack forms, superposition cannot be applied and the solution becomes far more complex.

In addition, the main advantage in using AAEMM rather than step-by-step methods is the reduction in the number of calculations required. The ageing coefficient is obtained from a table or equations and the long term deflection can then be calculated in a single step. In this case, as the method is being implemented on a computer, this advantage is largely irrelevant.

Design Procedures

Of the various preliminary design procedures considered, those which provide a rational, performance based criterion are to be preferred, particularly since

a major aim of the design is deflection control. Ideally, the preliminary design procedure will lead to near optimal or minimum cost designs, although this criteria is difficult to quantify and will depend upon the specific conditions applying.

Load balancing is an effective method which aims to provide good deflection control, so it was decided to make use of this method. However, the process is not critical as the detailed design involves systematic checks to ensure that all design requirements are met. It is in the detailed design that the method chosen above for the prediction of deflections is to be used. Details of such a method are given in Chapter 7.

Chapter 3

Analytic Techniques

3.1 General

Partially prestressed beams show deflections which vary over time as a result of creep and shrinkage coupled with prestress and the long term loads which are applied to the beam. Short term deflections produced by live load and variations in the temperature profile across the beam must also be considered. However deflections produced by thermal gradients are not included as part of the present study.

To trace the changes caused by creep and shrinkage, a model is required which takes into account the various construction stages, as well as the load history. As a first step towards this, the history of a plank is thought of as a set of stages and phases, with each phase requiring analysis [Warner (1986), Leong et.al. (1987)]. The term stage refers to the condition of the plank at a specific time instant; a phase is a process of change which takes place between two

adjacent stages.

The phases and stages chosen to represent the life of a plank are as follows:

Stage 0 This is the condition, just prior to transfer, when the concrete has been cast around the tensioned tendon in the prestressing steel.

Phase 0 Stress is transferred into the plank as the jacks are released.

Stage 1 This state exists immediately after transfer, when the self-weight of the plank is acting, but no creep or shrinkage have occurred.

Phase 1 Creep and shrinkage occur under the effects of prestress and plank self weight. This phase continues until TIME2 when the topping is poured.

Stage 2 Stage 2 is the state of stress, strain and deflection immediately before the topping is added.

Phase 2 Application of the topping. The plank is assumed to be unpropped After hardening, the topping concrete is in a state of zero stress, and the plank is carrying the full self weight, including the weight of the topping.

Stage 3 This stage exists just after the hardening of the topping concrete. The girder is now composite, but only the plank is stressed.

Phase 3 Under the effect of prestress and full self weight, creep and shrinkage proceed in the plank concrete, and creep and shrinkage commence in the topping concrete. These processes continue until TIME4, which is just prior to the application of the live load. For the purposes of the analysis, TIME4 is taken to approach time infinity, so that further creep and shrinkage beyond TIME4 are considered to be negligible.

Stage 4 Stage 4 occurs after the creep and shrinkage processes are complete, immediately prior to application of the of the live load at TIME4.

Phase 4 Application of the live load, which is assumed to cause cracking of the section.

Stage 5 Conditions under the full service load (G+Q).

Phase 5 Loading to failure.

Stage 6 Conditions at high overload as the peak moment is reached in the mid-span section.

A time-step procedure was adopted to analyse the time-dependent behaviour of a beam cross-section. The method involves ensuring that compatibility across a section, as well as force and moment equilibrium, are satisfied at a sequence of time instants. In the time interval between two adjacent time instants, the stress distribution is assumed to remain constant, while creep and shrinkage are allowed to occur freely in the concrete. At the end of the interval of time, compatibility in the section is restored by applying elastic stress increments to the steel, concrete and tendons, in such a way that the strain distribution is plane and strain compatibility between steel, concrete and tendons is achieved. Section analyses are carried out at several sections along the beam, so that numerical integration can be used to obtain the deflection from the calculated curvatures.

This chapter first describes the material properties and methods used to obtain the curvature and deflection due to an instantaneous loading. The approach is then extended to cover time-dependent deflections.

The method developed takes into account the effect of cracking in the beam under sustained loads. In addition, tension stiffening effects in the beam are taken into account, although non-linear creep effects at high tensile stresses are not modelled. Rather, a linear creep model is assumed, because it is considered undesirable to complicate the analysis further with a more complex creep model.

3.1.1 Sign Convention

The sign convention being used is compression positive in the concrete and tensile positive in the reinforcing and prestressing steel. As a results, signs are generally positive. Positive moments are defined as those which cause a tensile stress in the bottom fibre.

3.2 Short Term Loading

3.2.1 Material Properties - Steel

Reinforcing Steel

As this research is concerned primarily with behaviour in the service load range, an elastic-plastic stress-strain relation is considered to be sufficiently accurate for the analysis. The force in the j^{th} layer of reinforcing steel can thus be written as:

$$F_{sj} = \begin{cases} -f_{sy}A_{sj} & ; \epsilon(t) < -\epsilon_{sy} \\ E_s\epsilon(t)A_{sj} & ; -\epsilon_{sy} \leq \epsilon(t) \leq \epsilon_{sy} \\ f_{sy}A_{sj} & ; \epsilon_{sy} < \epsilon(t) \end{cases} \tag{3.1}$$

where F_{sj} is the force in the j^{th} layer of reinforcing steel,

A_{sj} is the area of the j^{th} layer of reinforcing steel,

f_{sy} is the yield stress of the steel, and

ϵ_{sy} is the strain at yield in the steel.

Prestressing Strand

For similar reasons, an elastic-plastic stress-strain relation is also used for the prestressing strand. The force produced in the k^{th} layer of strand is:

$$F_{pk} = \begin{cases} -f_{py}A_{pk} & ; \left(\epsilon(t) - \frac{\sigma_{p0}}{E_p}\right) < -\epsilon_{py} \\ (E_p\epsilon(t) - \sigma_{p0})A_{pk} & ; -\epsilon_{py} \leq \left(\epsilon(t) - \frac{\sigma_{p0}}{E_p}\right) \leq \epsilon_{py} \\ f_{py}A_{pk} & ; \epsilon_{py} < \left(\epsilon(t) - \frac{\sigma_{p0}}{E_p}\right) \end{cases} \tag{3.2}$$

where F_{pk} is the force in the k^{th} layer of prestressing tendons,

A_{pk} is the area of the k^{th} layer of prestressing tendons,

σ_{p0} is the stress in the tendons at transfer,

E_p is the Young's modulus of the prestressing steel,

f_{py} is the yield stress of the prestressing steel, and

ϵ_{py} is the strain at yield in the prestressing steel.

3.2.2 Material Properties - Concrete

Compressive Stress-Strain Relation

Both linear and non-linear stress-strain curves are used for the concrete in different computer programs. The linear relation is simply of the form:

$$\sigma_c = E_c\epsilon_c \tag{3.3}$$

With σ_c being the uniaxial stress in the concrete and ϵ_c being the uniaxial elastic strain.

The value of Young's modulus E_c is obtained from experimental data when this is available. When beams are being designed or experimental data is not available, E_c is estimated from the formula given in AS3600 (Cl. 6.1.2) [SAA (1988)]:

$$E_c = 0.043\rho_c^{1.5}\sqrt{f_{cm}} \tag{3.4}$$

where ρ_c is the density of the concrete in kg/m^3, and

f_{cm} is the mean value of the compressive strength of the concrete, at the relevant age.

To make a simple allowance for cracking of the concrete, Eqn. 3.3 is modified as follows:

$$\sigma_c = \begin{cases} 0 & ; \epsilon_c < 0 \\ E_c\epsilon_c & ; \epsilon_c \geq 0 \end{cases} \tag{3.5}$$

In order to study overload behaviour, a non-linear stress-strain equation is required. The one chosen is given in Warner and Lambert (1974). This equation utilises non-dimensional expressions to define the non-linear relation between stress and strain in concrete. The non-dimensionalised stress is represented as

$$\bar{\sigma_c} = \frac{\sigma_c}{\sigma_u} \tag{3.6}$$

and the normalised strain as

$$\bar{\epsilon_c} = \frac{\epsilon_c}{\epsilon_c'} \tag{3.7}$$

where σ_u is the ultimate strength of the concrete in the member at the appropriate age and ϵ_c' is the strain associated with that stress. This leads to the following set of equations, which produce a curve similar to that shown in Figure 3.1:

$$\bar{\epsilon_c} < 0 \quad : \quad \bar{\sigma_c} = 0 \tag{3.8}$$

$$0 \leq \bar{\epsilon_c} \leq 1.0 \quad : \quad \bar{\sigma_c} = \gamma_1 \bar{\epsilon_c} + (3 - 2\gamma_1)\bar{\epsilon_c}^2 + (\gamma_1 - 2)\bar{\epsilon_c}^3 \tag{3.9}$$

$$1.0 \leq \bar{\epsilon_c} \leq \gamma_2 \quad : \quad \bar{\sigma_c} = 1 - \frac{1 - 2\bar{\epsilon_c} + \bar{\epsilon_c}^2}{1 - 2\gamma_2 + \gamma_2^2} \tag{3.10}$$

$$\gamma_2 < \bar{\epsilon_c} \quad : \quad \bar{\sigma_c} = 0 \tag{3.11}$$

where γ_1 and γ_2 are parameters which define the shape of the curve. γ_2 is the strain at which stress reduces to zero and γ_1 is a non-dimensional stiffness.

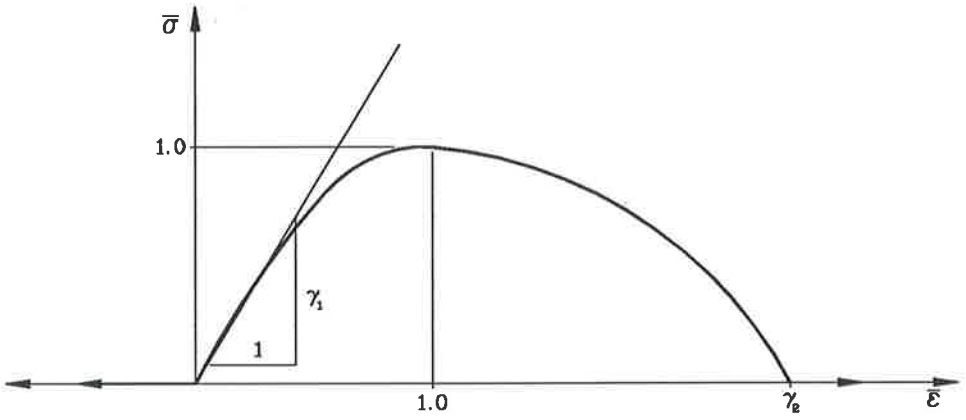

Figure 3.1: Compressive stress-strain curve for concrete (Warner (1969)).

Tension stiffening

Equation 3.5 above allows for no tensile stress in the concrete. To include tension stiffening effects in the analysis, a strain softening segment can be added to the tensile quadrant of the concrete stress-strain curve, as proposed by Bažant and Oh (1983b, 1984).

One disadvantage of this approach is that it ignores the fact that at a physically visible primary crack, the tensile stress in the concrete is zero, and that tension stiffening occurs because of the development of a complex tensile stress field in the region between primary cracks.

Bažant and Oh (1984) suggests that the effect on tension stiffening of the

transfer of tensile stresses to the uncracked concrete is relatively small and that it is the tensile strain softening behaviour of the concrete which is most important. Evidence for this is indirect.

In any case, while the approach might not be physically "correct", it has the advantage that it is very easy to implement and, at least in the present study, gives reasonable answers.

The method involves no change in the compressive section of the curve, but a tensile portion is added to the curve. The equations used for this are as follows:

$$\sigma_c = E_c \epsilon_c \quad : \quad \epsilon_c \leq \epsilon_{tp} \tag{3.12}$$

$$\sigma_c = f'_t - (\epsilon_c - \epsilon_{tp})(-E_t) \quad : \quad \epsilon_{tp} < \epsilon_c < \epsilon_{tf} \tag{3.13}$$

$$\sigma_c = 0 \quad : \quad \epsilon_c > \epsilon_{tf} \tag{3.14}$$

where $\sigma_c, \epsilon_c =$ uniaxial stress and strain of concrete,

$E_c =$ Young's modulus of concrete,

$f'_t =$ direct tensile stress,

$E_t =$ tangent strain-softening modulus,

$\epsilon_{tp} =$ strain at peak tensile stress, and

$\epsilon_{tf} =$ final strain when tensile stress is reduced to zero.

Bažant and Oh recommend calculating E_t using the formula

$$E_t = -\frac{0.483 E_c}{0.393 + f'_t} \tag{3.15}$$

with E_t, E_c and f'_t in MPa.

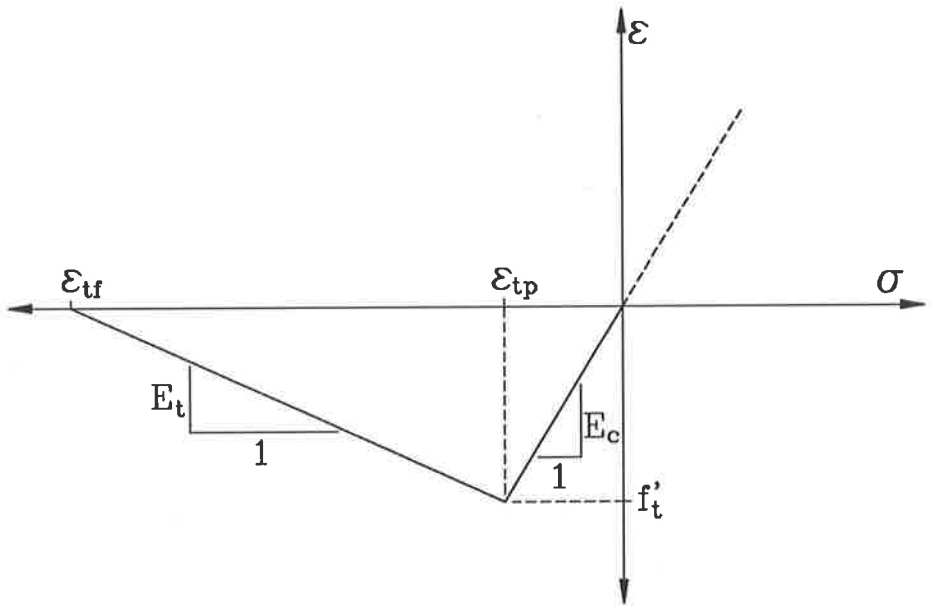

Figure 3.2: Tension stiffening segment of the concrete stress-strain curve (After Bažant and Oh (1984)).

The peak value of direct tensile stress f'_t is estimated using the formula given in AS3600.

$$f'_t = 0.6\sqrt{f'_c} \tag{3.16}$$

3.2.3 Analysis - Equilibrium, Compatibility

In the analysis of a composite, prestressed concrete beam section loaded in bending, the following assumptions are commonly made:

1. Plane sections remain plane;
2. There is no slip between the steel and concrete; and
3. The bond between the topping concrete and the plank is perfect.

These assumptions mean that the distribution of the total strain across a section can be described by a straight line, with the strains in the topping offset by known amounts. Temporarily ignoring the topping concrete, we can show the strain distribution for the plank as in Fig. 3.3. The line describing the strain distribution is defined in terms of the total strain occurring at the level of the surface of the topping and the strain at the bottom of the beam. The strain at the surface of the topping does not actually exist in any concrete, but only provides a reference. This strain distribution across the beam can be defined by the equation:

$$\epsilon(t) = \frac{\epsilon_0(t)(D-d) + \epsilon_b(t)d}{D} \tag{3.17}$$

where $\epsilon(t)$ = the strain at depth d, at time t,

$\epsilon_0(t) =$ the strain in the top fibre at time t,

$\epsilon_b(t) =$ the strain in the bottom fibre at time t, and

$D =$ the total depth of the beam.

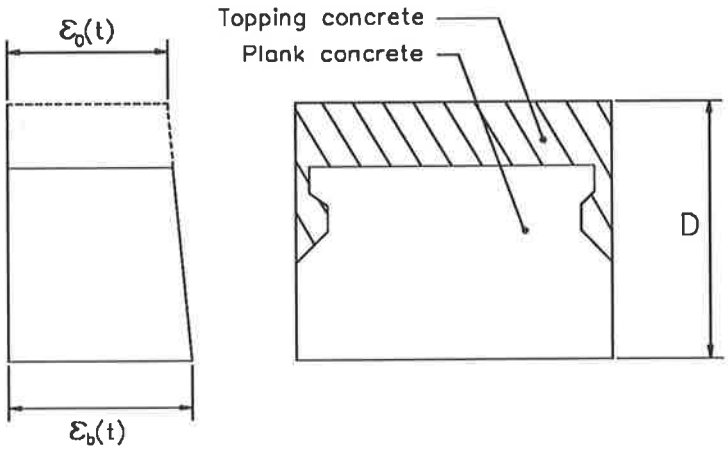

Figure 3.3: Total strain distribution in beam

To solve for ϵ_0 and ϵ_b is then a matter of ensuring that force and moment equilibrium are satisfied across the beam cross section. Previously, methods were shown which, combined with the equation of compatibility, allow the calculation of the forces contributed by the layers of reinforcing and prestressing steel. Various methods can be used to calculate the force and moment contributed by the concrete once the stresses across the section are known. The approach used in this analysis involves approximating the section by dividing it into a number of slices. This method has been used by many researchers. It is outlined by Bresler and Selna (1964) and is described in more detail by Warner and Lambert (1974). If stress across a slice is assumed to be constant, the force contributed by that slice can be calculated as:

$$F_{ci} = \sigma_{ci} b_{ci} t_{ci} \tag{3.18}$$

where F_{ci} = the force in the i^{th} layer of concrete,

σ_{ci} = the stress in the i^{th} layer of concrete,

b_{ci} = the width of the layer of concrete, and

t_{ci} = the thickness of the layer of concrete.

With the force produced by each element expressed in terms of the top and bottom strain, the equations of force equilibrium may be written as:

$$\sum_i F_{ci} + \sum_j F_{sj} + \sum_k F_{pk} = 0 \tag{3.19}$$

$$\sum_i F_{ci} d_{ci} + \sum_j F_{sj} d_{sj} \sum_k F_{pk} d_{pk} = M_{applied} \tag{3.20}$$

where d_{ci} is the depth to the i^{th} layer of concrete,

d_{sj} is the depth to the j^{th} layer of reinforcing steel,

d_{pk} is the depth to the k^{th} layer of prestressing steel, and

$M_{applied}$ is the moment being applied to the section.

This gives two equations with two unknowns and finding the strain distribution is simply a matter of finding a convenient solution technique.

3.2.4 Topping Concrete

The topping concrete is treated in a similar manner to that of the plank concrete. The main problem is that the total strain in the topping concrete, is not the same as in the adjacent plank concrete. However, the strain distribution in the plank concrete and the strain distribution in the topping concrete, must be related before the solution can be obtained. This is achieved by recording the

strain distribution at the time when the topping is added and subtracting this from the total strain over the section to obtain the total strain in the topping concrete. The effect of this is shown in Figure 3.4, where $\epsilon_{refc,i}$ is the reference strain at that level. Strains in the topping concrete are then written in terms of $\epsilon_0(t), \epsilon_b(t)$ and a series of reference strains. The strain in any steel in the topping concrete is calculated in the same way.

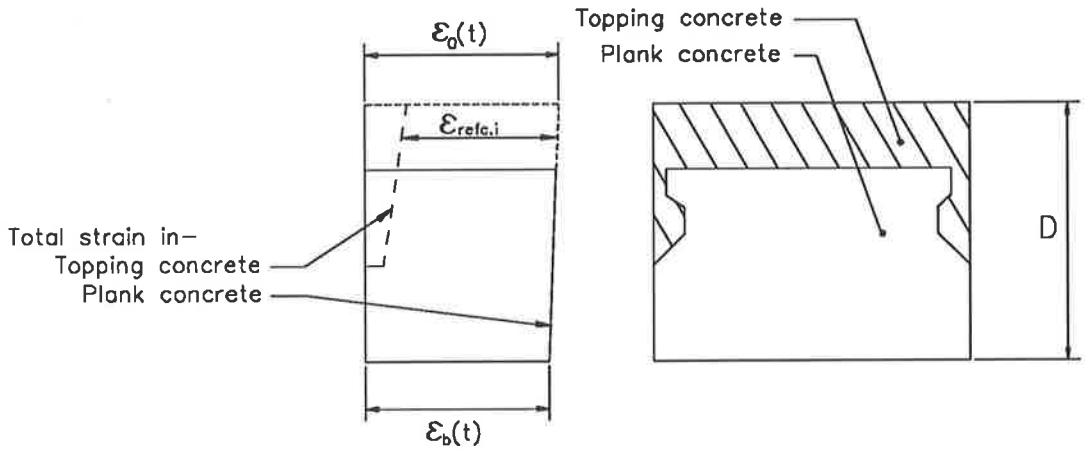

Figure 3.4: Total strain distribution in plank and topping

As these planks are usually unpropped when the topping is added, the reference strain distribution is recorded as the strain distribution produced after the self-weight moment of the topping concrete has been added. Calculations after this point then include the effect of the topping. If a plank is propped, the only difference in calculations is that the reference strain distribution is recorded as the strain in the section immediately before the topping is added, and topping effects are included from this time.

3.2.5 Solution Procedures

Several solution procedures are possible, the fastest of these works by assuming linear stress-strain relations for all of the materials. Then by substituting these

relations into the equations for force and moment equilibrium (Eqn. 3.19,3.20) and using the equation of compatibility (Eqn. 3.17), an equation of the following form may be written:

$$\begin{bmatrix} A11 & A12 \\ A21 & A22 \end{bmatrix} \begin{bmatrix} \epsilon_0[t] \\ \epsilon_b[t] \end{bmatrix} = \begin{bmatrix} A13 \\ A23 \end{bmatrix} \tag{3.21}$$

This method is based on a curvature prediction program developed by Warner (1986). However, in the present analysis the method used to model creep behaviour has been changed. A derivation of these equations is presented by Darby and Warner (1988a), along with an explanation of the values of A11, A12, etc. The form of these values is also shown in Appendix E. By writing the equations in this form, it is possible to solve directly for the top and bottom strains by simply inverting the equation given.

If any non-linearities such as cracking of the beam occur, then an iterative approach must be used, as shown in Fig. 3.5, where layers are removed from future calculations once they pass into tension. The layers must be removed, as in deriving the equation given above, it is necessary to replace concrete stress with $E_c\epsilon_c$. Unless the layers are removed, they will appear to have infinite tensile strength. The closed form solution must be applied repeatedly until all the layers which are in tension for a given solution, were removed before the calculation of that solution.

The method is shown in the diagram in the form of a Nassi - Schniedermann (N-S) diagram. Loops are represented in these diagrams by nesting the loop code within rectangles at the left and either the top or bottom, as appropriate. For, example, in Fig. 3.5 all of the statements are nested within the outer repeat loop. The thick bars on the box at the top indicate a subroutine. This technique is described in many computing text-books [For example D'Orazio (1984)].

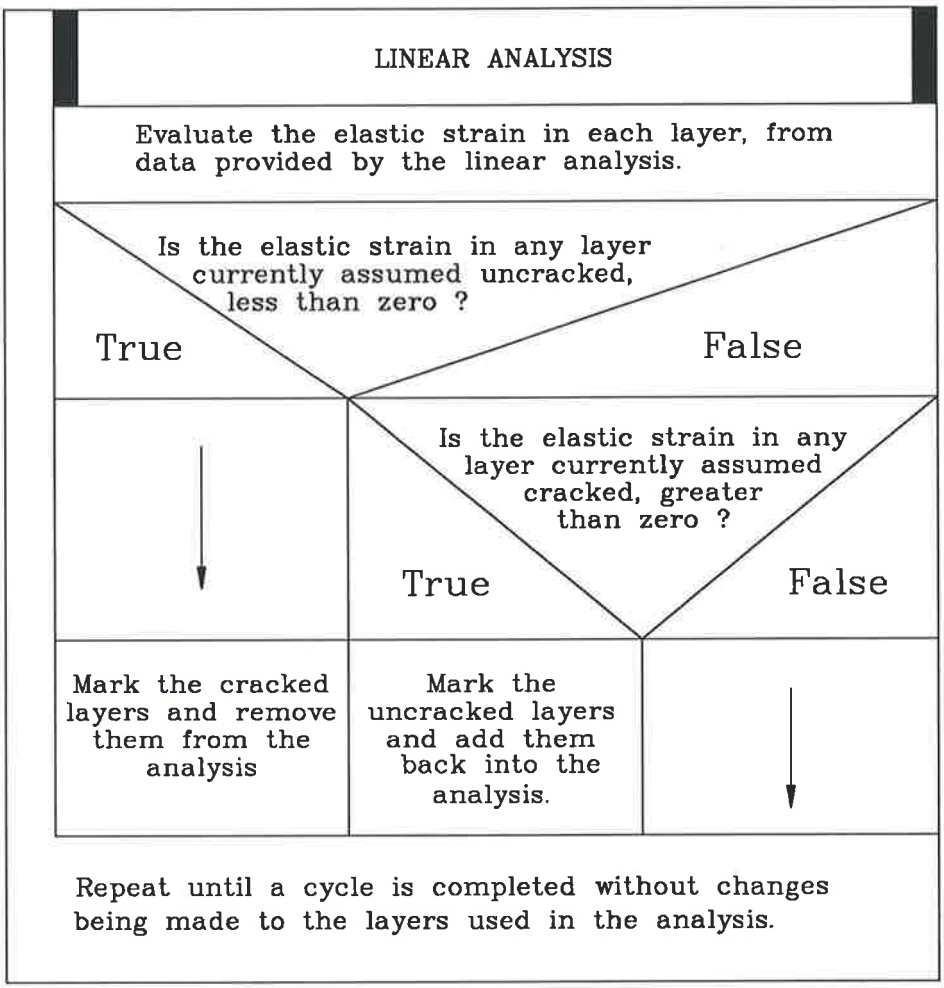

Figure 3.5: N-S diagram showing the allowance for cracking

One problem which is found in using this approach is that the program cycles between two or three guesses, without finding a solution. In particular, this occurs near the ends of the beam, where the first guess might give the top half of the beam fully cracked. The prestressing force was being applied close to the centroid of the remaining concrete, so the next iteration suggests that the beam was uncracked. The third iteration is then solving the first problem, and this cycle continues without a solution ever being found. Although this problem could occur in the midspan, it appears only to be a problem with the large cracks predicted to occur near the ends of the beam. As a result, the problem is avoided by forcing cracks in the plank concrete to begin at the bottom of the section. Debonding would be used to prevent cracks forming near the supports, so assuming that these cracks do not form does not affect the validity of the deflection calculations. Is this conclusive?

Introducing the tension stiffening curve described earlier makes it very difficult to use the closed form solution, and it becomes necessary to make use of an iterative method based on the guessing of a strain distribution. One very stable approach to this is described by Lai and Warner (1973). This method involves the use of two search loops. The inner loop varies the bottom strain until force equilibrium is satisfied for a given strain in the top fibre of the section. By incrementing, or decrementing, the bottom strain by a known amount, values of the force and corresponding strain can be obtained. Two strains are found, one which gives a force in the section greater than zero, the other which gives a force less than zero. The average of the two strains is calculated and the force produced by the strain distribution defined by the top and bottom strains is calculated. One of the two bounding values is replaced by the new value, and the cycle repeats until the desired tolerance is reached. The moment produced by this strain distribution is calculated and passed to the outer loop, which performs a similar search on the top strain, calling the inner loop on each iteration to ensure force equilibrium. The N-S diagram for the inner loop is

shown in Figure 3.6.

By calculating the strain distribution at a number of points along the beam, deflections can be obtained from the strain distribution, using basic theory, by calculating the curvature, κ, where:

$$\kappa = \frac{\epsilon_0 - \epsilon_b}{D} \tag{3.22}$$

Deflections are obtained by numerical integration of the curvatures:

$$\delta = \iint \kappa \, dx \, dx \tag{3.23}$$

The double integration can be performed using the "moment-area" method of calculating deflections. The curvature is obtained at a number of points along the beam and the area of the curve between these points calculated using a trapezoidal approximation. By summing the moments of these areas about the mid-point of the beam, the deflection can be obtained. As the beam is assumed to be simply supported, the slope will be zero at mid-span and the deflection at this point is easily obtained.

3.3 Time-Dependent Behaviour

The previous section dealt with the calculation of short term deflections. Before a description of the calculation of long term deflections is given, the methods used to model the materials must be described.

3.3.1 Non-prestressed Steel

Relaxation of the reinforcing steel can be ignored.

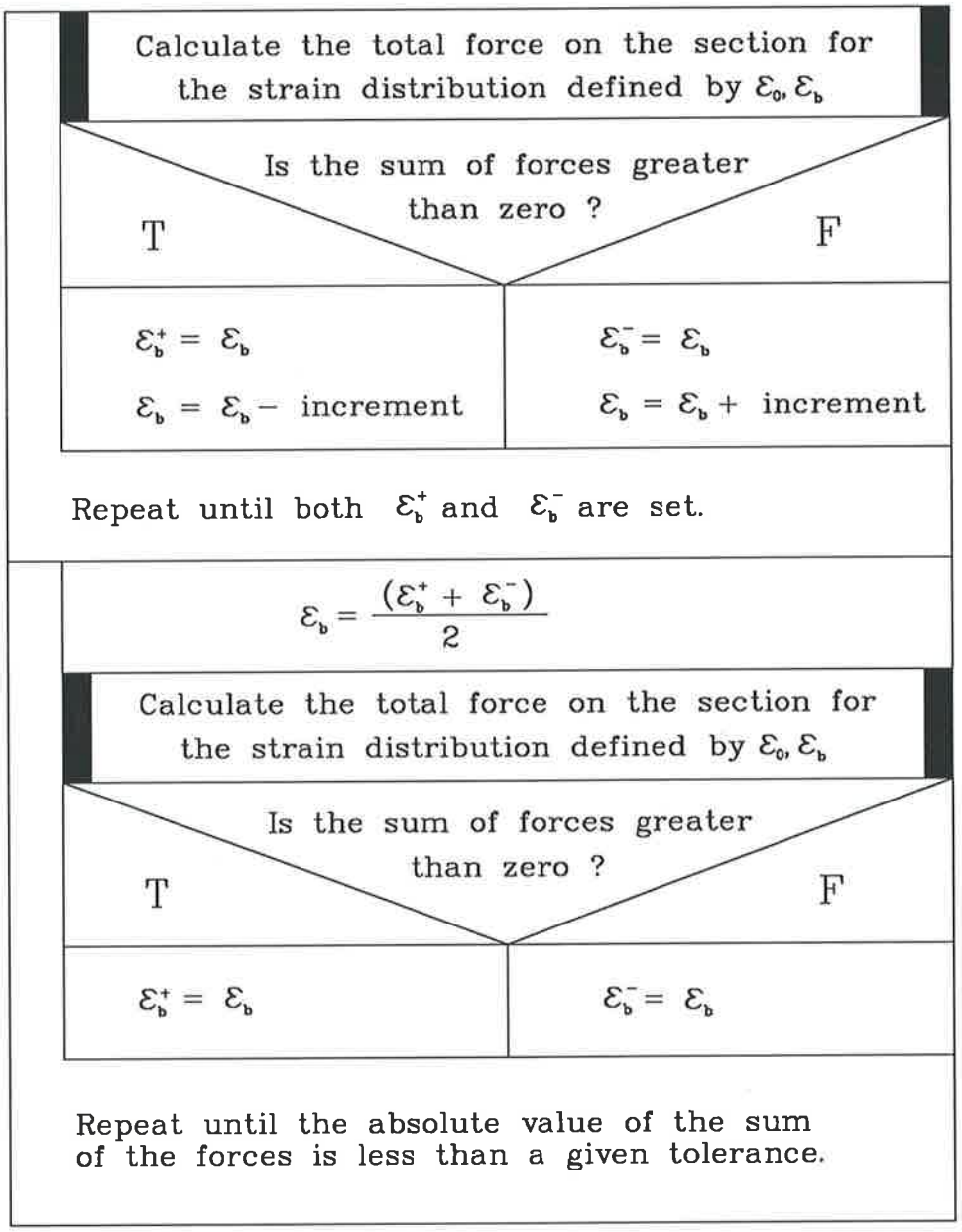

Figure 3.6: Inner loop of the search procedure

3.3.2 Prestressing Strand

All of the beams involved in this research project are precast in beds and steam cured overnight. It is therefore reasonable to assume that all of the relaxation of the prestressing strand occurred overnight, before the stress is transferred into the beam. The Australian concrete code AS3600, also allows for this, and suggests that the value of the relaxation loss is around 10% [SAA (1988), Koretsky and Pritchard (1982)]. The initial prestress value is dropped by this amount before entering the value into the program. This means that no further allowance is required to be made by the analysis procedure.

Relaxation effects can nevertheless be treated, simply by using one of the available formulae for the calculation of relaxation strains in tendons. The inelastic strain would then be introduced into the analysis in a similar manner to that used for the inelastic concrete strains.

3.3.3 Concrete

The step-by-step method of analysis was earlier chosen for use in accounting for the time-dependent effects in the concrete.

In applying the step-by-step method (SSM) of analysis [Gilbert (1986)] a continuously varying stress history is approximated by a series of stress increments. Over a given time interval the stress in a given fibre is constant. This is illustrated in Figure 3.7. The creep strain which is produced by any stress increment can be written in terms of the elastic strain increment and the appropriate value of the creep coefficient.

$$\epsilon_{ci}(t) = \epsilon_{ci}(\tau_j)[1 + \phi(t, \tau_j)] \tag{3.24}$$

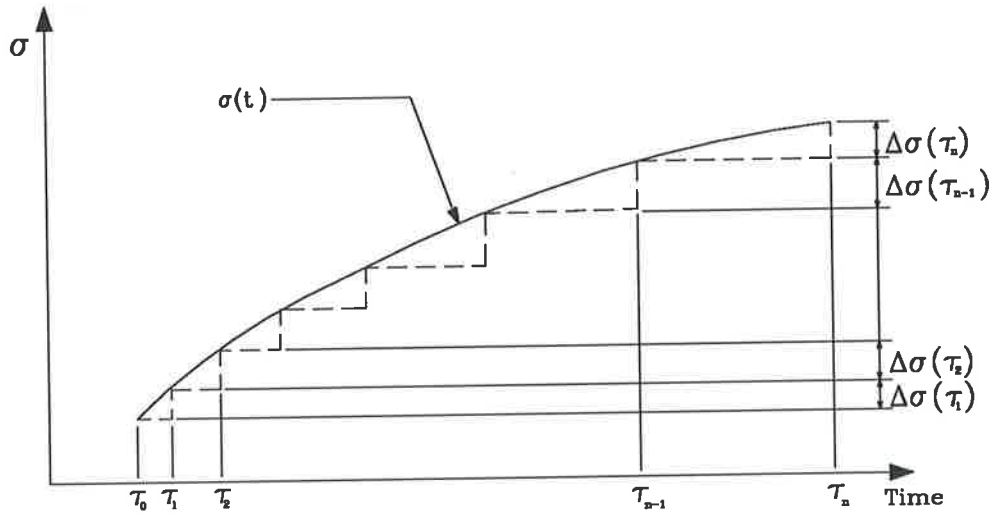

Figure 3.7: Approximation of a continuous curve with stress increments

where $\epsilon_{ci}(t)$ is the creep strain in the i^{th} fibre at time t caused by the stress increment applied at time τ_j,

$\epsilon_{ci}(\tau_j)$ is the initial strain caused by this stress increment, and

$\phi(t, \tau_j)$ is the value of the creep coefficient at time t for this concrete when it is loaded at time τ_j.

If it is assumed that concrete strains can be linearly superimposed, the strains from each of the stress increments, and the shrinkage strain, may be added, and an equation for the total strain on the section can be written.

$$\epsilon(t) = \epsilon(\tau_0)[1 + \phi(t, \tau_0)] + \sum_{j=1}^{i} \epsilon(\tau_j)[1 + \phi(\tau_i, \tau_j)] + \epsilon_{sh}(\tau_i) \qquad (3.25)$$

If sufficient time intervals are used it is possible to make fairly accurate predictions. The major disadvantage of this approach is the large amount of data

needed. In particular, a separate creep curve is needed for each stress increment to account for the ageing of the concrete. To overcome this the creep curves for different loading times are approximated by means of the equations given by ACI Committee 209 (1978).

ACI Committee 209 apply a correction factor to the basic creep curve to adjust for the age at loading. The implied assumption is that the shape of the curve remains the same, irrespective of the ultimate value of creep. Although this is not strictly accurate, it is unlikely to lead to serious error.

This assumption leads to an equation for the ultimate value of the creep coefficient for a loading at time τ_j of the form:

$$\phi^*(\tau_j) = \gamma_{la}\phi^* \tag{3.26}$$

where $\phi^*(\tau_j)$ is the ultimate creep coefficient for a loading at time τ_j,

ϕ^* is the ultimate creep coefficient for a loading at 1-3 days for steam cured concrete, and 7 days for moist cured concrete, and

γ_{la} is the factor used to adjust the final value.

The correction factor γ_{la} can be estimated using the following formulae:

$$\gamma_{la} = 1.25(\tau_j)^{-0.118} \text{ for moist cured concrete,}$$
$$\gamma_{la} = 1.13(\tau_j)^{-0.094} \text{ for steam cured concrete.}$$

where τ_j is the loading age in days.

The creep and shrinkage curves were also modelled using curves given by ACI Committee 209 (1978). These are as follows:

$$\phi(t) = \frac{t^{\psi}}{d + t^{\psi}}\phi^* \tag{3.27}$$

	Typical value	Normal range
ψ	0.60	$0.40 - 0.80$
d	10 days	$6 - 30$ days
α	1.00	$0.90 - 1.10$
f	35 days - moist cured 55 days - steam cured	$20 - 130$ days

Table 3.1: Typical values of the constants in the ACI-209 creep and shrinkage equations

$$\epsilon_{sh}(t) = \frac{t^{\alpha}}{f + t^{\alpha}} \epsilon^{*}_{sh} \tag{3.28}$$

where $\phi(t)$ is the creep coefficient at time t, and

$\epsilon_{sh}(t)$ is the shrinkage strain at time t.

The values of d, f, ψ and α are considered to be constants for a given member shape and size and define the time-ratio part. Typical values for these constants are suggested in ACI-209 (1978) and these are given in Table 3.1.

Variation in Young's modulus

To allow for variations in the Young's modulus of the concrete, the variables γ_1 and σ_u in the compressive strength curve need to be varied. The tensile portion of the curve is assumed to be constant as the actual values are not known very accurately anyway.

The ultimate compressive strength, σ_u, is varied using the formula given by ACI Committee 209 (1978).

$$\sigma_u(t) = \frac{t}{a + \beta t}\sigma_u(28) \tag{3.29}$$

where $\sigma_u(28)$ is the ultimate 28 day strength of the concrete,

t is the time at which the strength is being calculated, and

a and β are constants for a given concrete.

The value of γ_1, the non-dimensional stiffness parameter presented earlier, also needs to be adjusted. The relation for γ_1 is written as:

$$\gamma_1 = \frac{E_c \epsilon_c'}{\sigma_u} \tag{3.30}$$

The value of the Young's modulus of concrete, E_c, and the value of σ_u vary with time, so it is convenient to relate the two in some manner. This can be done by using the well-known empirical relation [Pauw (1969)]:

$$E \propto \sqrt{f_c'} \tag{3.31}$$

allowing the following formula to be written:

$$\gamma_1(t) = \sqrt{\frac{\sigma_u(\tau_1)}{\sigma_u(t)}}\gamma_1(\tau_1) \tag{3.32}$$

where τ_1 is some reference time at which both σ_u and γ_1 are known.

3.3.4 Analysis for Time Effects

The time step procedure is a simple cycle which evaluates the changes which occur over each time step. Beginning just after time instant t_{n-1} and assuming constant states of stress in all layers of materials, we evaluate the unrestrained creep and shrinkage which occur in each concrete layer over the time interval $\Delta t = t_n - t_{n-1}$.

At time instant t_n, strain compatibility will have been destroyed by the stress increments in the concrete. Elastic increments in strain, with corresponding strain increments are therefore found for all material elements such that, at time t_n, all equilibrium and compatibility requirements are satisfied. The new conditions in the section at time t_n provide the starting conditions for the next cycle.

The method of ensuring that compatibility and equilibrium are satisfied is essentially the same as before, except that now, the total strain in the concrete includes both an elastic and an inelastic component. Using Equation 3.25, the strain increment in the concrete at time τ_i is written as:

$$\epsilon(\tau_i) = \epsilon(t) - \epsilon(0)[1 + \phi(t, \tau_0)] - \sum_{j=1}^{i-1} \epsilon(\tau_j)[1 + \phi(\tau_i, \tau_j)] - \epsilon_{sh}(\tau_i) \qquad (3.33)$$

The elastic strain, ϵ_e, which is required for the calculations is simply the sum of all of the elastic strain increments. Thus, rearranging Equation 3.33 allows us to write the elastic strain in terms of the previous strain increments, which are known, and the total strain at that depth. The total strain $\epsilon(t)$ is, through the use of the equation of compatibility (Eqn. 3.17), expressed in terms of $\epsilon_0(t)$ and $\epsilon_b(t)$, which are the unknowns we wish to solve for.

$$\epsilon_e = \epsilon(0) + \sum_{j=1}^{i} \epsilon(\tau_j) = \epsilon(t) - \epsilon(0)\phi(t,\tau_0) - \sum_{j=1}^{i-1} \epsilon(\tau_j)\phi(\tau_i,\tau_j) - \epsilon_{sh}(\tau_i) \quad (3.34)$$

Substituting this equation into the equations of equilibrium allows force and moment equilibrium to be expressed in terms of the top and bottom strains on the section. One of the solution methods already described can then be used to obtain a solution to the problem.

3.4 Live Loading

As the analysis procedure is to be used primarily in the design of beams, it is useful to incorporate into the program a method for calculating the live load deflection increment. Procedures have already been presented in Section 3.2 for the calculation of deflections produced by instantaneous loadings, these must be extended to account for the inelastic conditions in the beam at the time when the load is applied.

This was implemented using the previous creep analysis by defining a time interval of zero length and changing the applied moment during this interval. The program will then calculate curvatures in the usual way, at the end of the zero time interval, by ensuring that compatibility and equilibrium are satisfied. As the time interval has zero length, creep and shrinkage have no effect, and the deflection increment is due purely to the increase in load.

3.5 Program - Camber

Using the analytic techniques presented, a program called CAMBER was written. The program was written in Pascal on a SUN-IV system, although it was

later moved down onto an IBM-PC computer. A user manual and program listing of Camber are given in Appendix A.

The time taken to run a problem depends on such factors as the number of sections used in the numerical integration along the beam, and how swiftly the iterative solution converges. It is worth timing the various methods to determine the sort of advantage which is gained through the use of the closed form solution technique. The results of such a comparison are shown in Table 3.2, where it can be seen that using the closed form solution allows large savings in solution time. This is especially important with the PC based techniques, where the solution time for the iterative solution is far too long for practical usage.

Solution technique	Time taken on	
	SUN-IV system	IBM-PC system
Closed form solution	19.6 sec.	303 sec.
Iterative closed form	28.2 sec.	358 sec.
Iterative solution	1079.3 sec.	11244 sec.

Table 3.2: Times to obtain a solution using different techniques.

3.5.1 Solution Accuracy

In developing a computer program, two sorts of error need to be considered. The first is a modelling error which is caused by differences between the theory used and the real world. The second type of error arises from the numerical approximations involved in implementing the theory. Modelling errors are investigated by comparing the predicted behaviour of the beams with behaviour observed in experiments. This is discussed in detail in Chapter 4, while the second type of error is considered here.

Real variables are implemented on the SUN-IV system using 64-bit IEEE float-

ing point format. This provides approximately 16 digits of precision, meaning that internal rounding errors are unlikely to be a serious cause of inaccuracy.

The number of time steps used within the program affects the accuracy of the model. With increasing numbers of steps the continuously varying curve, which represents the actual variation of stress with time, is more accurately approximated. On the other hand, an excessive number of steps causes the program to execute too slowly. Therefore, the program was run with an increasing number of time steps to determine the number of steps at which further increases did not give any significant increase in accuracy. Figure 3.8 shows the results of this test for plank PA10NT1 and indicates that ten time steps should give acceptable answers. Some beams were found to give unstable solutions when only ten time steps were used. It is therefore recommended that twenty steps be used.

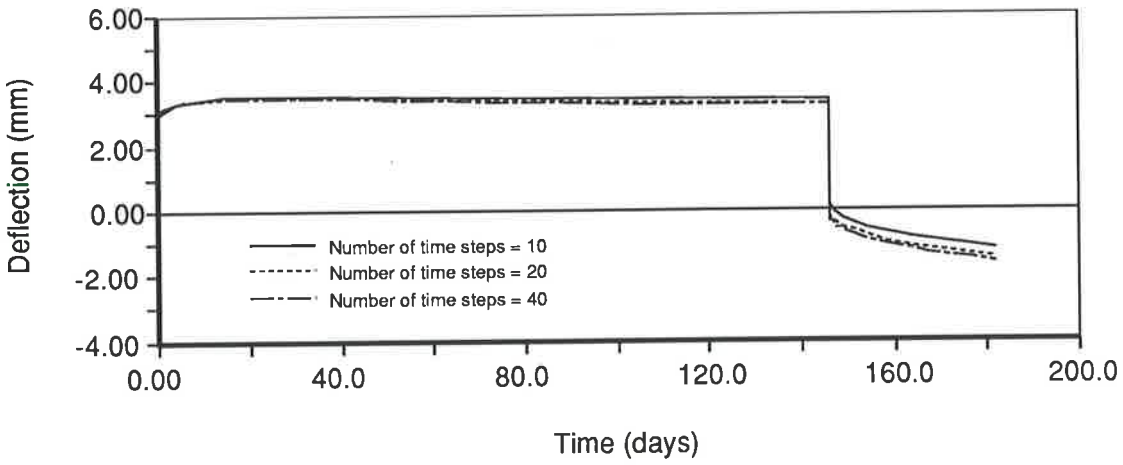

Figure 3.8: Effect of varying time steps on PA10NT1

The division of the section into a number of slices introduces a similar type of error. This is reduced in the program by recording the actual centroid of slices taken through the section and using this value in preference to the centroid of the rectangular slices used to approximate the section. Figure 3.9 demonstrates that the use of more than ten slices is not required.

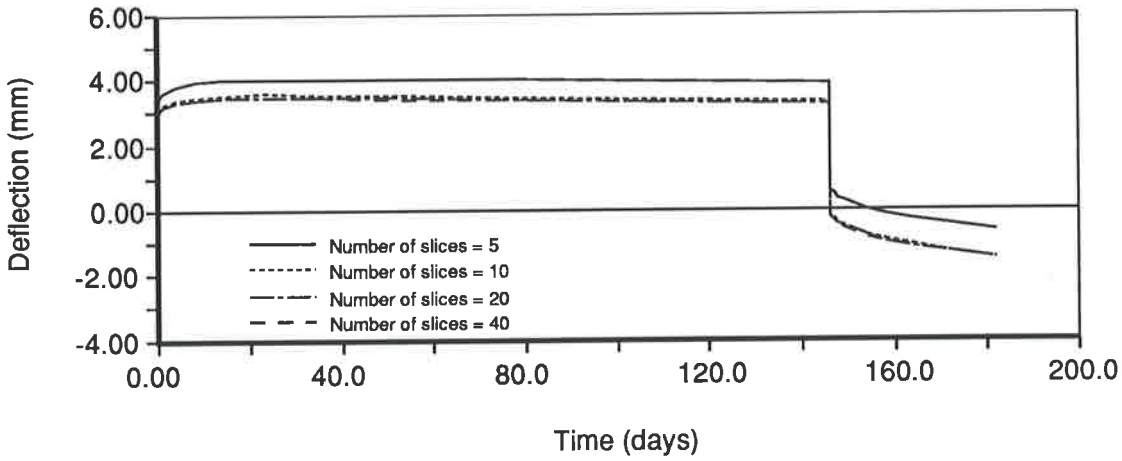

Figure 3.9: Effect of varying the number of slices on PA10NT1

Numerical integration of the curvatures along the beam is used to calculate the deflections. Increasing the number of stations at which curvature is calculated produces an answer which is closer to that which would be obtained if the calculated curvature could be integrated analytically. However, as cracks form at discrete intervals on a real beam, increasing the number of stations does not necessarily produce a more accurate result. As this is a basic difference between the model and the real world, a sufficient number of stations should be provided to ensure a good accuracy for the numerical integration, whether this provides a closer answer to the true value or not. In this case, as shown in Fig. 3.10, only five stations are required.

If tension stiffening is to be modelled, this can then be done using a model such as the one described earlier. The model attempts to allow for the effect by giving the average stress-strain relation, which might be measured over a long gauge length.

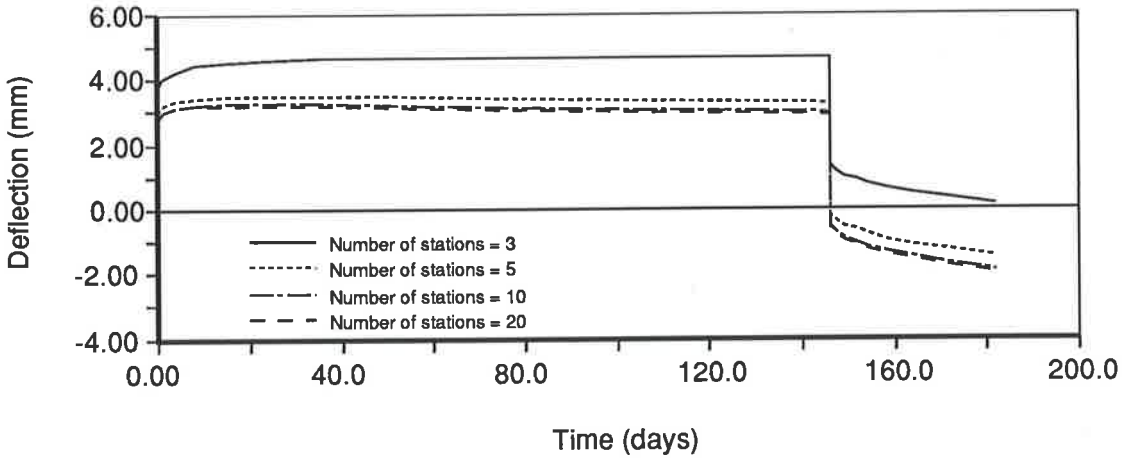

Figure 3.10: Effect of varying the number of stations on PA10NT1

3.6 Summary

Within this chapter, a procedure was developed for the prediction of the short term and long term deflections of composite, partially prestressed beams. This procedure must be checked against experimental data, to determine its accuracy under various conditions, before it can be used for the design of beams.

Chapter 4

Comparison with Leong's Plank Test Data

In some sections of Chapter 3, alternative procedures are outlined for the prediction of the long-term deflections of composite, partially prestressed composite beams. Comparisons with experimental data will help to determine whether the more complex procedures are required to produce accurate answers, or whether the simpler methods are adequate. Details of these comparisons are presented in this chapter, using the experimental data collected by Leong, Crawley and Warner (1987).

4.1 Leong's Data

The set of six planks tested by Leong et.al. were cast in Echuca, then transported to Adelaide, where they were kept inside to reduce the effect that the environment had on the results. Deflections and strains were monitored over a period of around two hundred days, which gave sufficient data for long-term

trends to be clearly seen. In addition, live load tests were performed at various times during the testing period, to gain information on their performance under load.

Measurements on creep and shrinkage prisms provided the creep and shrinkage data which were entered into the program.

4.1.1 Plank Details

Two designs of planks were tested. The PA10NT series consists of three planks with the cross section shown in Fig. 4.1. These planks contain only prestressing strand. The PR10NT series consists of a further three planks as shown in Fig. 4.1, which have mixed reinforcing and prestressing steel. In each series the planks are numbered 1,2 and 3 giving PA10NT1, PA10NT2, etc. Plank 1 in each series had the topping added after 146 days while the topping was added to planks 2 and 3 after 28 days. For the purpose of this analysis, planks 2 and 3 in each series are identical.

4.1.2 Material Properties

Prestressing Strand

The strand used was 12.7mm, low relaxation seven wire strand, supplied by BHP. Tensile tests gave values for Young's modulus of 191×10^3 MPa at a tensile force of 70kN and 187×10^3 MPa at 130kN.

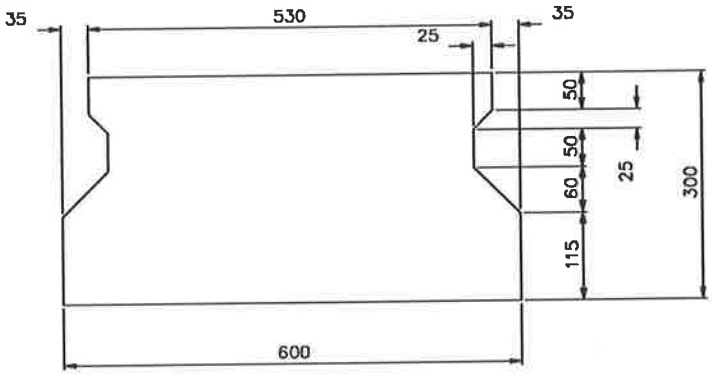

END ELEVATION
SCALE 1:10

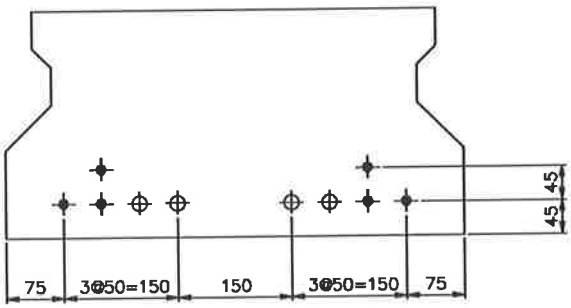

REINFORCEMENT AND STRAND DETAIL FOR PR1ONT
4/20 Y bars 8900 LONG
6/φ12.7mm LOW RELAXATION SUPER GRADE STRANDS
INITIAL PRESTRESS SHALL BE 128kN PER STRAND
STRANDS SHALL BE STRAIGHT
SCALE 1:10

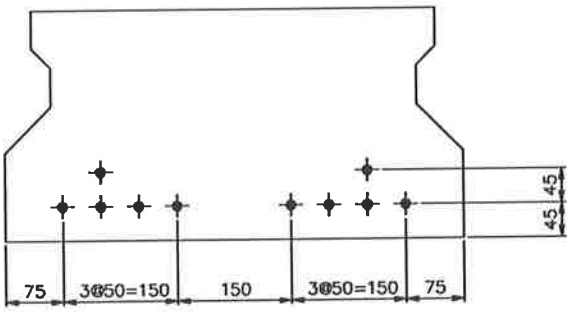

REINFORCEMENT AND STRAND DETAIL FOR PA1ONT
8/φ12.7mm LOW RELAXATION SUPER GRADE STRANDS
INITIAL PRESTRESS SHALL BE 67kN PER STRAND
STRANDS SHALL BE STRAIGHT
SCALE 1:10

Figure 4.1: Details of beam cross-sections

Reinforcing Bar

The reinforcing bars used were Tempcore deformed bars of 20mm diameter. The actual yield stress was assumed to be 480MPa and the Young's modulus was assumed to be 2×10^5 MPa.

Concrete

Four concrete pours occurred during the production of the composite planks. Pour 1 formed the PA series of planks and pour 2 the PR series. These pours were conducted at Echuca using concrete supplied by the Hume precasting yard at Echuca. The topping concrete placed on planks PA10NT2, 3 and PR10NT2, 3 came from pour 3, while the topping concrete for the remaining planks came from pour 4. Pours 3 and 4 both occurred in the Chapman Laboratory at the University of Adelaide, the concrete for these pours being supplied by an Adelaide ready mix concrete company.

Tests were conducted to obtain a value of Young's modulus for each of the concrete pours. The values are shown in Table 4.1.

	Pour	Age of concrete when E_c was determined (days)	E_c (from test) (MPa)
Plank concrete	1	1	23704
	2	1	33247
Topping concrete	3	7	26627
	4	7	21531

Table 4.1: Test values of Young's modulus for the concrete

Tests to obtain the creep and shrinkage parameters for each of the pours were also conducted using standard test prisms (100mm x 100mm x 500mm). To allow the experimental creep and shrinkage data to be used in the program, the curves given earlier (Eqns no. 3.27,3.28) were fitted to the data.

Figures 4.2 and 4.3 show that the fits provide a reasonable approximation to the data over the time of interest. Data were only collected over about fifty days for the Pour 4 concrete, so the final values of creep and shrinkage which were estimated may be considerably in error. However, over the time period for which the program was run the curves fit the data well, so this should not affect the comparisons with experimental results.

Ultimate creep and shrinkage values were adjusted to account for the difference in theoretical thickness between the plank and the prism, using the method in AS3600, giving the values shown in Table 4.2. The shape of the curves was assumed to remain the same.

When the topping is added to the plank, the cross-section of the beam is changed. As cross-section has a large effect on the final values of creep and shrinkage, this change must be taken into account in some way. The method chosen was to calculate two limiting values for ultimate creep and shrinkage and then choose a value within the range thus obtained. One limiting value was obtained by ignoring the topping altogether. The other was obtained by assuming that the topping was added immediately and acted like an impervious membrane. The mean value was then chosen from this range.

To account more accurately for the addition of the topping, it would have been necessary to allow for the change in the flow of moisture as the topping is added. This would greatly complicate the program and require the use of a different approach to the prediction of creep and shrinkage. As the results have been found to be relatively insensitive to the values of creep and shrinkage used, it was decided that the above method would be sufficiently accurate.

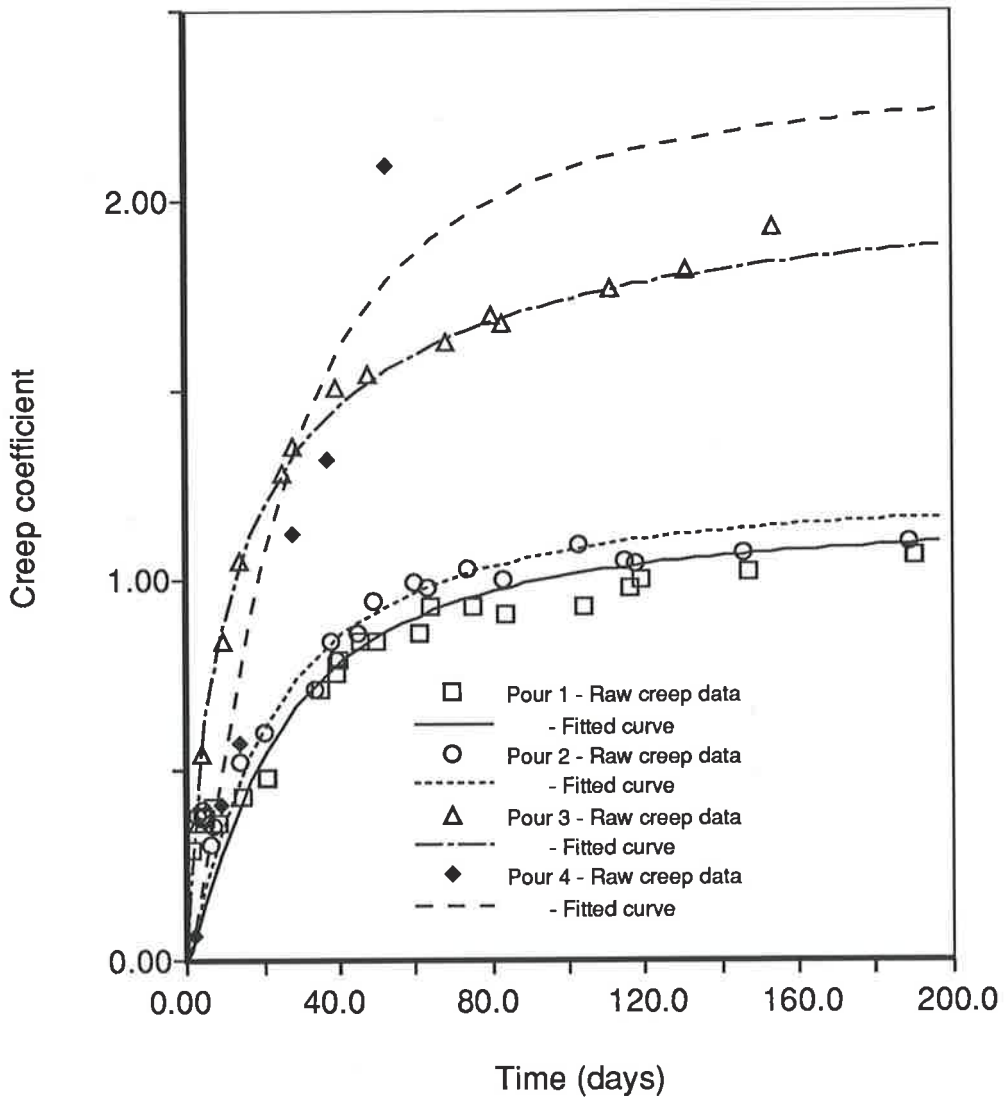

Figure 4.2: Plot of creep data and fitted curves

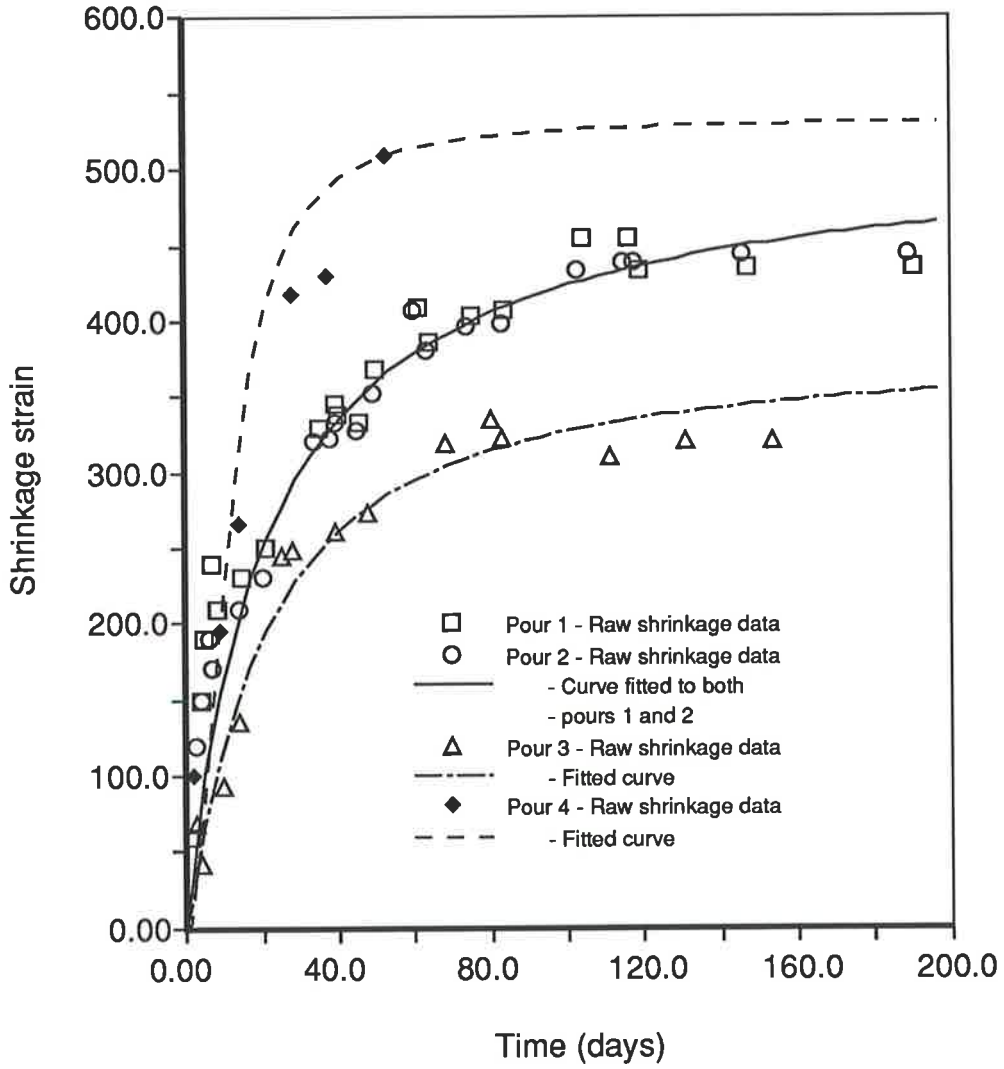

Figure 4.3: Plot of shrinkage data and fitted curves

Values were also calculated using the data given in AS3600 for when experimental data are not available. These would be the values used in any preliminary design. The curve shapes were defined by using typical values of ψ, d, α and f, which are the variables in the ACI 209 creep and shrinkage equations. (See Equations 3.27 and 3.28) These values are also included in Table 4.2.

Pour No.		ϕ^*	ϵ^*_{sh}	ϕ^*	ϵ^*_{sh}	ψ	d	α	f
		with topping		without topping					
1	Test	0.82	312×10^{-6}	0.93	390×10^{-6}	1.27	54.4	0.97	19.9
	Code	1.76	420×10^{-6}	1.98	525×10^{-6}	0.60	20	1.00	55
2	Test	0.88	312×10^{-6}	0.99	390×10^{-6}	1.18	37.0	0.97	19.9
	Code	1.76	420×10^{-6}	1.98	525×10^{-6}	0.60	20	1.00	55
3	Test	1.69	287×10^{-6}	—	——	0.79	8.5	1.11	28.1
	Code	2.69	525×10^{-6}	—	——	0.60	20	1.00	35
4	Test	1.86	532×10^{-6}	—	——	1.42	88.5	2.04	148
	Code	2.69	525×10^{-6}	—	——	0.60	20	1.00	35

Table 4.2: Creep and shrinkage parameters

4.1.3 Prestressing Force

Load cells were used to obtain the values of prestress before steam curing, prior to release and after release. These values are shown in Table 4.3 along with the values of prestress estimated from the strand extension tests.

Initial values of prestress in the strand were obtained from these test values and used within the program. Test data were available showing the level of prestress in the strand after the steam curing was complete, and hence, the amount of relaxation in the strand. However, AS3600 [SAA (1988)] gives a method for use when no test data is available, which was tried to allow some

indication of its accuracy to be obtained. The method involves reducing the initial value by 10% to account for relaxation. The results in the table show this to be a reasonable assumption.

	Initial MPa	Prior to release MPa	After release MPa
	PA series		
Load cell	672	594	577
Strand extension	701	—	—
Program	670	603	542
	PR series		
Load cell	1278	1234	1129
Strand extension	1291	—	—
Program	1280	1152	1107

Table 4.3: Prestressing force in planks

4.2 Short-term Deflections (First 24 hours)

During the period in which the planks were monitored at Echuca, before transport to Adelaide, significant variations in deflections were recorded. These are shown in Figure 4.4. The most likely cause of these variations comes from temperature gradients forming across the beam. The planks tended to hog up during the day as their top surface was heated, and return to the old level overnight. The light rain on the second day, coinciding with a large increase in deflections, probably caused the top surface to be quickly cooled, decreasing the strain in the top fibres and pulling the plank down.

No attempt is made to predict these deflections, as temperatures were not mon-

itored and the prediction would simply involve guessing suitable temperature gradients.

The graph of short-term deflections (Fig. 4.4) also shows that within each set of three supposedly identical beams, differences of several millimetres are apparent. These could easily be caused by small differences in the manufacturing process or errors during the measurement of the camber prior to transfer of the prestress. It is not proposed to try and explain these variations, but it should be remembered when comparing predicted and experimental results that random variations of this order must be expected to occur.

4.3 Long-Term Deflections

Calculated and observed long-term deflections are presented in graphical form in Figures 4.5 to 4.8. There is a plot of experimental data on each graph along with the results for a particular run, or set of runs, from the computer. These runs are discussed in the following sections.

4.3.1 Linear Analysis

By using a linear stress-strain curve, computer solutions can be effected which run very quickly. The results obtained are acceptable providing the stresses remain within the range of about f'_t in tension to $0.4f'_c$ in compression. But while it was initially thought that this condition would be satisfied with dead load only acting, it was found that the effect of differential shrinkage between the topping and plank concretes caused the formation of cracks in the topping concrete. This suggests that the simple linear analysis will only give reasonable results when the topping is applied at an early age, so that cracking does not occur.

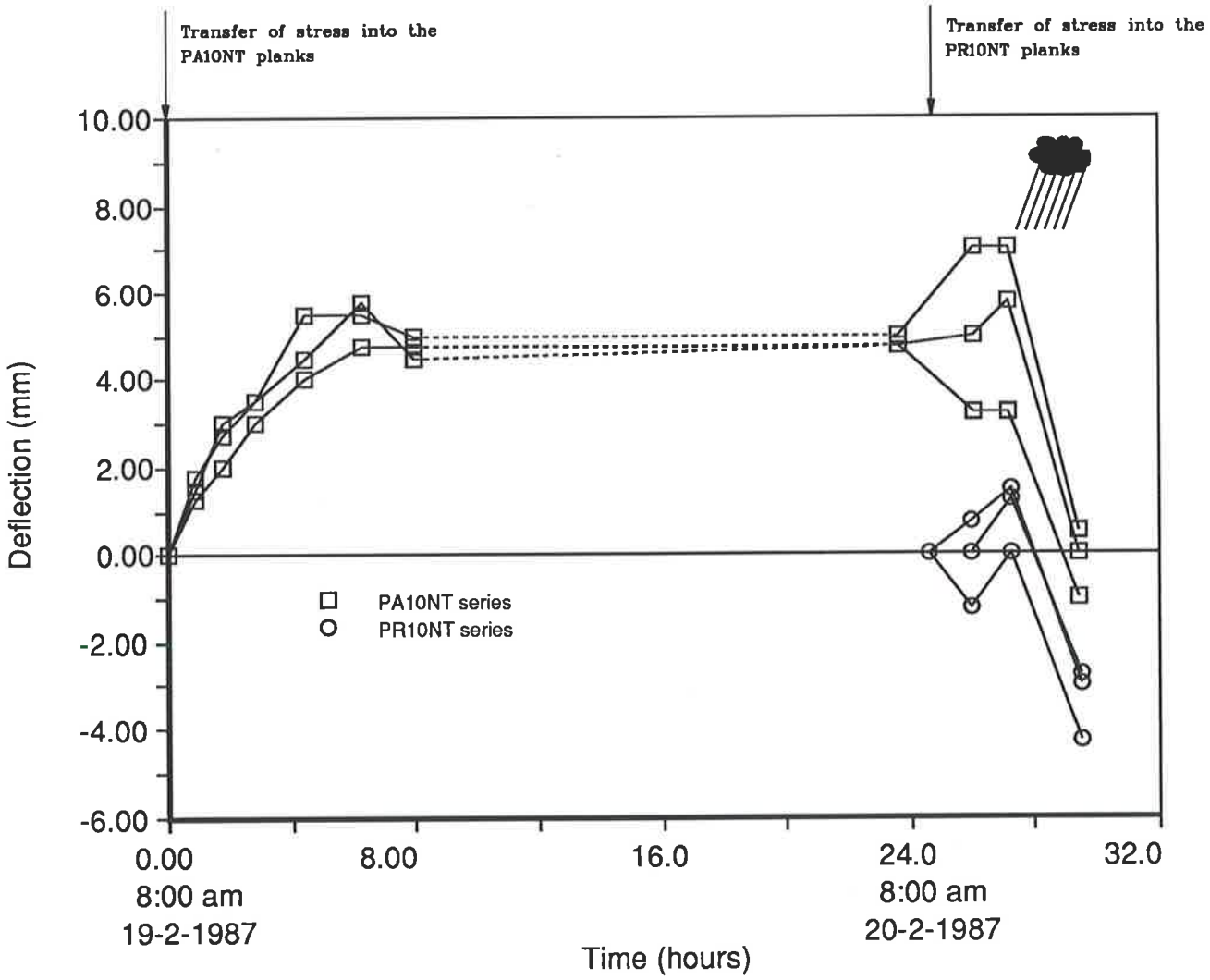

Figure 4.4: Short-term variation in deflections

A modification to the closed form linear analysis to allow it to handle cracking can, nevertheless, be made, by removing from the analysis slices of concrete which exceed a given tensile stress. This procedure is described in Chapter 3.

The solid line in Figure 4.5 shows the effect on predicted deflections of disregarding cracking. The deflections are greatly overestimated after the topping is added because of the differential shrinkage between the topping and plank concretes.

Figure 4.6 shows similar results although the increase in deflection is relatively small. This is because the topping was added at an early age and the differential shrinkage is correspondingly small. The final results from this curve are good, but the initial values are in error by several millimetres. It was stated earlier that errors of this order should be expected, however the general shape of the curve should also be correct. In this case it was not, and the good final result was probably just coincidence as the deflections prior to the addition of the topping concrete are inaccurate.

Figures 4.7 and 4.8 show that similar results were obtained for the PR series of planks.

4.3.2 Non-Linear Analysis

This method gave much better answers than the linear analysis, chiefly because it allowed for the occurrence of cracking. The dashed line labelled "non-linear" results shows the result of using a non-linear curve for the concrete stress-strain relation, however similar results can be obtained using the modification to the linear analysis which makes an allowance for cracking. The second method is preferred, as the predictions are obtained much more quickly.

The shape of the curves produced using this procedure were similar to those

obtained experimentally. While differences of several millimetres are apparent, it is probably not realistic to expect the predictions to be more accurate.

4.3.3 Tension Stiffening

Tension stiffening can have a significant effect on the deflections measured for a beam. One method of accounting for this effect is to add a strain-softening portion to the tensile quadrant of the concrete stress-strain curve. A complicating factor for beams under long-term loading is the effect of non-linear creep, which will occur when the tensile stress in the concrete rises above about half of the tensile strength. Even though non-linear creep effects cannot be accounted for using the present model of creep and shrinkage, it was still thought worthwhile investigating tension stiffening effects.

In Figures 4.5 to 4.8 the dashed line labelled "Tens. stiffening in plank concrete only", represents the effect of ignoring tension stiffening effects in the topping concrete, while including them in the plank concrete. As the plank concrete was uncracked under dead load in these tests, the close correspondence with the curve which ignores tension stiffening altogether is to be expected. This run is far more relevant when studying the live load deflections in the next section.

Cracks do form in the topping concrete. Unfortunately, as can be seen from the line labelled "tension stiffening", attempting to account for any tension stiffening in the topping leads to inaccurate answers. Indeed, the best answers were obtained by ignoring the tensile strength of the topping concrete altogether.

As cracks form at discrete intervals along the plank, the sections of uncracked concrete would be expected to have some stiffening effect. However, the complexity of the situation, with non-linear tensile creep effects, shrinkage and the

topping interacting with the plank, make it difficult to form any definite conclusions. Also, the situation is very different from the usual situation where cracks open in the bottom of the beam, as a result of bending. From the limited data available, it seems satisfactory to simply state that ignoring the tensile strength of the topping concrete appears to result in good predictions.

4.3.4 Variation in Young's Modulus

The value of Young's modulus for concrete varies with time, increasing as the concrete ages. This effect was included in several runs for the PA series of planks, but was found to only have a minor effect on the outcome, while complicating the program. For these reasons, the effect was ignored in future runs.

4.3.5 Use of AS3600 Creep Data

A final set of runs was made using creep data predicted by the methods given in AS3600. The shape of the curves was defined using the "typical" values given by ACI-209 (1978). These are the values which would have been used in design calculations, where the properties of the concrete mix are not known exactly. As can be seen from the graph, predictions are not greatly affected using these values and it is likely that any inaccuracy, from this source, would not be too great.

4.4 Live Loading

A set of live load tests were also performed by Leong, Crawley and Warner. Beam 2 in each series was loaded at an age of about sixty days, while all

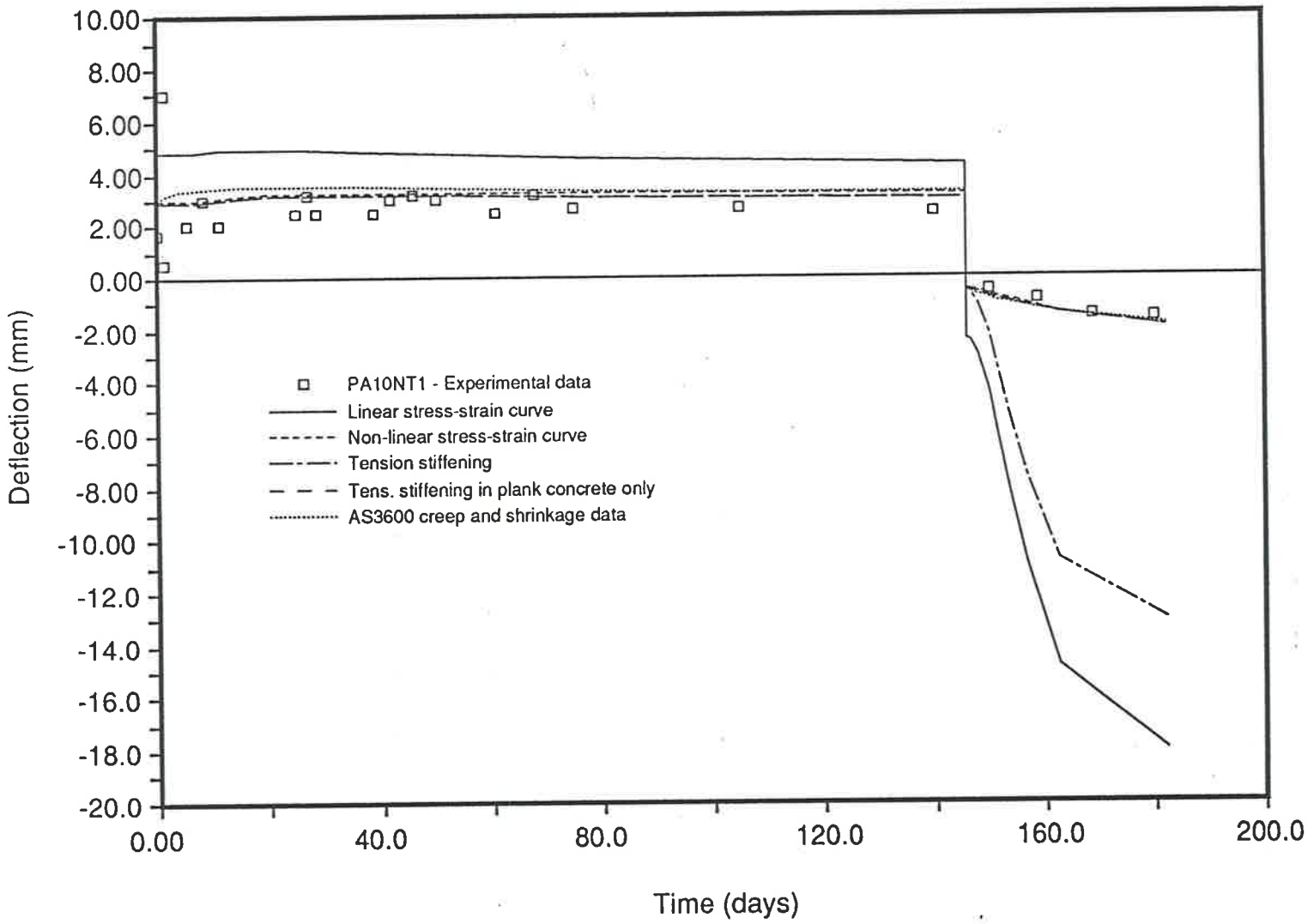

Figure 4.5: PA10NT1 - Plots of deflection vs. time

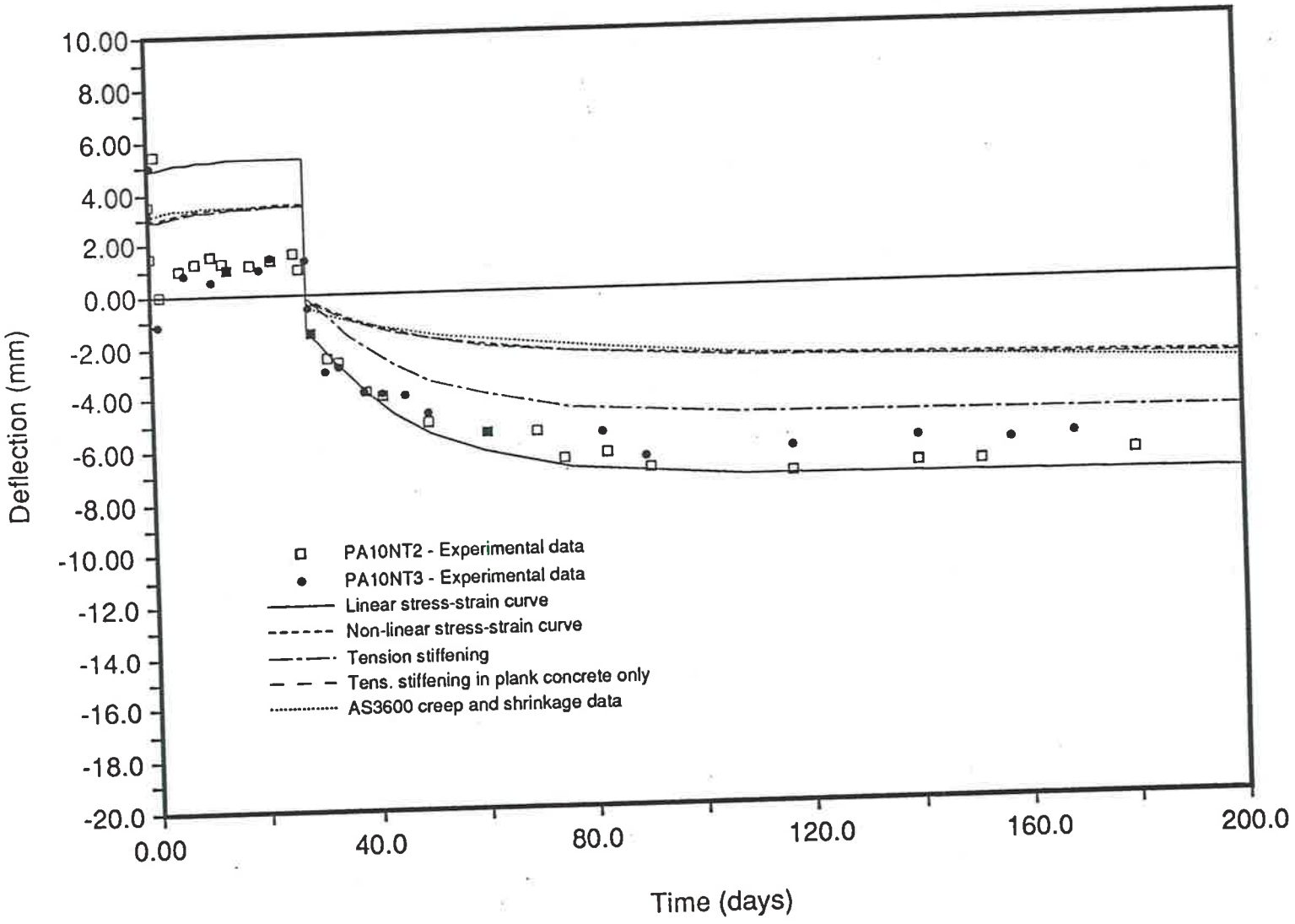

Figure 4.6: PA10NT2,3 - Plots of deflection vs. time

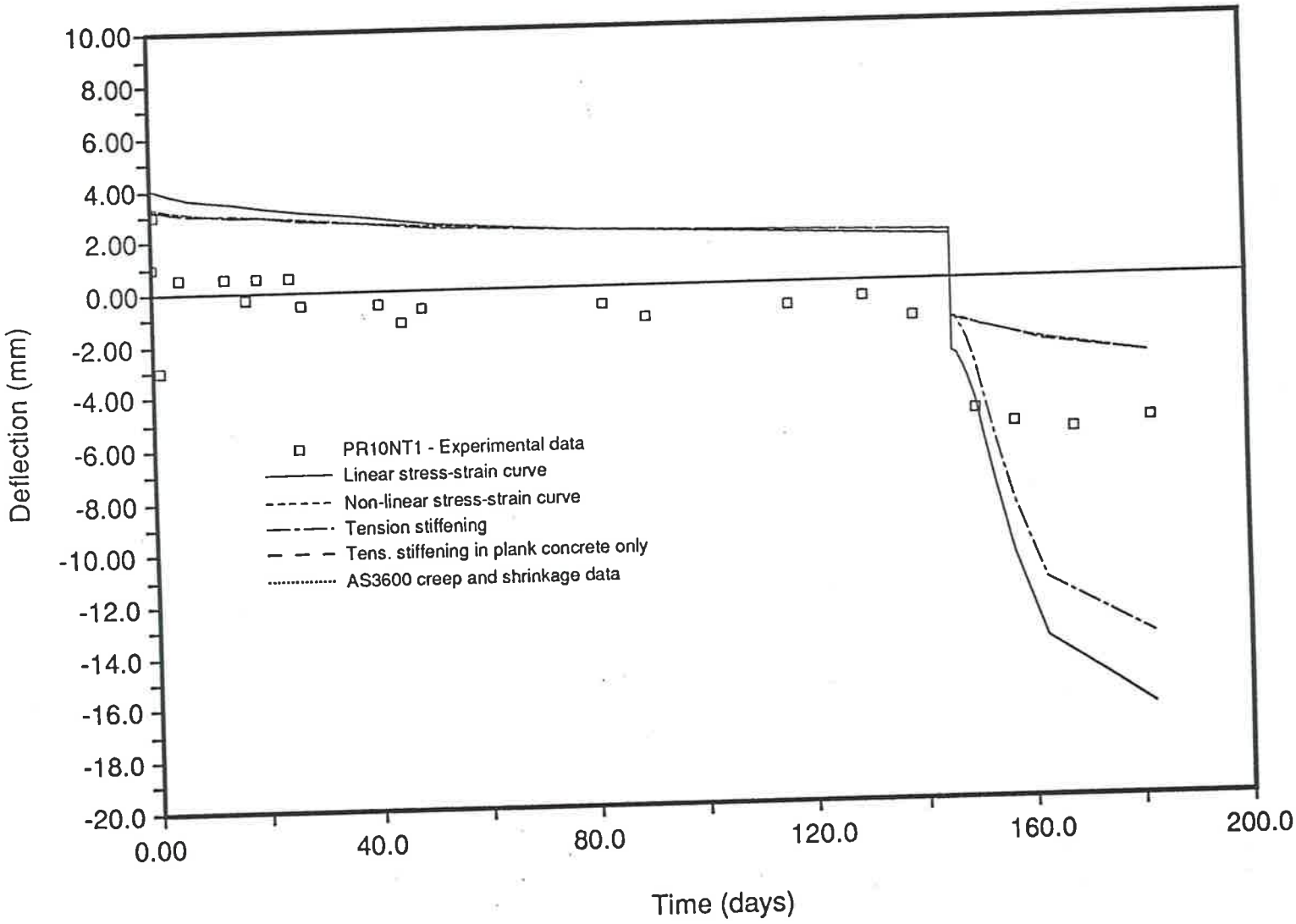

Figure 4.7: PR10NT1 - Plots of deflection vs. time

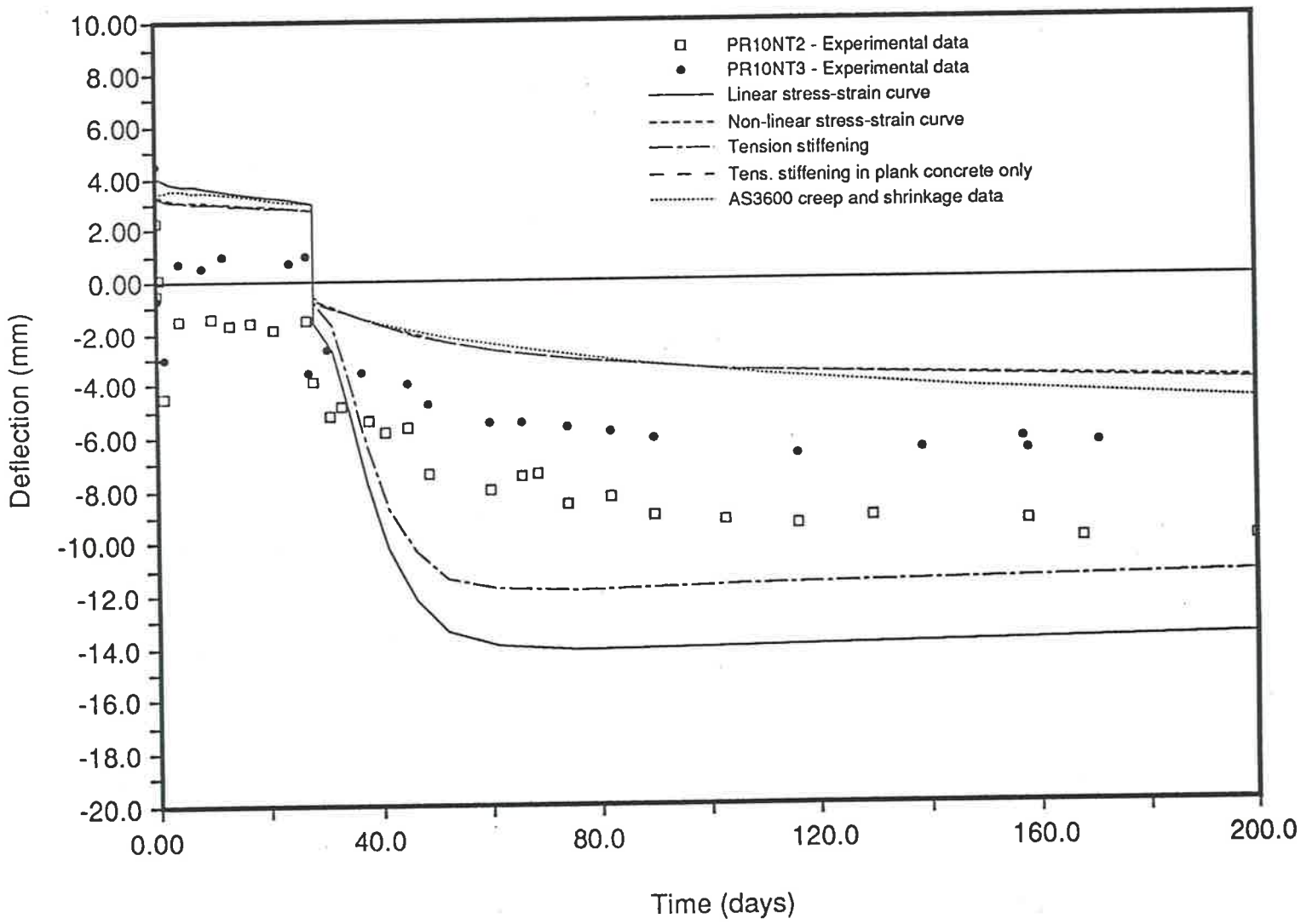

Figure 4.8: PR10NT2,3 - Plots of deflection vs. time

the beams had ultimate load tests performed at approximately one hundred and eighty days. The experimental rig used to test the beams is shown in Figure 4.9.

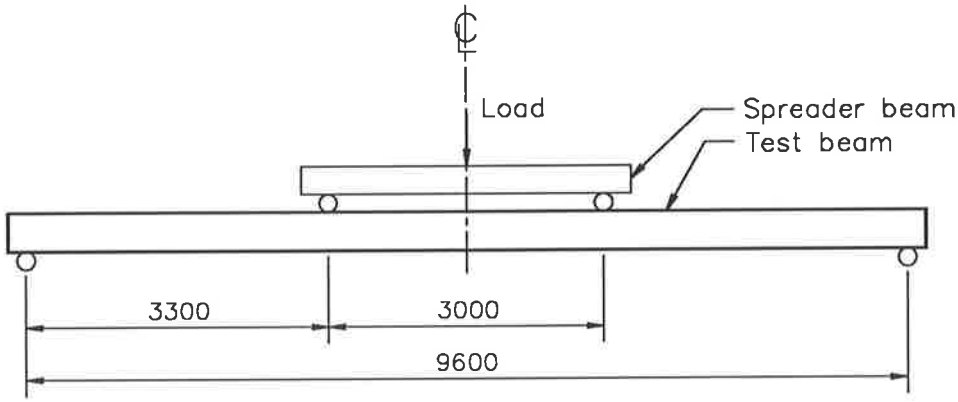

Figure 4.9: Test frame for live loading

The ultimate load results have been compared with the results of several runs of the program Camber, using different assumptions about the concrete properties. In all cases the strain distribution assumed to be in the beam at the start of the loading was that predicted by Camber as being in existence at an age of 180 days.

Three different runs were made, using different stress-strain curves for the concrete in each case. The curves used are shown diagrammatically in Fig 4.10. The first run ignored tension stiffening effects in the concrete. As expected, this curve provides a lower bound for the rest of the predictions. Figures 4.11 and 4.12 show the results for plank PA10NT1. Results for the other planks are included in Appendix B.

Run 2 added Bažant's tensile quadrant to the stress strain curve of the plank concrete as was described earlier. This provides a convenient method of introducing tension stiffening effects into this type of analysis. For the reasons mentioned earlier, tension stiffening effects were only included in the plank concrete. As can be seen, this produces a significant increase in the level of

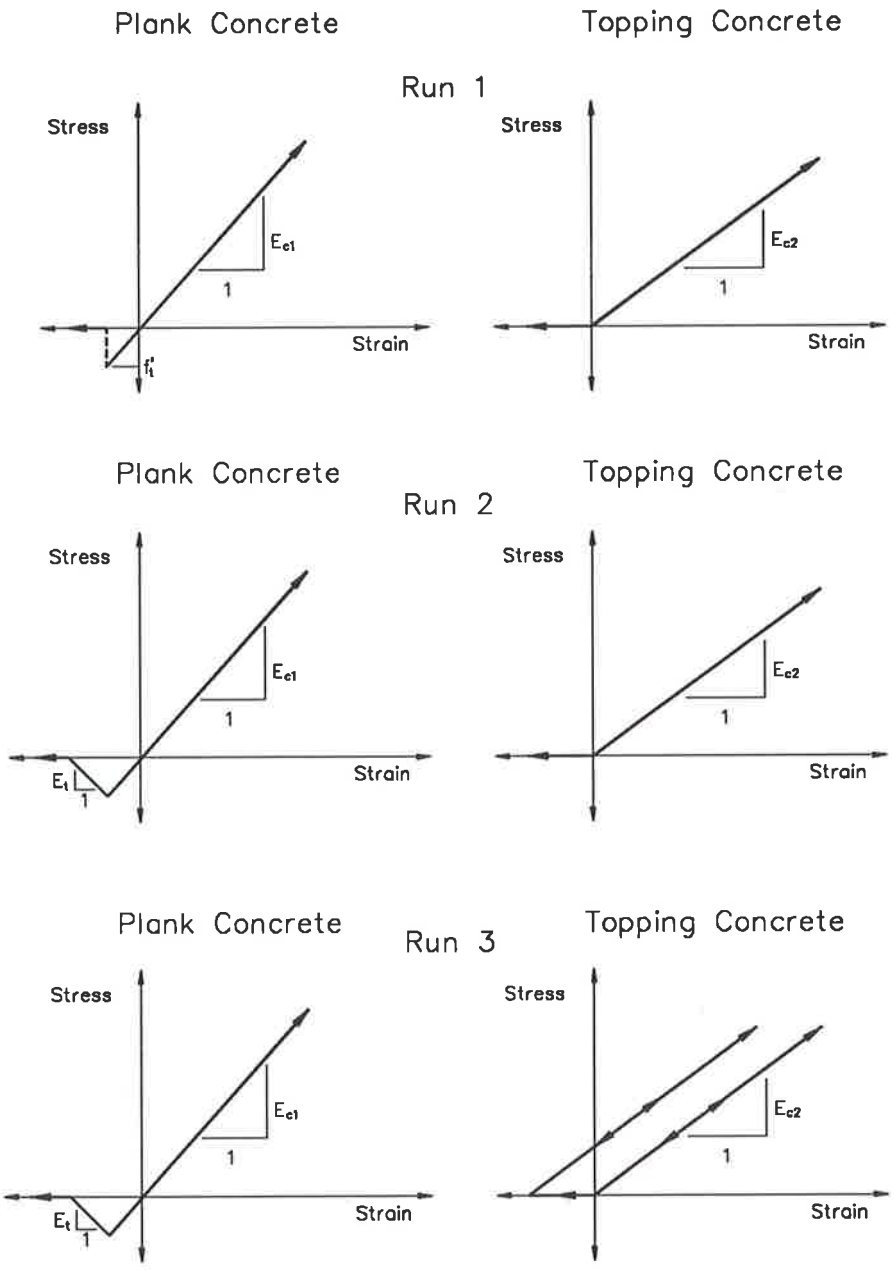

Figure 4.10: Stress-strain curves used for Live Load predictions

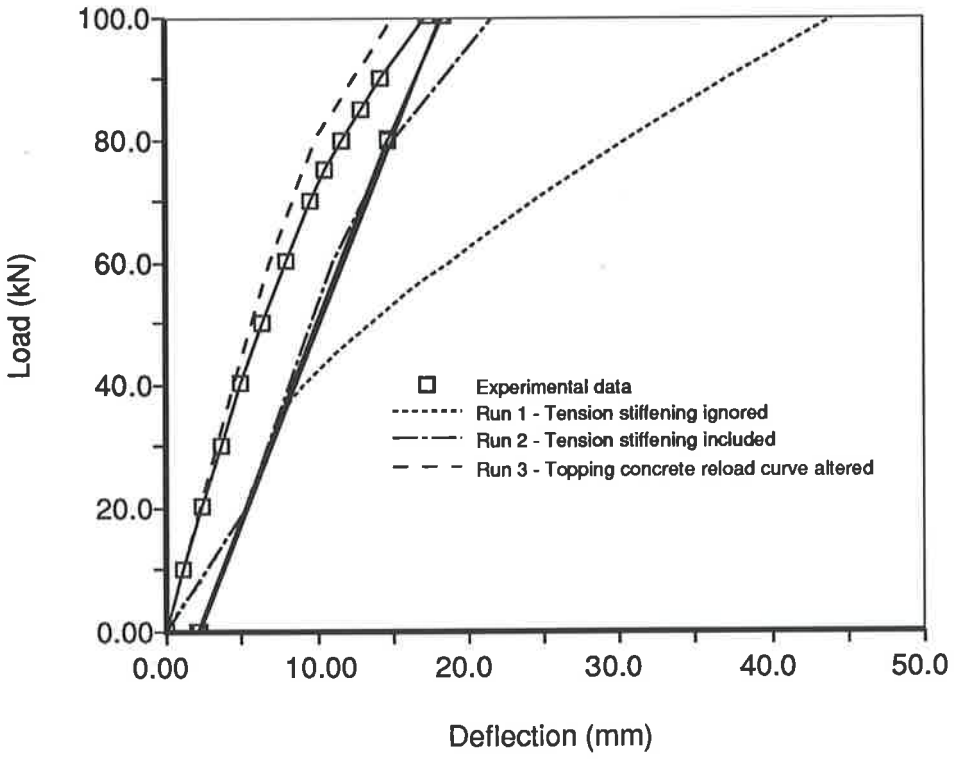

Figure 4.11: Load deflection curve for PA10NT1 - Load range 0-120kN

accuracy. Inspection of the initial loading shows that the predicted deflections move suddenly away from the measured deflection curve, but subsequently increase with the same slope.

The initial drop is produced when the cracks in the topping concrete, which were predicted to form, close up. When the topping is added at an early date, as with PA10NT2, no cracks form and this effect is not observed. Several possible explanations were considered to explain why evidence of the cracks closing was not observed in the experimental data. These are:

- Some type of "tension stiffening" effect.
- Non-linear creep effects were excluded from the analysis. When the ten-

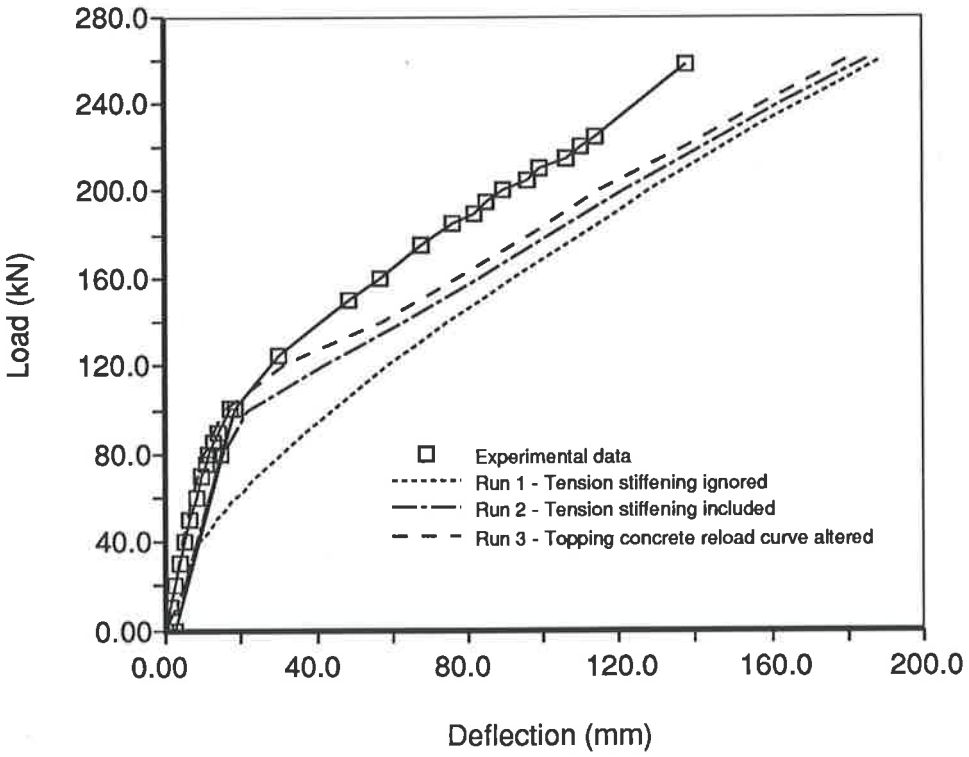

Figure 4.12: Load deflection curve for PA10NT1 - Load range 0-260kN

sile stress is above about half the tensile strength of the concrete, these effects will become significant and possibly affect the formation of cracks. Two factors are relevant, the first is that an increased rate of creep would decrease the tensile stress in the topping, the second that the ultimate strength under long term loading is likely to be less and cracks may form at a lower moment than was predicted [Domone (1974)].

The fact that the tensile strength of the topping concrete was ignored to enable reasonable predictions of the long-term deflections indicates that we do not understand exactly what is happening here.

- Incomplete closure of the cracks due to a mismatch between opposing crack surfaces and debris within the cracks. Foo (1986) reported observing this during fatigue tests of prestressed beams. While those cracks

formed in the bottom of the beam, the basic principle may still apply.

Although the reasons for the difficulty in predicting deflections when the topping is in tension are not clear, an attempt is made to allow for them. This is done by assuming a crack blocking mechanism, whereby the topping concrete starts taking stress as soon as it is reloaded, even if it is in tension. The stress-strain curve assumed is shown in Figure 4.13. Run 3 on the graphs shows the improvement in the initial stages of the loading as a result of this change.

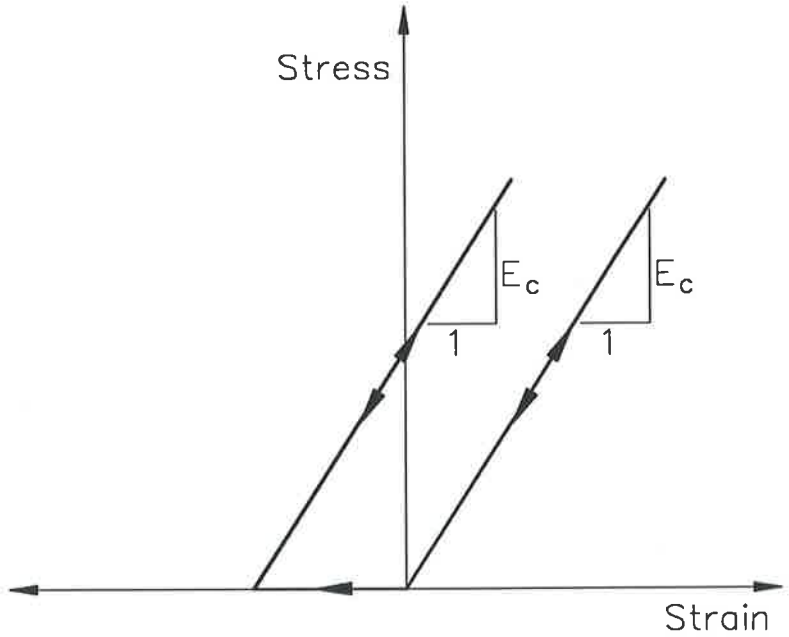

Figure 4.13: Topping concrete Stress-strain curve assumed for Run 3

The deflections at higher levels of loading are still inaccurate. Two possible causes for this are:

- The stress distribution across the beam is not correct. This might be caused by an inaccuracy in the modelling of creep and shrinkage.
- The method used to model the tension stiffening effect is inaccurate.

Of the two, the second is more likely to have a major influence on the problem.

This could be checked by using a different approach to modelling the tension stiffening effect.

4.5 Summary

Comparisons with test data have allowed the development of a method which provides reasonable predictions of the long-term deflection of partially prestressed beams. A reasonably quick solution time is achieved through the use of a closed form solution technique to find the strain distribution on a section.

The experimental data on both long-term and live load deflections indicated the importance of accounting for cracking in the topping concrete. The limited data made it difficult to determine the processes occurring in the topping concrete, however methods were obtained which provided reasonable predictions of the behaviour. These effects were only of importance when the topping concrete was added at a relatively late date, however ignoring them could sometimes lead to a significant error.

In the next two chapters, further verification of the method is sought through comparison with test data. This needs to be done before the method can be used in the design of beams. In addition, as the test data is from relatively short span beams (7700mm. to 10000mm.), it would be desirable to obtain some data from longer span beams to ensure that the behaviour observed, applies over the full range of spans.

Chapter 5

Gawler Beams

In order to provide further verification of the computer program, four fully prestressed planks were monitored from the time of casting in July, 1988. Data are still being collected. These beams were designed by the Highways Department of South Australia for use in a bridge over the Gawler River. A topping slab was subsequently cast over them. As the planks are fully prestressed, the measured camber is larger and the percentage error smaller. The large camber also provides an opportunity to obtain data for planks undergoing significant deflection changes with time. In addition, access to the underside of the plank is fairly easy, meaning that deflections can be monitored over a period of several years if this is desired.

5.1 Details of Gawler Beams

5.1.1 Beam Cross Section

The beams, which have a span of 7.7 metres, have the cross-section shown in Fig. 5.1. Four planks out of a series of seventy six cast were chosen to be monitored. These planks were poured at around 2 p.m. on the twenty seventh of July, 1988. The weather conditions at the time were cool, overcast and dry, with a temperature of around 15°C.

After casting, the planks were steam cured overnight at a temperature of around 70°C. Casting of the planks occurred at Hy-Stress Pty. Ltd., an Adelaide precasting works.

5.1.2 Properties of Prestressing Strand

The prestressing steel came from a coil of 12.7mm strand supplied by BHP. The test results supplied by BHP for the strand were assumed to be accurate, so no tests were performed.

5.1.3 Concrete Properties

Concrete used in the planks was mixed in a batching plant at the prestressing works. Standard compressive strength cylinders (150mm. diam. × 300mm. length) were taken from the pour. The cylinders were placed under the covers and steam cured with the planks.

The strength of the cylinders was obtained at various ages and is shown in Table 5.1. As this project is ongoing, some cylinders remain to be tested at a

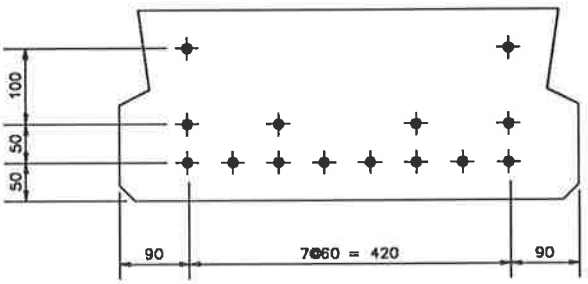

STRAND DETAILS
φ12.7 mm SUPER GRADE LOW RELAXATION STRAND
INITIAL PRESTRESS SHALL BE 147 kN per STRAND
SCALE 1:10

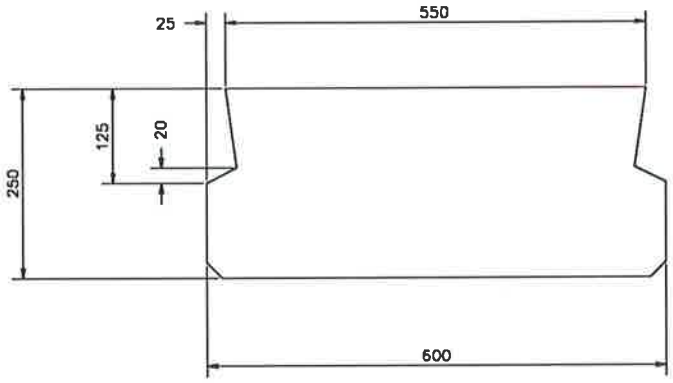

CROSS SECTION OF GAWLER BEAM
SCALE 1:10

Figure 5.1: Cross section of planks used in Gawler Bridge

later date.

Age of Concrete (Days)	Strength (MPa)	E (MPa)
1	38.4	—
7	50.9	40200
28	61.8	—

Table 5.1: Strength of plank concrete

In addition, three cylinders had demec points placed on them and are being used to determine the shrinkage properties of the mix. A further three cylinders were placed in a creep rig and loaded to about $0.4f'_c$ so that the creep characteristics could be determined. These cylinders were loaded at an age of about seven days.

The bridge planks were stored outside, so to ensure that temperature and humidity effects were similar in the planks and cylinders, the cylinders were stored in an exposed position.

5.2 Details of the Test Program

As the planks came from part of a production run and were placed into a road bridge, the range of data which could be collected was restricted. The most important information was the deflection readings which were obtained using precision levels from points on the top of the beam. After the beams were placed into the bridge, these points were transferred to the underside of the beams, so that deflections could be collected after the topping was poured.

To gain an indication of the effect that the temperature profile was having on the deflections, it was decided to place some temperature probes in the planks. Small semiconductor probes were used, which, after calibration, should have

an accuracy of $\pm 0.1°C$. Readings from these probes were taken whenever the deflection of the bridge was obtained.

One probe was placed near the bottom of the section, and one near the top, to give the difference in temperatures across the section. In general the temperature profile is not linear.

Deflection readings were usually taken in the early morning, before the sun had struck the planks, to minimise the size of any thermal gradient across the beam. Under these conditions, the assumption of a linear stress distribution would not introduce a significant error.

5.3 Load History

The load history of these beams was complicated by the preloading which was carried out during storage of the planks, in order to reduce the creep-induced increase in camber. About two and a half weeks after the beams were poured, a point load was placed at the midspan of the beams. To enable the computer analysis of these planks, phase 1 of the load history was adapted as follows:

Phase 1(a) Creep and shrinkage occur in the plank under the effect of self-weight and prestress.

Phase 1(b) The plank is preloaded by a point load at the midspan.

Phase 1(c) Creep and shrinkage occur under the effect of self-weight, prestress and the point load.

Phase 1(d) The preload is removed prior to the plank being transported to the bridge.

Phase 1(e) Creep and shrinkage continue under self-weight and prestress.

Changes were accordingly made within the computer program CAMBER. Few major changes are required as the analysis remains basically the same, however a different moment distribution is applied over some of the time intervals. The additional input data required are the time at which the preload is added and removed, the size of the preload and the moment distribution which the preload introduces into the beam.

As a result of the preloading, the assumption that total strain is always increasing will be violated. The assumption of linearity of creep strains is thus less accurate [Bažant (1982)], and the error in any predictions is likely to be somewhat larger, than for the other tests.

5.4 Test Results

5.4.1 Deflection History - Day one

Deflections recorded during the first day of the planks' life show a rapid increase as the thermal gradient produced by the steam curing dissipates. The measured deflections and the thermal deflection predicted from the temperature measurements are shown in Fig. 5.2. The difference between the predicted deflections and the measured deflections can be largely explained by the temperature gradient.

5.4.2 Long-Term Deflections

Using the experimental data on long-term deflections obtained by Leong et.al. (1987), a method for predicting deflections is developed in Chapter 4. This method is also used to predict the long-term deflections of the planks from the

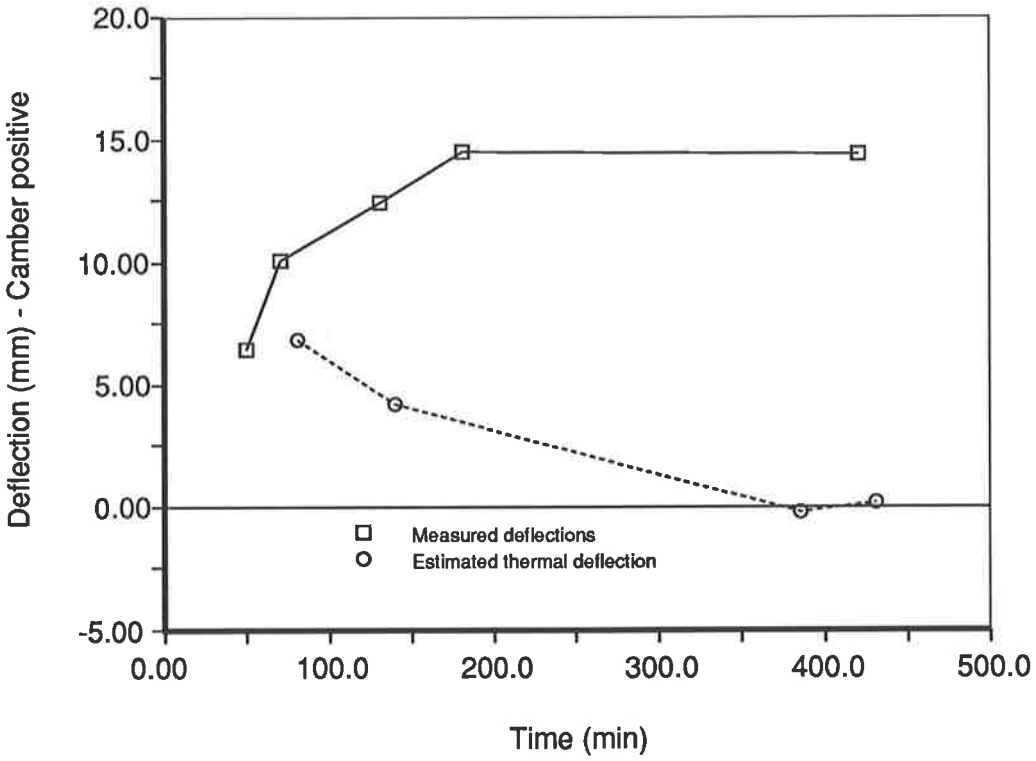

Figure 5.2: Total and thermal deflections in Gawler planks

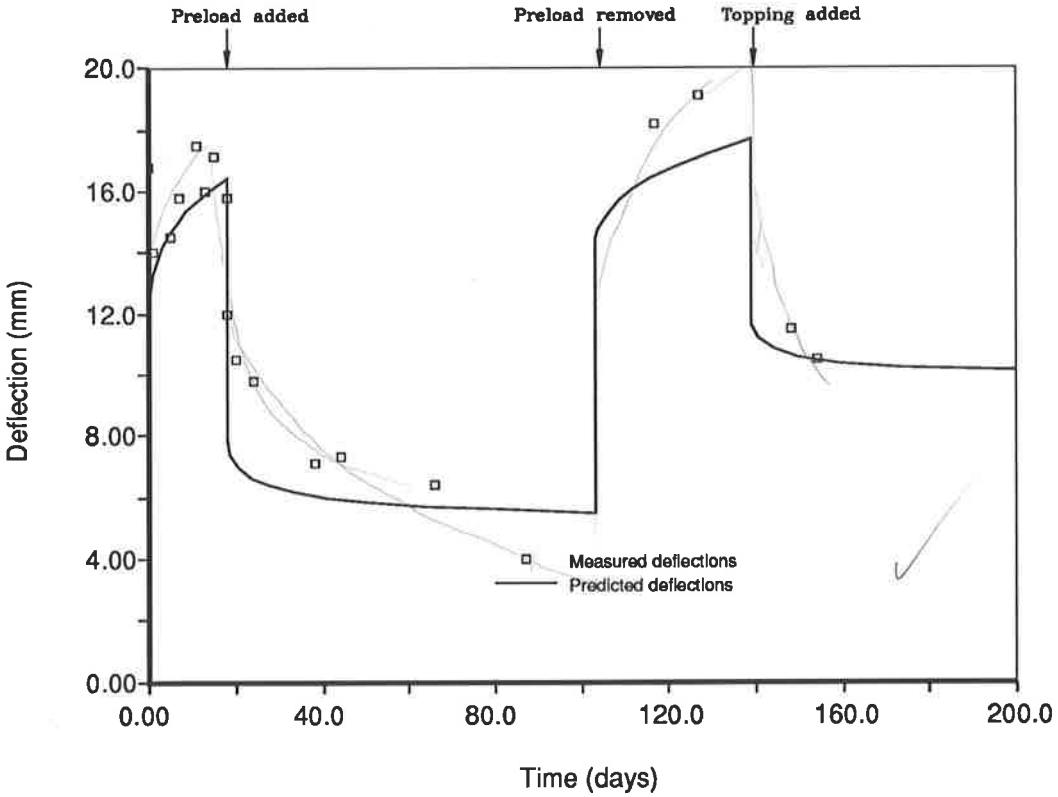

Figure 5.3: Long-term deflections measured on Gawler planks

Gawler bridge. A graph of measured deflection versus predicted deflections is shown in Fig. 5.3.

Deflection values shown on the graph, before the removal of the preload, are the average of the deflections from four planks. During transport to the bridge site, one of the reference points was lost, so future readings are the average of only three planks. The results are considered to be very satisfactory.

The values of deflections measured on individual planks were scattered over a range of several millimetres. This confirmed the assumption made earlier that the predictions will have a maximum accuracy of a few millimetres, because of random variations during the manufacturing process and inaccuracies in the experimental technique.

It is interesting to note that the unloading of the beam did not introduce a particularly large error, in spite of the inability of the step-by-step method to model unloading well.

Chapter 6

Moama Bridge Load Test

During 1988, a bridge over the Murray River flood channel at Moama was built out of prototype, partially prestressed, composite beams. The bridge consists of thirteen spans of either 9.2 metres or 8.9 metres, the arrangement of which can be seen in Fig. 6.1 which shows the general layout of the bridge. The plank cross-section is almost identical to that of the PR series of planks used in the laboratory tests, the only difference being the addition of two Y20 bars in the top of the section and the placement of shear steel along the full length of the beam.

To learn something about the behaviour of composite, partially prestressed planks within an actual structure, a load test was performed on the bridge. The information gathered during the load test is presented within this chapter, along with the procedures which were used to obtain the data and simple evaluations of the test results.

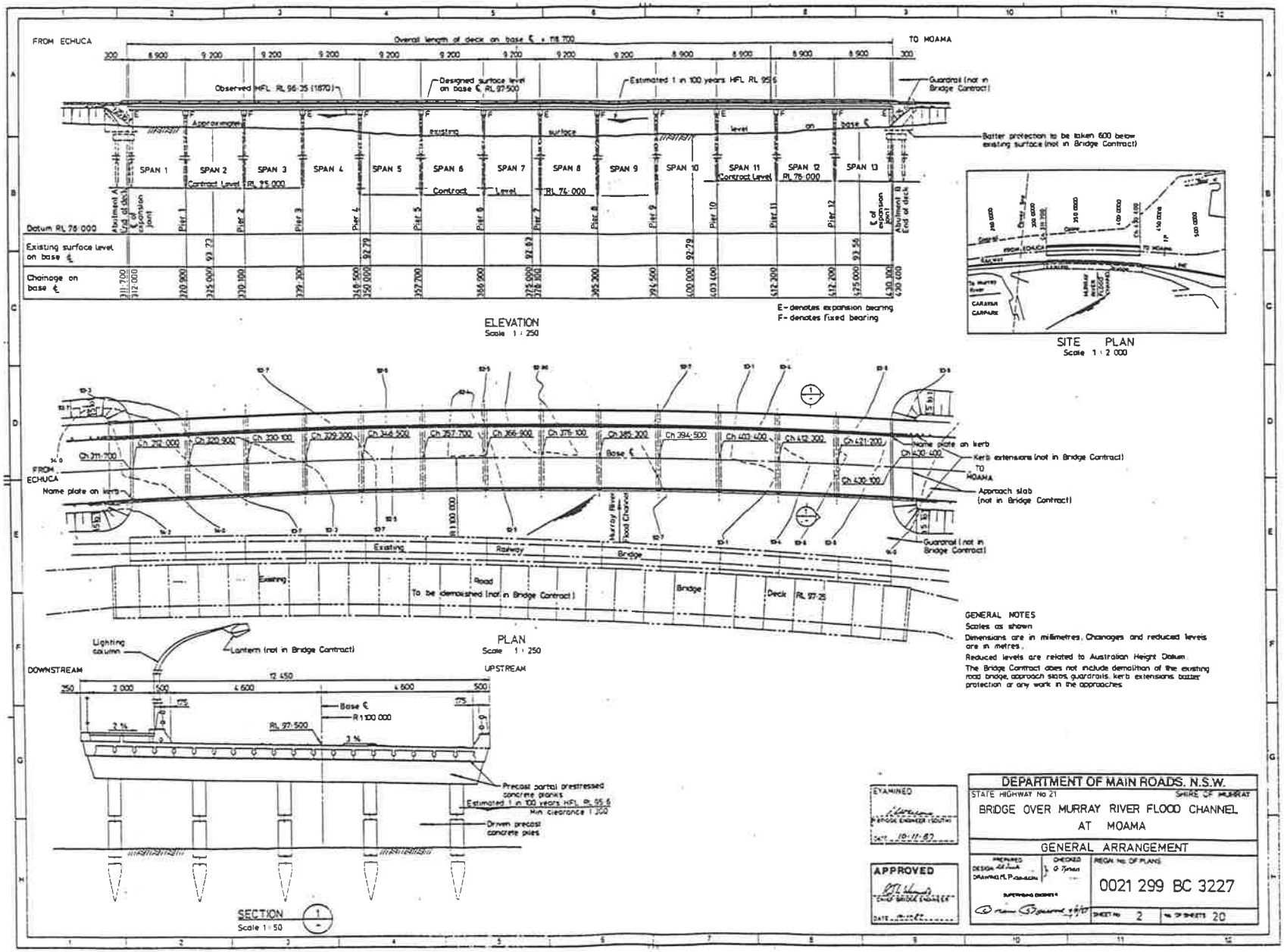
FROM ECHUCA
TO MOAMA
Overall length of deck on base ℄ = 118.700
Observed HFL RL 96.25 (1870)
Designed surface level on base ℄ RL 97.500
Estimated 1 in 100 years HFL RL 95.6
Guardrail (not in Bridge Contract)
Batter protection to be taken 600 below existing surface (not in Bridge Contract)
SPAN 1
SPAN 2
SPAN 3
SPAN 4
SPAN 5
SPAN 6
SPAN 7
SPAN 8
SPAN 9
SPAN 10
SPAN 11
SPAN 12
SPAN 13
Contract Level RL 75.000
Datum RL 75.000
Existing surface level on base ℄
Chainage on base ℄
E- denotes expansion bearing
F- denotes fixed bearing
ELEVATION
Scale 1 : 250
SITE PLAN
Scale 1 : 2 000
Name plate on kerb
Kerb extensions (not in Bridge Contract)
TO MOAMA
Approach slab (not in Bridge Contract)
Guardrail (not in Bridge Contract)
Existing Railway Bridge
Existing Road To be demolished (not in Bridge Contract)
Murray River Flood Channel
Bridge Deck RL 97.25
PLAN
Scale 1 : 250
Lighting column
Lantern (not in Bridge Contract)
DOWNSTREAM
UPSTREAM
Base ℄
R1100 000
RL 97.500
Precast partial prestressed concrete girders
Estimated 1 in 100 years HFL RL 95.6
Min clearance 1.300
Driven precast concrete piles
SECTION
Scale 1 : 50
GENERAL NOTES
Scales as shown
Dimensions are in millimetres. Chainages and reduced levels are in metres.
Reduced levels are related to Australian Height Datum.
The Bridge Contract does not include demolition of the existing road bridge, approach slabs, guardrails, kerb extensions, batter protection or any work in the approaches
EXAMINED
APPROVED
DEPARTMENT OF MAIN ROADS, N.S.W.
STATE HIGHWAY No 21
SHIRE OF MURRAY
BRIDGE OVER MURRAY RIVER FLOOD CHANNEL AT MOAMA
GENERAL ARRANGEMENT
DESIGN
CHECKED
DRAWING
REGN. No. OF PLANS
0021 299 BC 3227
SHEET No 2
No OF SHEETS 20

6.1 Details of Bridge

The bridge construction involved the placing of the planks between the piers, before pouring topping concrete over the middle section of each span. This was done before pouring topping concrete over the supports to ensure that the planks are simply supported when the dead load due to topping is applied.

Two types of joints exist over the piers, between the planks. These are shown in Fig 6.3. As can be seen, the expansion joints will prevent the transmission of moment between planks at some of the piers, while a degree of continuity will be produced by the concrete topping at the other supports. The stiffness of these joints is unknown.

The bridge cross-section (See Fig. 6.1), shows the presence of three concrete parapets across the bridge's width. In the regions near these a significant stiffening effect will be exerted.

6.2 Experimental Methods

6.2.1 Temperature

As it was not practicable to place temperature probes within the cross section, less sophisticated methods were used to give some indication of the temperature profile across the beam.

Thermometers were used to measure the temperature of the top and bottom surfaces of the bridge during the load test. To reduce the effect of sunshine on the temperature readings, a polystyrene cover was placed over each thermometer and a thermal conducting compound applied to provide a better contact

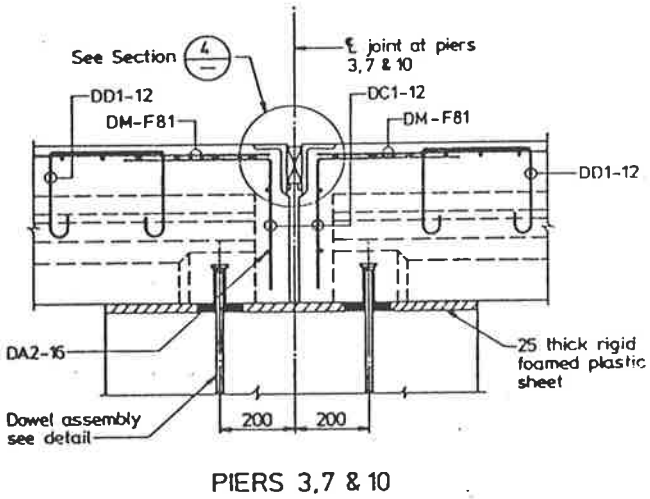

Figure 6.2: Detail of expansion joint

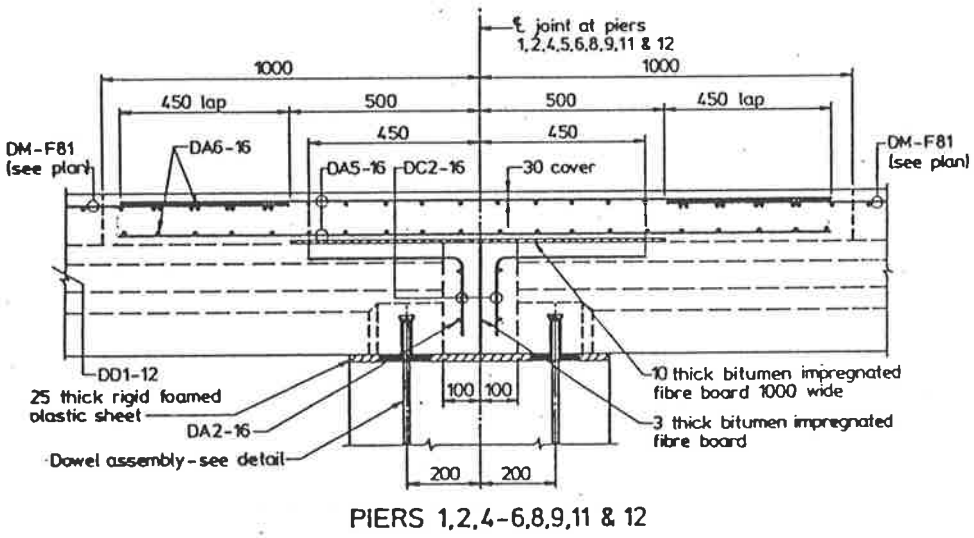

Figure 6.3: Detail of joint over piers

between the plank and thermometer.

Although the exact shape of the temperature profile across the bridge is unknown, knowledge of the top and bottom temperatures gives some data from which estimates can be made.

In addition, measurements of strain and deflection, with the bridge unloaded, were taken throughout the day. These provide an indication of the effect which the temperature profile had and allowed the values of strain and deflection to be adjusted to allow for the effect of temperature.

6.2.2 Strain

Demec points were placed on the top of the bridge at the locations shown in Fig. 6.4. The second span of the bridge was studied, strains being measured over each of the supports and at the centre of the span, giving readings from the regions of maximum negative and positive moments. Strains were measured at several points across the bridge in these regions, to allow the lateral distribution of strain to be determined. Three demec points were placed at each of these locations, allowing two separate readings to be taken and the results averaged.

On the underside of the bridge, demec points were placed at the midspan only. Scaffolding was required to reach the bottom of the bridge. As the scaffolding was placed off-centre to allow deflections to be obtained at the mid-span of the bridge, it was impossible to safely place or measure more than a single pair of demec points at most of the locations.

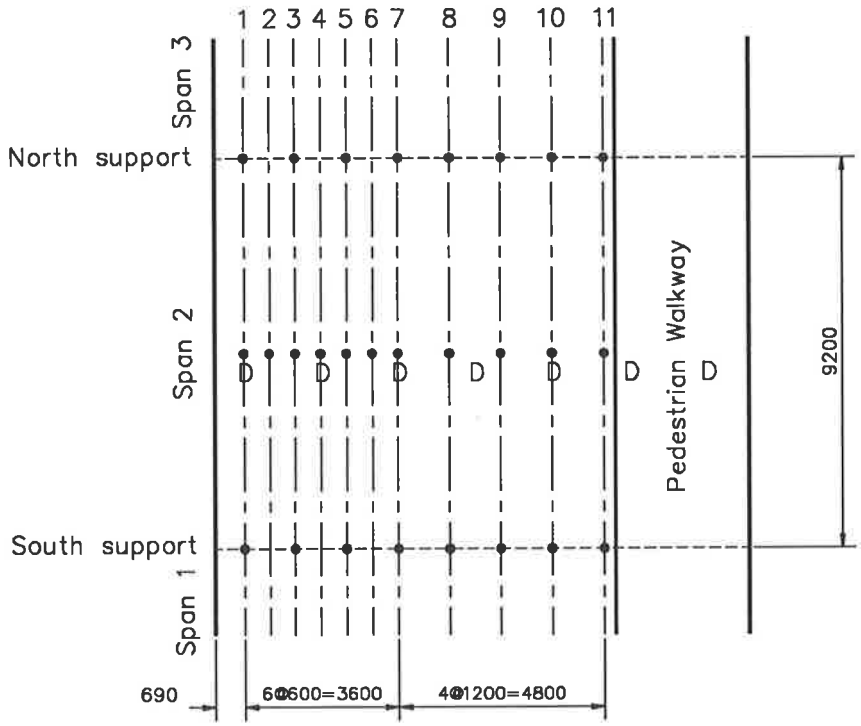

Figure 6.4: Layout of strain gauges for load test

6.2.3 Measurement of Deflection

Measurements were taken with a precision level of deflections at important times during the life of the beams as well as during load testing of the bridge. Results are shown in Figures 6.9, 6.11, 6.13 and 6.15.

6.2.4 Observation of Cracking

A visual inspection was made of the planks and topping, while the maximum positive and negative moments were being applied to the bridge. To aid in the detection of cracks, water was applied and the area watched while it dried, so that cracks could be spotted more easily.

When cracks were found, a portable microscope was used to measure the size of the cracks under the various load cases.

6.2.5 Loadings

Loading of the bridge was conducted using six trucks. The trucks had each been loaded with sand and weighed at a weigh-bridge before the tests commenced. Details of the truck weights and sizes are given in Table 6.1. In the table, 'A' refers to the distance between the front axle and the rear axle, 'B' to the distance between the front axle and the forward axle of the rear axle pair and 'C' is the distance between wheels, along an axle.

Four different patterns of trucks were used, allowing various aspects of the bridge's behaviour to be investigated.

Pattern 1 has the rear axles from all six trucks placed as close as possible to the centre of the span being tested. This produces the maximum positive

Plate 6.1: During test loading of bridge - Pattern #1

Plate 6.2: Measuring strains during load test

Truck		Load		A	B	C
Owner	Reg. No.	Front Axle (tonnes)	Rear Axle Pair (tonnes)	(mm)	(mm)	(mm)
Valuntas	FOB-083	5.080	14.300	4600	3300	1800
Leetham	ORO-328	5.160	16.300	4500	3150	1800
Buckley	MQX-081	4.300	15.100	4300	3100	1800
DMR	JMR-510	4.620	14.620	4700	3350	1800
Chapman	FSS-881	5.020	15.820	5700	4450	1800
Reddish	BAV-817	4.820	14.320	5400	4100	1800

Table 6.1: Trucks - Load and size information

moment which was possible using these trucks. The test was important as it provided information on the size of cracks formed under a large live load, as well as information on deflections.

Pattern 2 puts the rear axles from three trucks into the centre of one span, while the rear axles of the other three trucks are in the centre of an adjacent span. A large negative moment is produced under this loading, allowing the presence of cracks over the support to be investigated. In addition, this loading provides information about the behaviour of the joint. The behaviour of this joint must be understood, if the correct assumptions are to be made in the design of individual planks for these bridges.

Pattern 3 used only two trucks which were placed at the east edge of the bridge, with both of their rear axles near the centre of the span. This test was designed to give information about the lateral distribution of load. The shear key is relied upon to transmit shear between planks, but it is difficult to say

how far the load from a single wheel will be transmitted.

Pattern 4 is similar to Pattern 3 but has the two trucks placed in the centre of the bridge.

6.3 Results - Long term deflections

The program CAMBER was used to produce predictions of the long term deflections of these beams. Figure 6.5 shows that the results were in error by around four millimetres. A check on the initial deflection using hand calculations, gives virtually the same deflection as that which was calculated by the program, suggesting that the error is in the input data.

An indication of the size of error needed to produce this difference can be gained by calculating the error needed in any one input to produce the measured initial value. The percentage errors required were a 10% error in the prestressing force, a 25% error in the initial Young's modulus or a 20% difference in the self weight of the concrete. Obviously, a combination of several factors would require smaller differences in each. An error of this size in the Young's modulus of the concrete is quite possible as a constant value was used for all of the calculations. The value in the plank at transfer could be significantly less than the value assumed, although this problem was not found to be significant with other experimental data.

This is what I said earlier about time dependency.

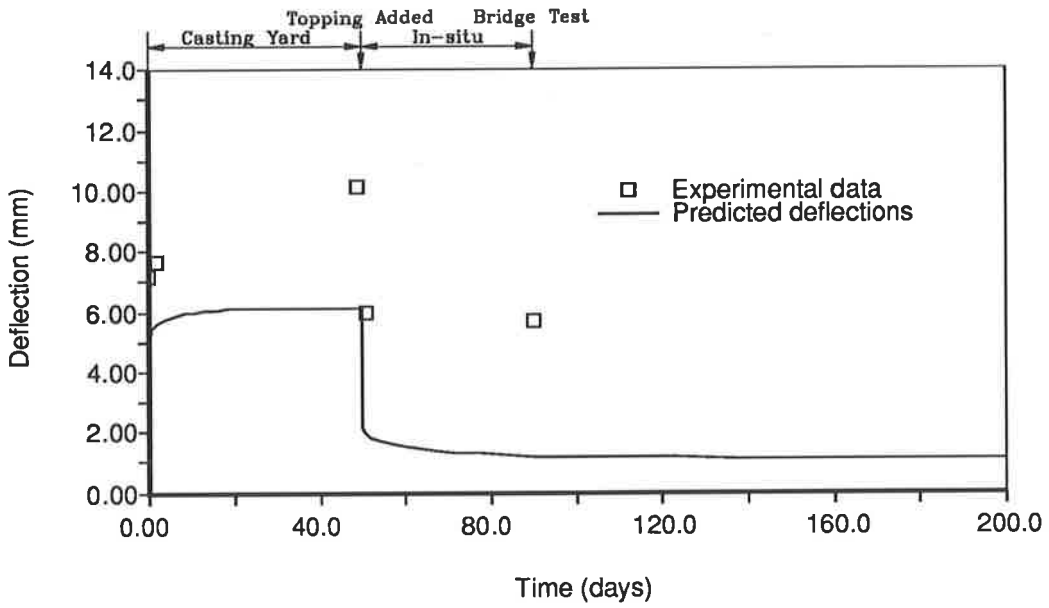

Figure 6.5: Predicted deflections vs. Experimental deflections - Moama Bridge

6.4 Live Load Test

6.4.1 Base Load

Readings of strain and deflection were taken with the bridge unloaded, to provide a series of references, which could be used to account for the effects of temperature on the strain and deflection readings. As it was only possible to collect temperature readings on the top and bottom of the beam, there was insufficient data to predict the thermal strains with any accuracy. For this reason, no attempt was made to predict these variations.

However, it is interesting to note that the total strains are generally compressive initially, but become tensile during the day. The averages of the values (See Fig. 6.7) show this effect most clearly, although it is also evident at most

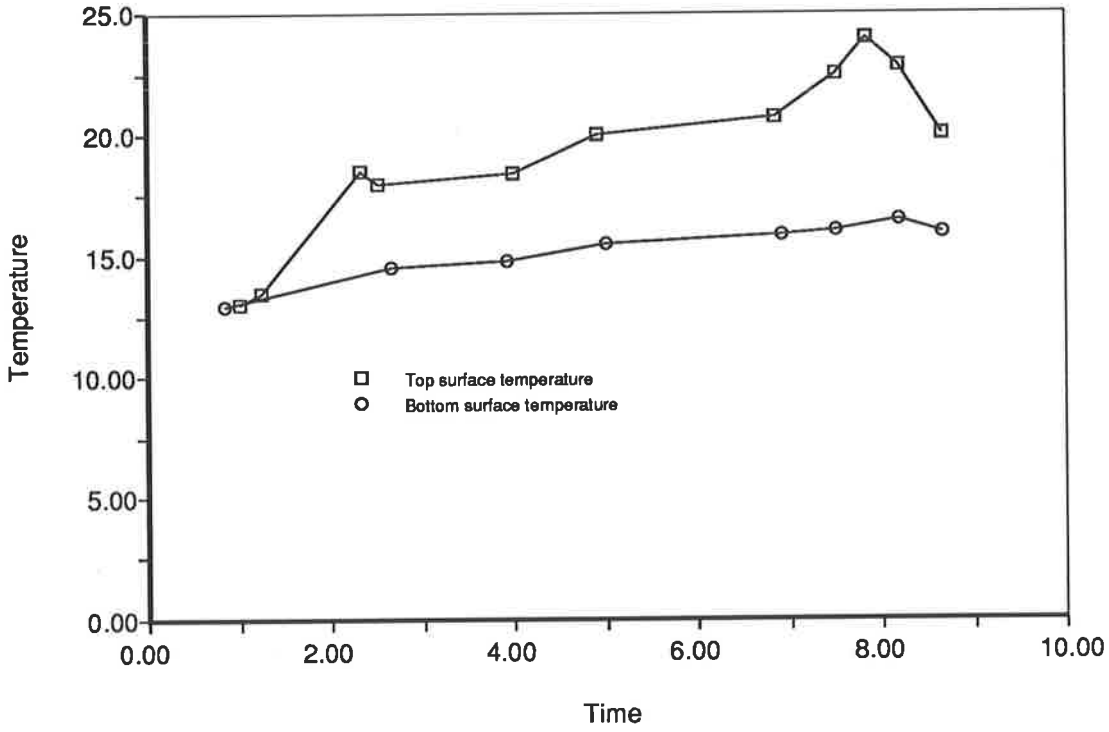

Figure 6.6: Temperature variation during the day

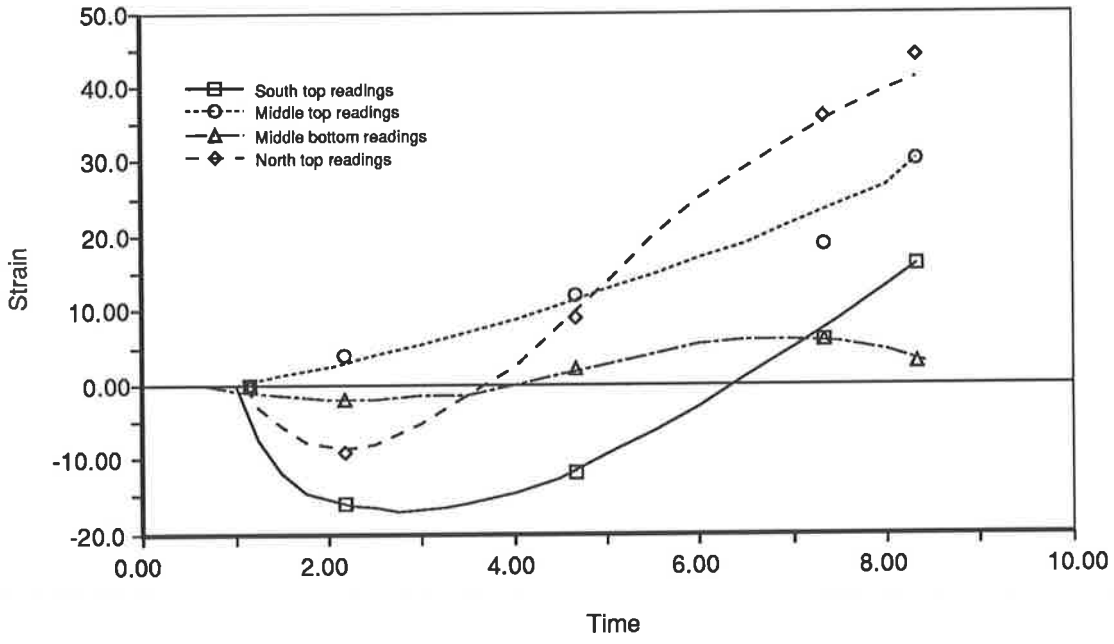

Figure 6.7: Average strain variation due to temperature at each set of points

individual locations. This is probably caused by the slow development of the temperature profile across the beam. Self-equilibrating stresses would produce compressive stresses in the top and bottom fibres as the temperature increased in these areas. As a linear profile becomes set up, the self-equilibrating stresses would decrease and the strain would become tensile as the effect of the inelastic tensile strain, produced by the temperature increase, becomes apparent. Results will be further complicated as stresses are produced by the hyperstatic reactions.

6.4.2 Live Loading

The following procedure was used to obtain a simple estimate of the strains which would be expected under live loads: The bridge was assumed to act like a three-span continuous beam, mounted on pin supports. As there are expansion joints at every third support, this assumption is not unreasonable. However, the support detail shown in Fig. 6.3 indicates that the stiffness over the piers is likely to be less than that of the rest of the beam, so this is a large simplification. Strains and deflections were also estimated by assuming the deck to be a simply supported beam between adjacent piers, however this approach proved to be extremely inaccurate.

For this simple analysis, Young's modulus was taken to be 40,000MPa and cracking was ignored, giving a linear, elastic material. Finally, lateral distribution of loads was assumed to be perfect. The strains measured on the bridge were divided by those estimated using this approach, the resultant factor giving an indication of both the lateral distribution of load and the accuracy of the analysis.

Graphs are presented for each of the load cases, demonstrating how this factor varies across the bridge. One axis of the graphs contains the factor described

above, while the other is the position across the bridge. Deflection readings were taken from every third beam, these being numbered MD83, MD85, MD93, MD84, MD86, MD94 and MD95. The distribution of strain gauges is shown above in Fig. 6.4. The numbering on the graphs, corresponds to the numbering of the strain gauges in the figure.

Load Pattern #1

The strain measurements from the top of the deck, all showed maximum values in the centre of the deck (See Figure 6.9). This is probably caused by the stiffening effect of the concrete parapets at the edge of the road. As these rise around 400mm. above the level of the deck and the deck is only 425mm. thick, they would have a significant stiffening effect near the edge of the bridge, and reduce strains near these locations.

Measured strains over the supports are somewhat higher than were predicted using the three span approximation. It is likely that the joints over the piers are less stiff than the deck, which would cause the strain measured over the piers to be larger. Another possible explanation is that there is some resistance to rotation at the expansion joints, which would cause in increase in moment at the supports, and a decrease at the midspan. This resistance could come from the connection to the piers. The fact that the measured deflection is lower than the predicted deflection, would also be explained by this.

No cracking of the partially prestressed planks was observed, although the beams were closely inspected while the load was applied. As this was the peak positive moment which could be applied using the trucks available, it was not possible to study the effect of cracks forming in the beams.

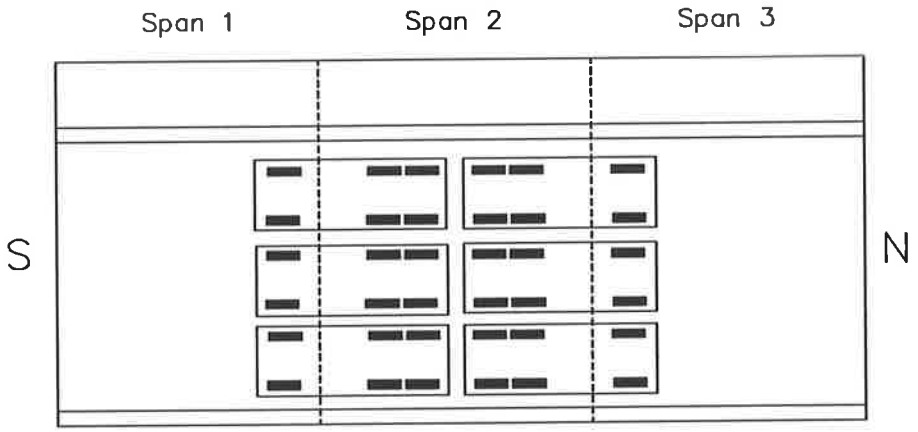

Figure 6.8: Load Pattern 1

Load Pattern #2

The results from this loading, shown in Fig. 6.11, are reasonable. It is again noticeable that strains are generally lower near the edges of the bridge. The predicted midspan deflection is, however, somewhat lower than was measured off the bridge. A possible cause for this, is the cracking which was observed to occur over the supports in the topping concrete, under the negative moment which was applied. These cracks would cause an increase in the deflections measured, as well as an increase in the moment at the adjacent support. Strains measured at the adjacent support were significantly higher than was predicted, indicating that the moment at the adjacent support was probably higher than predicted.

As the cracks did not form between any of the pairs of demec points, they did not have a direct effect on the strains measured. However, the cracks may have caused a drop in the value of strain measured at the North support, by reducing the strain in the concrete.

One curious aspect of this data is the large scatter evident in some of the

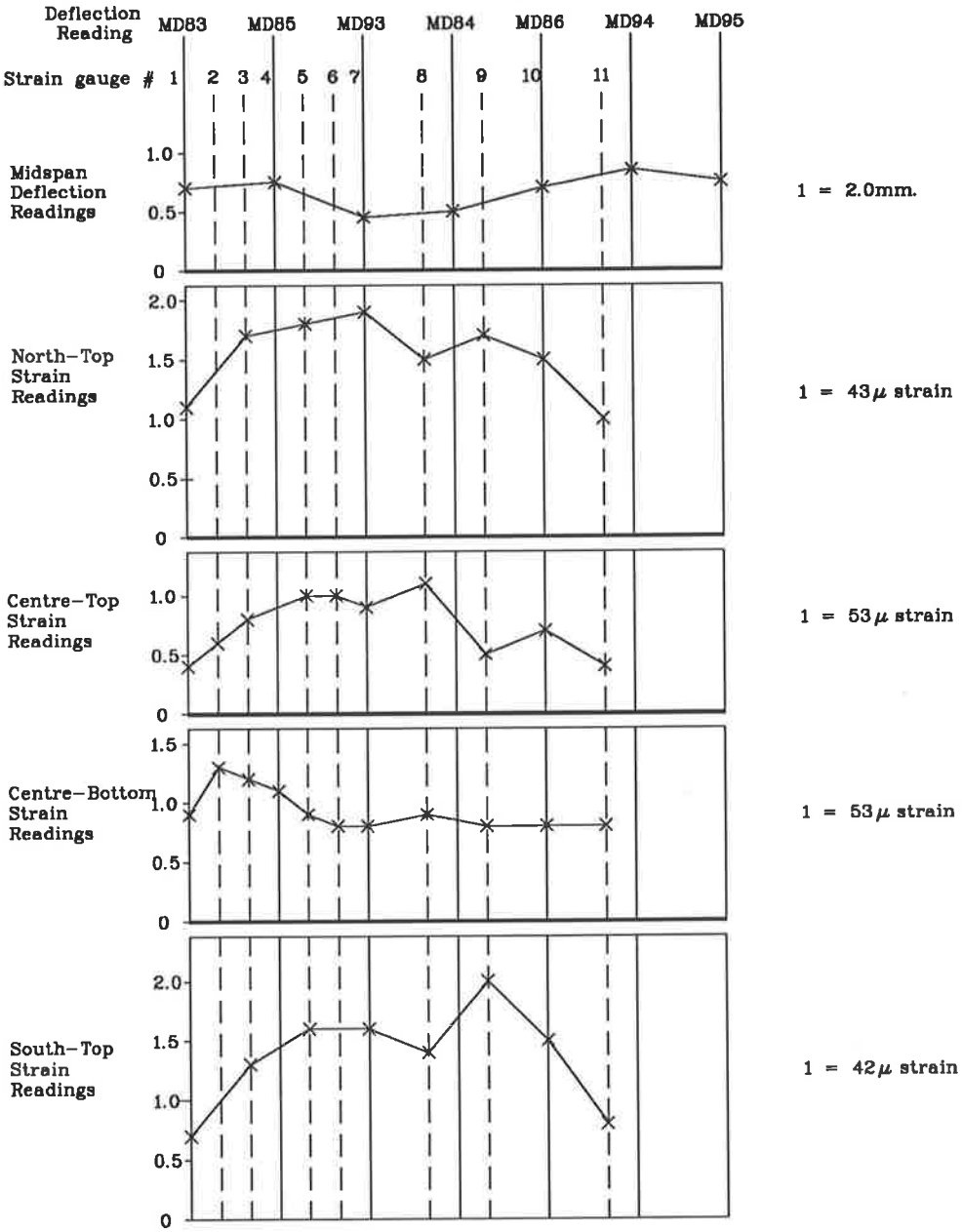

Load Pattern #1

Figure 6.9: Strains and Deflections measured during Load Pattern 1

values. The absolute value of the scatter with the "South top" readings, is only around 10 microstrain, which is reasonable, as it is only the small predicted value which, divided into the actual value, makes the error seem large. The scatter of the "middle bottom" values is somewhat larger, suggesting some other cause apart from random error. As this is the only loading where a line of truck wheels was across the demec points, it was thought that the loads might still be concentrated and not have spread out into the adjacent planks. However, the pattern of strains does not follow the pattern of the wheels, so this seems an unlikely explanation.

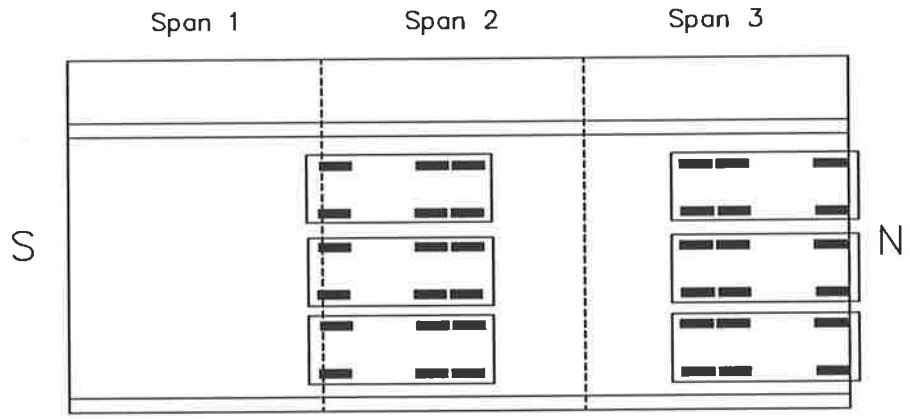

Figure 6.10: Load Pattern 2

Load Pattern #3

This test was designed to give an indication of the lateral distribution of load. Only two trucks were used in this test, so the strains were smaller, and the percentage error correspondingly larger.

Fig. 6.13 show the load to be concentrated to the side of the bridge where it is applied, tapering off to very small strains on the far side as would be expected. This trend is not as noticeable with the deflection data. However the predicted deflection is only 0.7mm, which is a similar size to the error expected from a

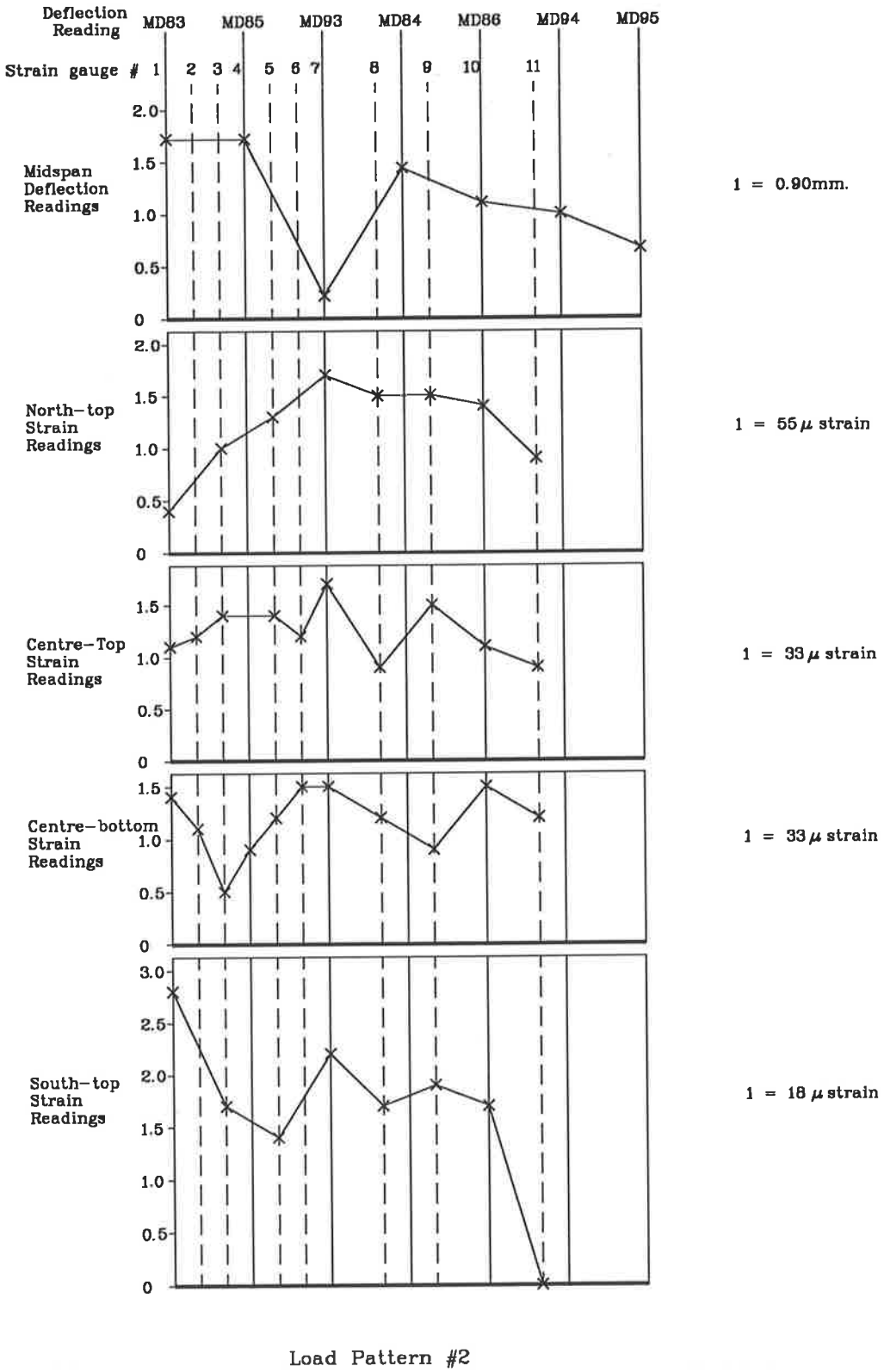

Figure 6.11: Strains and Deflections measured during Load Pattern 2

precision level under field conditions, so it is difficult to read anything into these results.

There some indication that the load is spreading out towards the supports, however the error again makes it difficult to reach a conclusion.

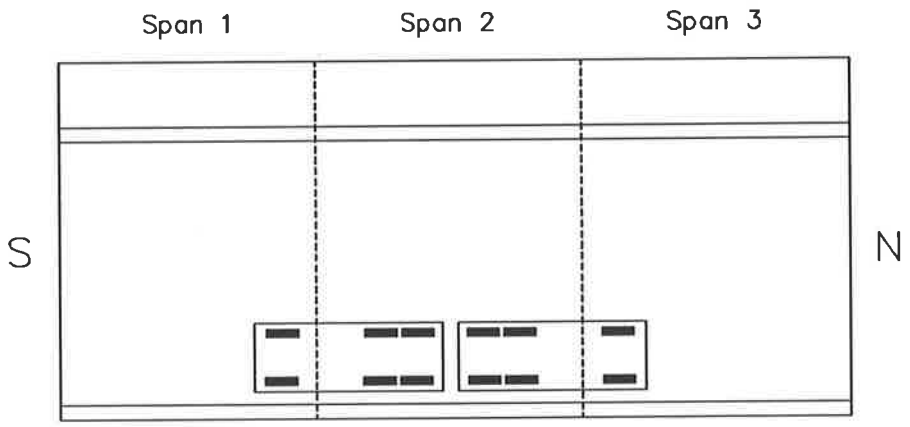

Figure 6.12: Load Pattern 3

Load Pattern #4

The only difference between the loads applied in patterns 3 and 4, is that the trucks are centrally located in pattern 4. As can be seen in Fig. 6.15, the strains are now at a peak along the centre of the bridge. However, the load seems to concentrate towards the ends of the span, which seems somewhat unusual, as the concentrated loading is at the centre of the span.

6.5 Summary

The live load test of the bridge demonstrated the beneficial effects of continuity on service load behaviour. No cracks were observed to form on the underside of the bridge planks and the measured deflections were significantly less than

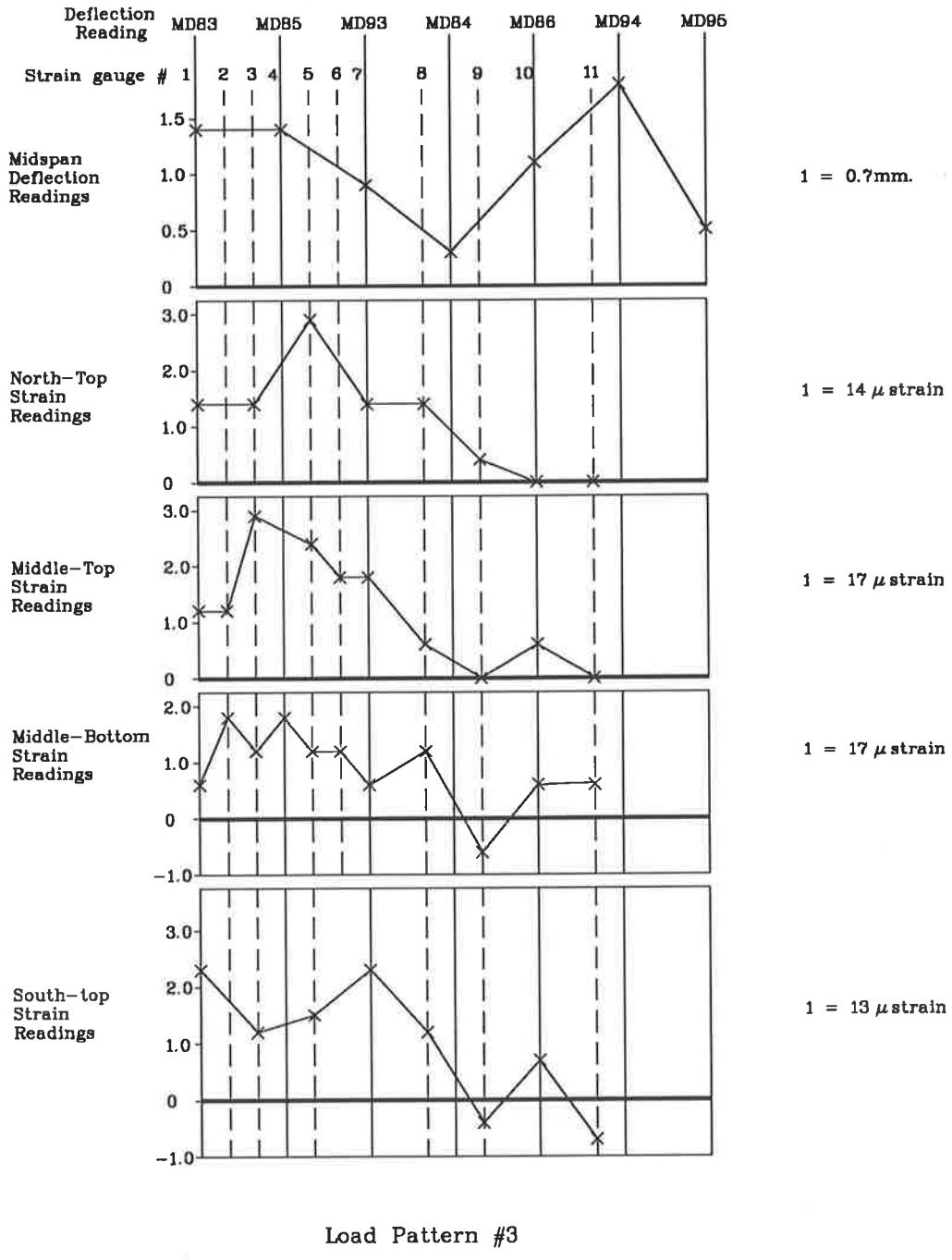

Figure 6.13: Strains and Deflections measured during Load Pattern 3

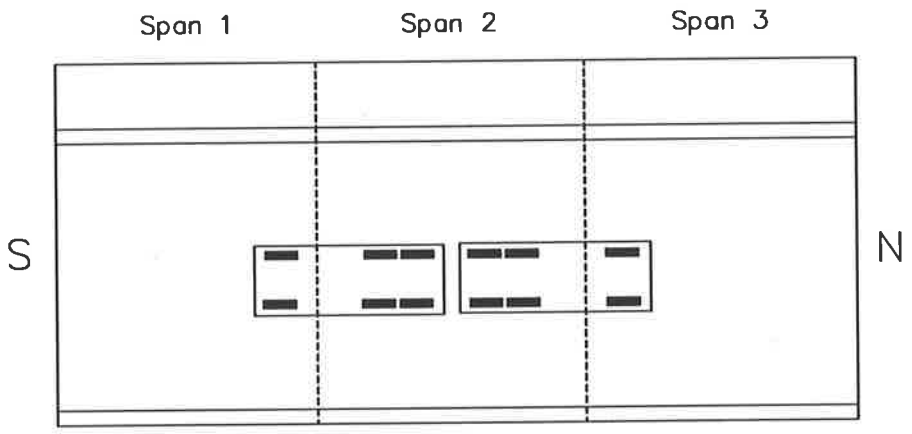

Figure 6.14: Load Pattern 4

those which had been predicted during design, using the assumption that the bridge was simply supported. Ignoring continuity during design is quite reasonable as it gives a conservative bound to the values of deflection and crack size. However, it does not indicate the size of cracks forming over the support.

Better agreement with the experimental results was obtained by considering the bridge to be continuous over three spans, this being the distance between expansion joints in the bridge deck. Lateral distribution of the load was not modelled.

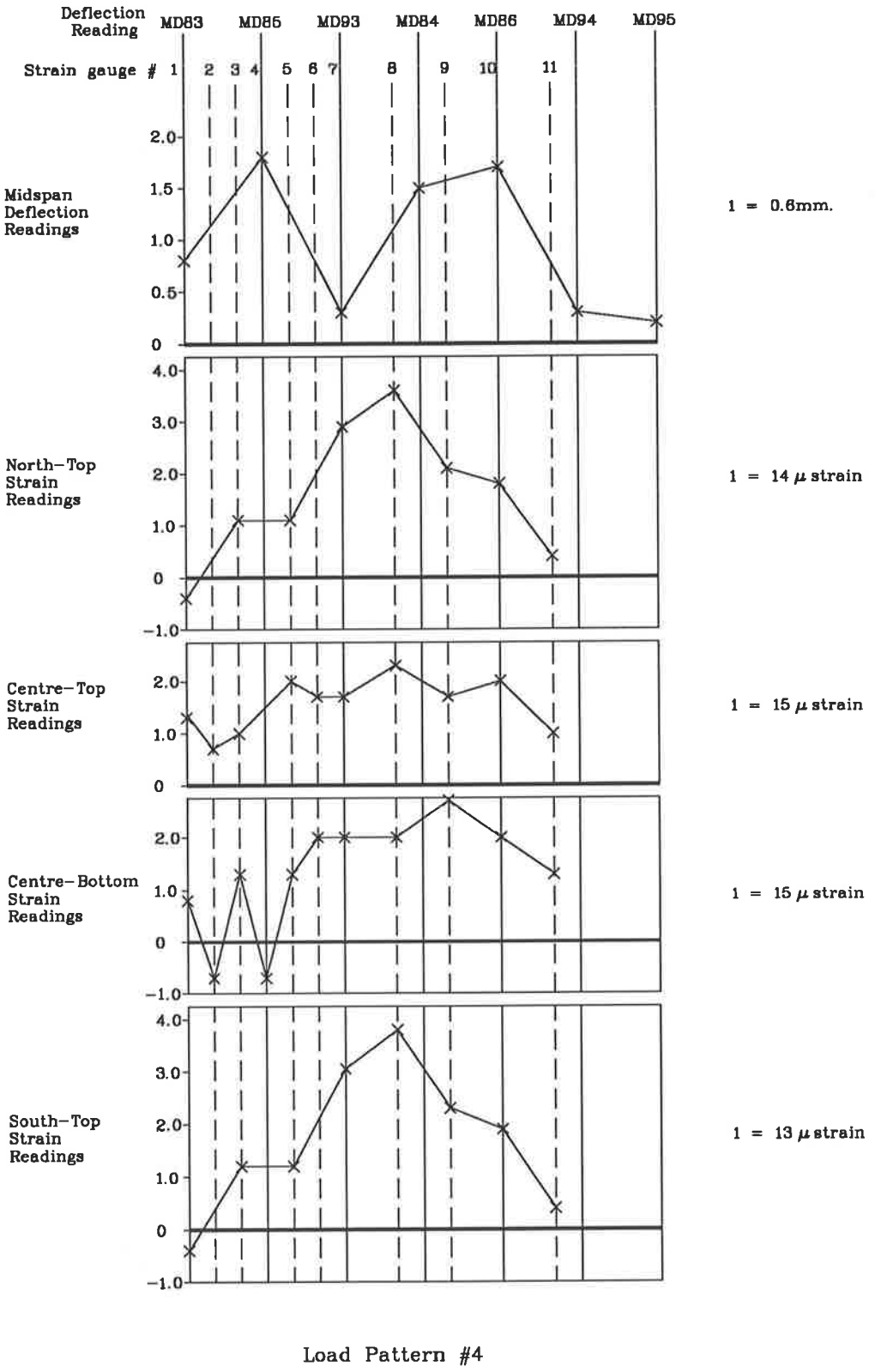

Figure 6.15: Strains and Deflections measured during Load Pattern 4

Chapter 7

Design of Composite Planks for Deflection Control

With the procedure available for predicting deflection at all significant stages of construction and service, it is possible to produce preliminary and detailed designs. In the present chapter, preliminary designs are carried out for progressively increasing spans up to twenty metres.

The designs have been carried out using the basic cross-sections currently used by the Dept. Main Roads, NSW. The resulting preliminary designs provide a means for checking the economy of the partially prestressed planks in comparison with the fully prestressed designs which are in current use. Another purpose for this work was to examine the feasibility of extending the plank designs up to twenty metre spans.

7.1 Choice of steel

Partially prestressed beams generally require more steel for ultimate moment purposes, than is required to provide the prestressing force in the section. Two approaches may be adopted to provide the additional steel, one adds additional non-prestressed reinforcement to the section, the other requires additional prestressing steel, but uses a lower level of prestress in each tendon.

Using mixed reinforcing and prestressing steel has the advantage that the section will be more ductile. In order to determine how important that may be for this type of beam, designs were produced containing mixed steel, as well as prestressing steel only. Once the designs had been prepared, values of k_u, the neutral axis parameter, were calculated to give an indication of the ductility of the section. Moment curvature plots were also produced for each section which allowed the calculation of another measure of ductility as the ratio of the curvature at the peak point to the curvature at yield [Naaman et.al. (1986), Kgoboko (1987)].

$$F = \frac{\kappa_p - \kappa_0}{\kappa_y - \kappa_0} \tag{7.1}$$

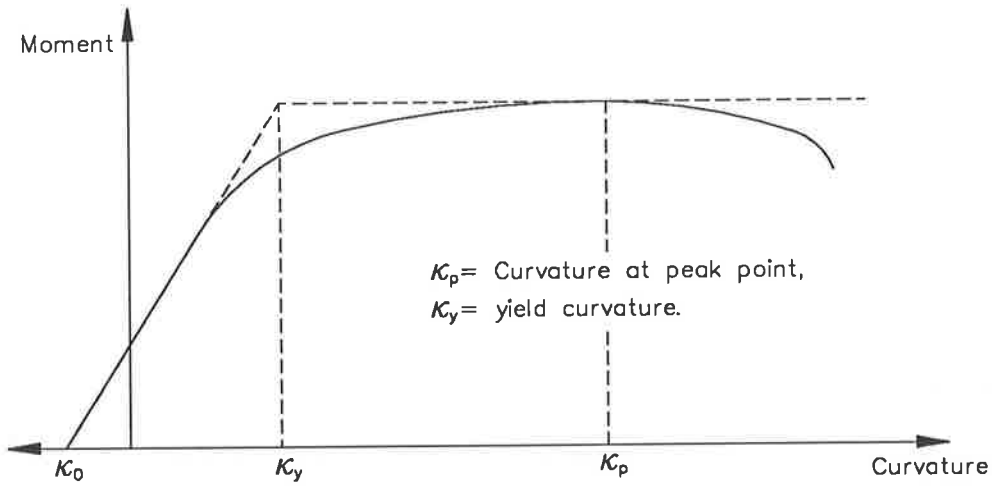

Figure 7.1: Peak and yield ductilities on a typical moment-curvature relation

Placing non-stressed steel into the section can also lead to a better control of

cracks. A rather indirect indication of this is given by the stress increment in the lowest layer of steel as the section is taken from the decompression moment to the service moment.

The main advantage in a design containing prestressing steel only, is one of economy. Various prestressing yards have indicated that they could place the steel for a design with no reinforcing steel faster. Any cost advantage from this would of course depend on many other factors. In addition, prestressing strand is presently slightly cheaper, on a pro-rata basis, than Y16 reinforcing bars.

Some steel is also needed in the top of the section to complete the shear cage. In these designs, prestressing steel was always placed here, as this allowed the overall level of prestress on the beam to be increased, reducing live load deflections, while not significantly affecting deflections under dead loads. One disadvantage of increasing the level of prestress is that a higher concrete strength is then required at transfer. Investigation of the relative cost advantages was beyond the scope of this project.

7.2 Design Criteria

The beams were designed in accordance with the Australian Standard for Concrete Structures AS3600 (1988) and the draft NAASRA limit state Bridge Design Specification (1987).

7.3 Design Procedure

In Chapter 2, design methods are reviewed and the approach which is used for preliminary design is chosen. This procedure is described here in detail.

1. The section depth can be estimated by choosing an uncracked section which is sufficiently large to control the allowable live load deflection increment. A good first guess of the section depth was generally obtained by increasing this value a little. The cross-section used was the standard cross-section used by the DMR.

2. The moment required to be applied by the prestressing force to produce a uniform stress distribution at the midspan of the plank, at transfer, is then calculated. The condition when only the dead load of the plank is acting was found to give good results, with the final prestress often being within a few percent of the initial estimate.

3. Two alternative steel arrangements are now determined, one contains only prestressing steel, the other contains mixed reinforcement.

   a) Prestressing steel only The amount of prestressing steel required can be calculated from-

$$A_p \geq \frac{M^*}{\phi f_{py} 0.85 d_p} \tag{7.2}$$

   where A_p = the area of prestressing steel (mm^2),

   M^* = the factored design moment,

   ϕ = safety factor = 0.8 for bending, and

   d_p = an estimate of the depth to the prestressing steel.

   The required stress in the steel can then be calculated from the moment found in the second part of the design procedure.

   b) Mixed steel The amount of prestressing steel required is calculated by assuming the steel to be prestressed to its maximum allowable value. The amount of additional steel required is estimated as:

$$A_{st} = \left[\frac{M^*}{\phi} - A_p f_{py}(d_p - 0.15 d_s)\right] \frac{1}{f_{sy} 0.85 d_s} \tag{7.3}$$

Prestressing steel was always added in increments of 200mm^2 as 12.7mm super strand (Area = 100mm^2 per strand) was being used and it was undesirable to place strands centrally in the section.

Reinforcing steel was assumed to be either Y16 or Y20 bars, again being added in pairs.

4. Steel was then arranged in the section and the ultimate moment checked using the actual steel arrangement.

5. The data was entered into the program Camber to allow deflection checks to be made. Once set up, steps 4 and 5 can be conducted fairly quickly giving suitable reinforcing details in two or three iterations.

6. Details such as the stress increment in the steel can then be checked.

7.4 Beam Designs - General

The design of the 12m. beam is shown on the following pages as an example. Details of the other beams, as well as the data used in the program Camber for the beams are contained in Appendix D.

Table 7.1 contains a summary of the calculated ductilities for the beams, which only shows small differences in the values calculated. To some extent this is caused by the relatively small amount of reinforcing steel in the sections, however the values of k_u indicate lower ductility in the sections containing mixed reinforcement. This does show the difficulty in trying to place a quantitative value on ductility.

Qualitatively, relative ductilities can be evaluated by viewing the moment curvature relations for the beams. This is done for several of the beams in Fig. 7.2 which shows that the beams with mixed reinforcement are slightly more ductile

Beam	Mixed Reinforcement		Prestressing steel only	
	k_u	F	k_u	F
12m.	0.32	6.38	—	—
14m.	0.32	5.33	0.31	5.20
16m.	0.31	5.21	0.30	5.00
18m.	0.33	5.16	0.32	4.59
20m.	0.35	4.71	0.33	4.71

Table 7.1: Calculated ductilities of beams

than those with only prestressing steel. The difference appears to be relatively small, so it is not a major disadvantage.

The beams are not predicted to crack under service loads making it unlikely that improved cracking behaviour will be of importance.

7.5 12m. Plank

1. **Deflections**

- At transfer 2.78 mm.
- Topping added at 28 days
  - Before addition of topping 4.97 mm.
  - After addition of topping 0.48 mm.
  - At 500 days -2.31 mm.
  - Under live load -13.66 mm.

Live load increment / span = $\frac{\Delta}{L} = \frac{1}{1057}$

- Topping added at 300 days
  - Before addition of topping 5.02 mm.

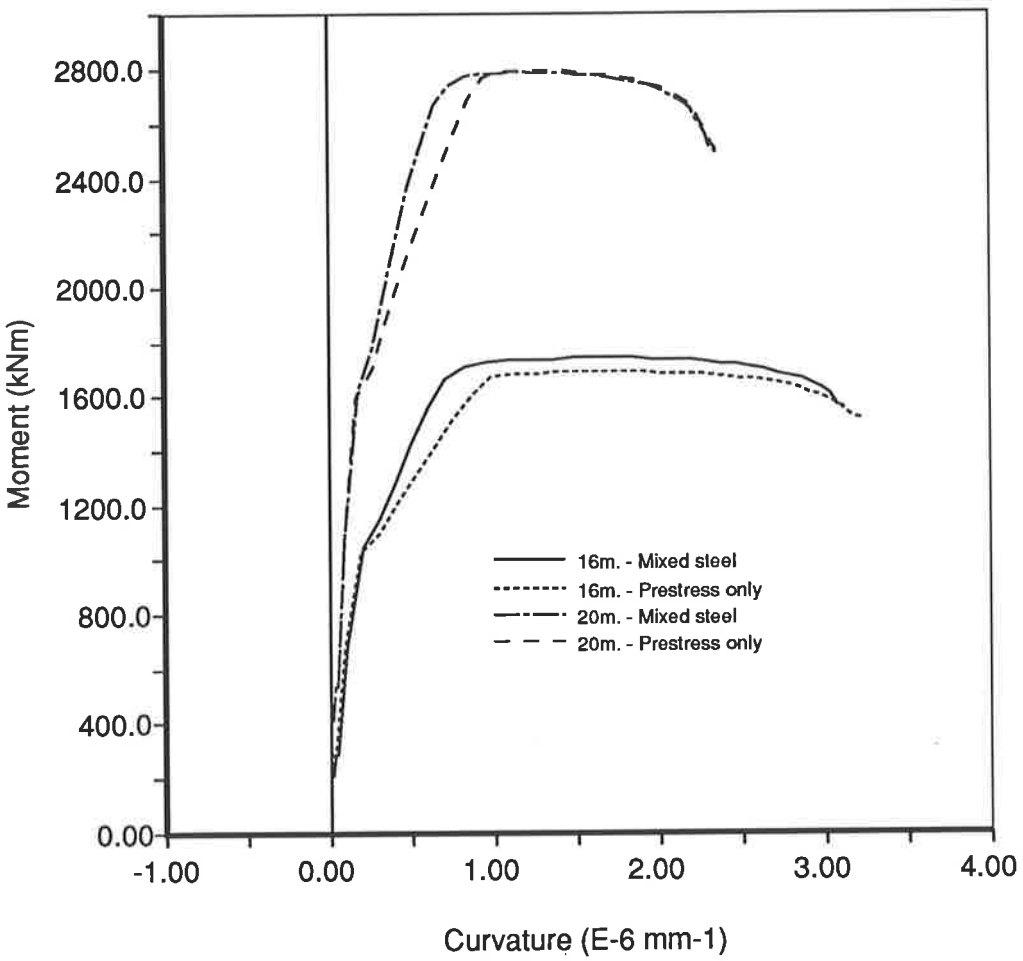

Figure 7.2: Moment-curvature plots for the 16m. and 20m. beam designs

After addition of topping	0.69 mm.
At 500 days	-3.61 mm.
Under live load	-16.94 mm.

Live load increment / span $= \frac{\Delta}{L} = \frac{1}{900}$

2. **Crack Increment**

   Crack Increment = 46.2 MPa.

3. **Ultimate Strength**

   - $M_u = 934\text{kNm}$
   - $\frac{\phi M_u}{M^*} = 1.05$

4. **Shear Details** Yet to be designed

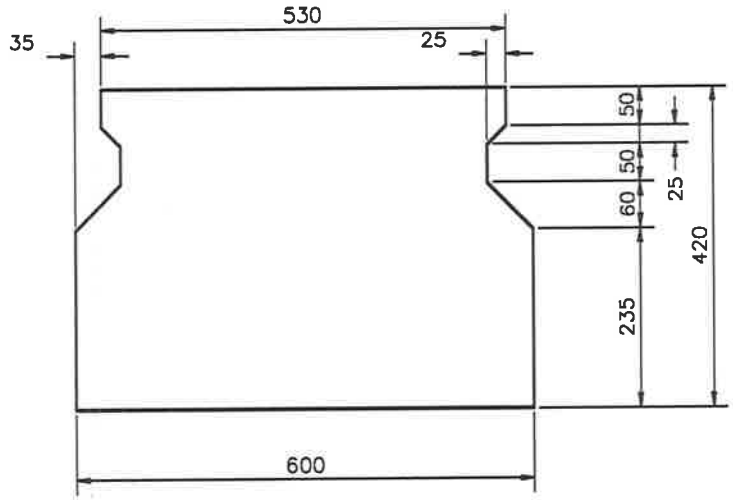

END ELEVATION
SCALE 1:10

The force in these strands at the midspan of the plank, immediately after the release of the tensioning jack shall be 139kN.

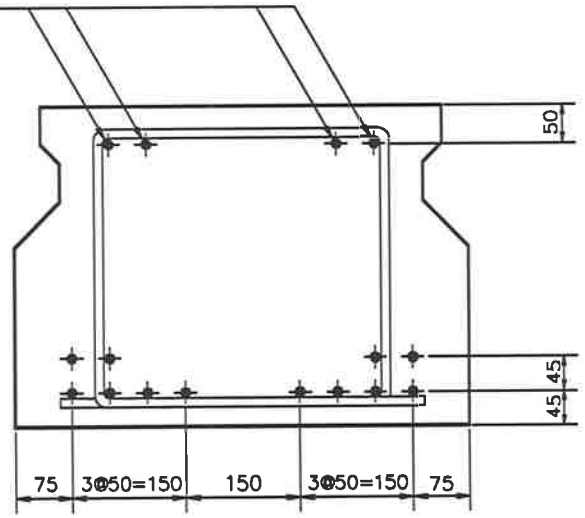

REINFORCEMENT AND STRAND DETAIL
16/φ12.7mm LOW RELAXATION SUPER GRADE STRANDS ✦
STRANDS SHALL BE STRAIGHT
SCALE 1:10

General Notes

Minimum 28 day strength of concrete shall be 40MPa.
Minimum compressive strength of concrete at transfer of prestress shall be 32MPa. Debonding could be used to reduce this.

The force in each 12.7mm strand, at the mid-span of the plank, immediately after the release of the pretensioning jack, shall be 128kN unless otherwise shown.

PRELIMINARY DESIGN	
12m. SPAN PARTIAL PSC PLANK	
DESIGN DRAWN	Sheet No. 1
DATE 24-11-88	No. of sheets 1

Chapter 8

Conclusions and Recommendations

8.1 Conclusions

The following conclusions were drawn as a result of the investigation:

- A computer based procedure was developed to predict long-term and short-term deflections of composite, partially prestressed concrete planks. The essential elements of the calculation procedure include:
  - Step-by-step method of creep analysis.
  - Linear stress-strain relation for concrete, with an allowance for cracking.
  - Ability to model tension stiffening effects if desired.

– Linear stress-strain relation used for the reinforcing and prestressing steel.

Using this procedure, predictions can be made to within several millimetres. Variations of this order are expected as a result of random variations in material properties, beam dimensions, etc. The error is acceptable and largely unavoidable.

While the procedure was designed particularly for use with bridge beams, it can also be applied to composite girders in other forms of construction.

- Without changing the basic analysis procedure, it is possible to account for the effects of continuity. The effect of continuity on the long-term deflection was small in the cases considered, so this was not required for the present study.

- An experimental program was carried out to obtain data on the long-term deflections of fully prestressed planks. The planks measured formed part of a road bridge.

- A live load test was performed on a bridge built out of composite, partially prestressed planks to investigate their behaviour under short-term loading. The long-term deflections of these beams were also recorded at important times in their history.

- The deflection calculation method was verified using three sets of test data. The results indicate that the program can predict deflections with a reasonable degree of accuracy.

- The formation of cracks in the topping concrete as a result of differential shrinkage was found to have a significant effect on both the short and long-term behaviour of the beams. While methods were developed which allowed reasonably accurate predictions to be made in spite of this effect, the exact nature of the process was not determined. This is one aspect which a future investigation could consider.

- For the bridge which was studied during the live load test, it was found reasonable to assume that the bridge was continuous at the supports, except where the bridge was interrupted by an expansion joint. The assumption made in the design of the beams, that they act as simply supported beams under live loads, was thus shown to be conservative, and some reduction in depth might therefore be possible. However, until more is known about the vibratory behaviour of these beams, this conservative assumption should be retained.

- ACI-209 (1978) creep and shrinkage curves, combined with predictions of the final values of creep and shrinkage from AS3600 [SAA, (1988)], were shown to provide sufficient accuracy for their use in design. The deflections predicted were relatively insensitive to the shape, or even the final values of the creep and shrinkage curves.

- The deflection prediction program was incorporated into a simple method for the design of composite, partially prestressed beams to give good deflection control. The method was used in the design of a series of beams for spans ranging from twelve to twenty metres.

8.2 Recommendations

The present study needs to be extended into a number of areas. Some of these are as follows:

- While it appears possible to reduce the depth of the beams to make an allowance for the effect of continuity, the dynamic behaviour of the beams would have to be investigated before this is undertaken.

- Before the preliminary designs of Chapter 7 are widely adopted, deflections from a set of planks with spans greater than about fifteen metres

should be monitored. In the present study there was no data available for planks with spans greater than 10 metres.

- The load factors used for the preliminary designs were obtained from the NAASRA Draft Bridge Specification and may vary in future drafts. For this reason, the designs are only preliminary and may well need to be revised.

- The computer program CAMBER should be generalised to allow for relaxation of the prestressing steel in members which are not steam cured and to account for the effects of continuity.

- Variations in ambient temperature during the day, were observed to have a large effect on short-term deflections. This effect should be studied as the next step in this project.

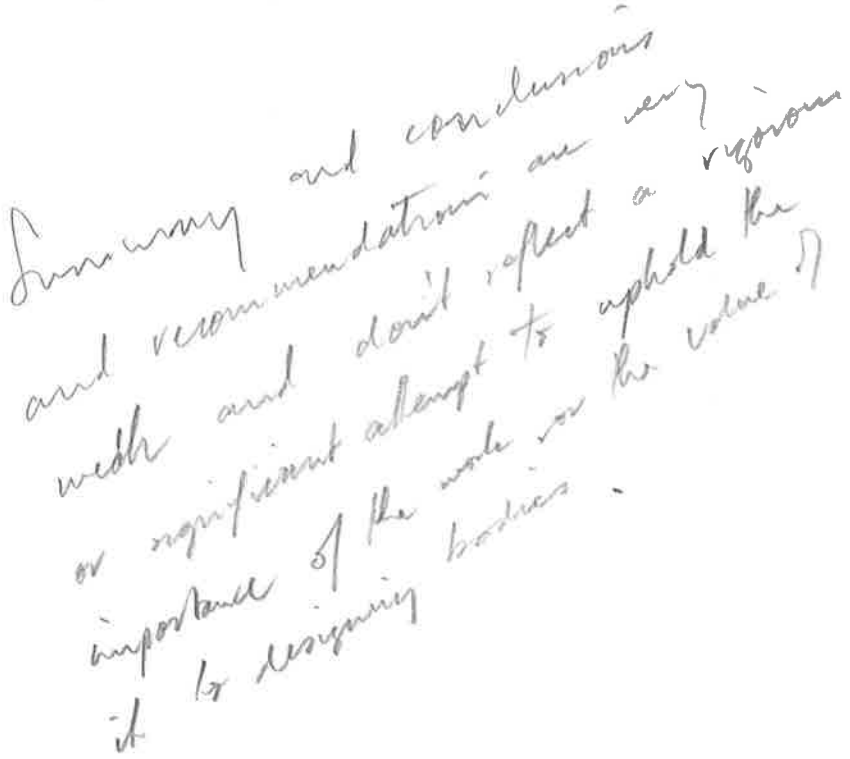

Appendix A

User Manual and Program Listing

A.1 Introduction

This appendix describes the use of the program CAMBER. It also contains information which may be useful to anyone involved in altering the program. The program is used to calculate the short and long term deflections of composite, prestressed concrete girders. These planks are cast in a prestressing yard, before being transported to the bridge site. At the bridge site they are laid side-by-side and a composite concrete layer is poured on top of them.

To account for this construction sequence, the analysis is divided into a number of phases and stages. These are as follows:

Stage 0 Stage 0 is the condition, just prior to transfer, when the concrete has

been cast around the tensioned tendon in the prestressing steel.

Phase 0 Stress is transferred into the plank as the jacks are released.

Stage 1 This is the state immediately after transfer when the self-weight of the plank is acting, but no creep or shrinkage have occurred.

Phase 1 Creep and shrinkage occur under the effects of prestress and plank self weight. This phase continues until TIME2 when the topping is poured.

Stage 2 Stage 2 is the state of stress and strain immediately before the topping is added.

Phase 2 Application of the topping. The plank is assumed to be unpropped so, after hardening, the topping concrete is in a state of zero stress.

Stage 3 Stage 3 occurs just after the hardening of the topping concrete. The girder is now composite, but only the plank is stressed.

Phase 3 Under the effect of prestress and full self weight, creep and shrinkage proceed in the plank concrete, and creep and shrinkage commence in the topping concrete. These processes continue until TIME4, which is a time just prior to the application of the live load. For the purposes of the analysis, TIME4 is taken to approach time infinity and further creep and shrinkage beyond TIME4 are considered to be negligible.

Stage 4 Stage 4 occurs after the creep and shrinkage processes are complete, immediately prior to application of the of the live load at TIME4.

Phase 4 Application of the live load, which is assumed to cause cracking of the section.

Stage 5 Conditions under the full service load (G+Q).

Phase 5 Loading to failure.

Stage 6 Conditions at high overload as failure is approached.

Full details of the method of analysis can be found in the reports DMR5 and DMR6 [Darby (1988a, 1988b)]

At present the program is running on a Sun 4 system. However it is intended to port the program onto an IBM computer in the near future. The program is written in Pascal. Use of the real data type on this system gives approximately sixteen digits of accuracy. The type is implemented using 64-bit IEEE floating-point format.

A.2 Input Files

Two separate files are required to start up the program on the Sun system.

A.2.1 Start-up file

Example

```
Moama Bridge Planks - PA10NT1
pa10nt1
```

Explanation

The first is a start-up file which is only two lines in length. This file is assigned to Standard input when the program is first run and tells the program where to go to find the rest of the data.

The first line contains a one line header which is placed at the start of each

of the output files. The second line should have the prefix from the data file name. For example, if the data file name is "DMR20.DAT" then the prefix would be "DMR20". The second part of the data filename must be ".DAT".

A.2.2 Data Files

Example

```
9600  40
40    30
20    0    2    0    9    125    20
0    0    600
124.999   0    600
125    530    0
175    530    0
200    480    0
250    480    0
310    600    0
405    600    0
425    580    0
0    0
800    380    600
200    335    600
23700    207900    191000    21530
47400000    21600000    77500000
1.85  4.80E-004   60   0.8500000238418579
2.69  5.25E-004   60   0.699999988079071
10    146
20    182
```

```
2     3     47     2E-003
2     3     35     2E-003
410      1770
0.60  20    1.00   55
0.60  20    1.00   35
```

Explanation

This file contains the information needed to run the program. It should have the following format:

length,numberofcycles	Length of span, Number of points to be used in the numerical integration. (Suggested value = 5)
fcp[1],fcp[2]	Characteristic strength of plank, topping.
nc,ns,np,nt,nr,topdep, slices	nc=number of slices into which the section is divided, ns=number of layers of reinforcing steel, np=number of layers of prestressing steel, nt=number of layers of steel in the topping, nr=number of points in the users's section description, topdep=depth of topping concrete, slices=nc
dpl[i],wpl[i],wto[i]	nr lines containing the section description, where dpl is the depth to the section being described, wpl is the width of plank concrete at this depth, wto is the width of topping at this depth.
circ[1,1],circ[2,1]	depth to void, radius of void. Should be 0,0 if there is no void in the section.

aas[j],ds[j]	ns lines containing the area of steel in the j^{th} layer and the depth to it.
ap[k],dp[k],sigp[k]	np lines containing the area of prestressing steel in the k^{th} layer, the depth to that layer and the prestressing force.
aat[m],dt[m]	nt lines containing the area of each steel layer in the topping concrete and their depth.
ec[1],es,ep,ec[2]	ec[1]=Young's modulus of plank concrete, es= Young's modulus of the reinforcing steel, ep= Young's modulus of the prestressing steel, ec[2]=Young's modulus of topping concrete.
mplank,mtopping,mll	The moment at midspan caused by the plank concrete, the topping concrete and the live load.
phistar[1],eshstar[1], x,y	The final creep coefficient, the final shrinkage strain and two numbers left for compatibility with older versions but no longer required.
phistar[2],eshstar[2], x,y	The same for the topping concrete.
m2,time2	The number of steps until the end of phase 2, and the time at which phase 2 ends.
m4,time4	The total number of steps until the end of phase 4, and the time at which phase 4 ends.
gamma1[1],gamma2[1], fcmax[1],ecmax[1]	Parameters for the non-linear stress-strain curve for the plank concrete.
gamma1[2],gamma2[2], fcmax[2],ecmax[2]	Parameters for the topping concrete.
fsy,fpy	Yield strength of reinforcing steel, Yield strength of prestressing strand.

ksi[i],daci[i], alpha[i],faci[i]	Parameters for the shape of the creep and shrinkage curves. See variable explanations.

A.3 Error Messages

The program may occasionally return an error message such as:

```
Warning: Convergence error in Mfind
```

This means that the program has been unable to find a solution within forty cycles of the iterative search. It is usually caused by an error in the data input producing a section where a solution is impossible. (For example - stressing the strand to 12500 MPa.)

It may also be possible for this error to occur when the solution converges very slowly. If this happens the number of steps allowed can be increased within the procedure where the error is reported.

A.4 Output Files

The program produces three output files from every run. Each file name will begin with the prefix given in the startup file. The suffixes used are ".dto", ".ot1" and ".ot2".

A.4.1 Data output (.dto) file

Explanation

The input data is echoed in this file in a more readable form. This is useful for checking the validity of input data, and for keeping track of what was done in a particular run.

Example

```
Moama Bridge Planks - PA10NT1
Date: 21 Sep 88
File: pa10nt1

Section details-                          Number of slices=  20
```

#	Depth	Plank width	Topping width
1	0.0	0.0	600.0
2	125.0	0.0	600.0
3	125.0	530.0	0.0
4	175.0	530.0	0.0
5	200.0	480.0	0.0
6	250.0	480.0	0.0
7	310.0	600.0	0.0
8	405.0	600.0	0.0
9	425.0	580.0	0.0

```
No void in section

                        Plank concrete     Topping concrete
```

Youngs modulus	23700	21530
Phistar	1.85	2.69
Eshstar	0.000480	0.000525
Tv	60.0	60.0
Alphad	0.85	0.70
alpha	1.00	1.00
daci	20.0	20.0
ksi	0.6	0.6
faci	55	35
gamma1	2.00	2.00
gamma2	3.00	3.00
fcmax	47.0	35.0
ecmax	0.002000	0.002000

Prestressing tendons-

Youngs modulus 191000

Yield stress 1770

Layer #	Depth	Cross sectional area	Initial prestress
1	380.0	800.0	600.0
2	335.0	200.0	600.0

Loading details-

Plank self-weight moment 47.4

Topping self-weight moment 21.6

Live load moment 77.5

Topping is added at t= 146.0 days

```
Final time is t= 182.0 days

 Number of intervals in the first time period=  10
Number of intervals in the second time period=  10
```

A.4.2 Analysis output (.ot1) file

Explanation

The results of the analysis of the mid-span section are output in this file. Output is structured using the phases and stages mentioned earlier in this report. Stresses in the top and bottom fibres, as well as the corresponding strains are reported in this file.

Example

```
Moama Bridge Planks - PA10NT1
Date: 21 Sep 88
File: pa10nt1

Phase 0 - Strains due to prestress only.
Time  Strain in top fibre   in    Stress in top fibre  Stress in
       topping    plank  bottom fibre  top  plank  bottom fibre
 0.00  --------- -0.000228    0.000264   ------    0.00    10.88

Stage 1 - Strains due to prestress and plank self weight.
  Plank moment= 47.4
Time  Strain in top fibre   in    Stress in top fibre  Stress in
       topping    plank  bottom fibre  top  plank  bottom fibre
```

0.00	---------	0.000062	0.000091	------	2.85	4.13

Phase 1 - Time march during phase 1 commences here.

Time	Strain in top fibre	in	Stress in top fibre		Stress in
	topping	plank bottom fibre	top	plank	bottom fibre
1.08	---------	0.000078 0.000107	------	2.86	4.08
3.76	---------	0.000106 0.000135	------	2.90	3.99
8.14	---------	0.000143 0.000171	------	2.94	3.88
14.54	---------	0.000189 0.000214	------	2.98	3.75
23.47	---------	0.000239 0.000261	------	3.04	3.61
35.66	---------	0.000292 0.000309	------	3.09	3.46
52.14	---------	0.000344 0.000357	------	3.14	3.32
74.39	---------	0.000394 0.000401	------	3.19	3.18
104.58	---------	0.000441 0.000442	------	3.24	3.05
146.00	---------	0.000482 0.000478	------	3.28	2.94

Stage 2 - End of phase 1

Phase 2 - Application of topping

Topping moment= 21.6

Time	Strain in top fibre	in	Stress in top fibre		Stress in
	topping	plank bottom fibre	top	plank	bottom fibre
146.00	0.000004	0.000541 0.000428	0.00	6.05	0.70

Stage 3 - End of phase 2

Phase 3 - Time march with topping added

Time	Strain in top fibre	in	Stress in top fibre		Stress in
	topping	plank bottom fibre	top	plank	bottom fibre
146.24	0.000007	0.000542 0.000427	0.00	6.04	0.70

```
146.84  0.000011   0.000545    0.000426   0.00    6.04    0.70
147.83  0.000015   0.000547    0.000425   0.00    6.04    0.70
149.29  0.000019   0.000550    0.000425   0.00    6.04    0.70
151.36  0.000025   0.000554    0.000424   0.00    6.04    0.70
154.23  0.000031   0.000558    0.000424   0.00    6.04    0.70
158.19  0.000038   0.000564    0.000425   0.00    6.05    0.70
163.65  0.000047   0.000570    0.000426   0.00    6.05    0.69
171.25  0.000058   0.000578    0.000428   0.00    6.05    0.68
182.00  0.000071   0.000588    0.000431   0.00    6.06    0.67

Phase 4 - Live loading of beam
Time  Strain in top fibre   in    Stress in top fibre  Stress in
      topping    plank  bottom fibre  top  plank  bottom fibre
182.00  0.000393   0.000704    0.000048   6.02    11.51    0.00
```

A.4.3 Deflection output (.ot2) file - Example

Explanation

The deflections calculated by the program are output in this file. The corresponding times are also reported. In this file a negative deflection is a hog (upwards movement of the plank).

Example

```
Moama Bridge Planks - PA10NT1
Date: 21 Sep 88
File: pa10nt1
```

	Time (days)	Deflection (mm)
1	0.0	-2.99
2	1.1	-3.19
3	3.8	-3.35
4	8.1	-3.45
5	14.5	-3.50
6	23.5	-3.50
7	35.7	-3.48
8	52.1	-3.43
9	74.4	-3.36
10	104.6	-3.29
11	146.0	-3.21
12	146.0	0.39
13	146.2	0.48
14	146.8	0.59
15	147.8	0.71
16	149.3	0.83
17	151.4	0.96
18	154.2	1.11
19	158.2	1.26
20	163.6	1.43
21	171.2	1.62
22	182.0	1.83
23	182.0	16.53

A.5 Procedures

Setuptime - The procedure produces a series of time steps which have approximately equal increments of the creep coefficient. It is called during the initialisation procedure.

The times are generated using the inverse of the assumed creep function-

$$t = \left(\frac{d}{\left(\frac{\phi^*}{\phi(t)} - 1 \right)} \right)^{\frac{1}{\psi}} \tag{A.1}$$

Convertdata - Section data is entered into the program in a form which the user finds relatively easy to enter but which the program finds difficult to use. This subroutine converts the data into a more useful form.

Init - Initialises several sets of program variables. Both setputime and convertdata are called from this routine.

Sigreinf - Contains the stress-strain curve for the reinforcing steel.

Sigprest - Contains the stress-strain curve for the prestressing steel.

Sigconc - Contains the stress-strain curve for the concrete.

Ftotal - Sums the forces on the section for a given set of values of eps1,eps2.

Mtotal - Calculates the moment needed to balance a given strain distribution.

Mfind - Varies ϵ_2 to find the value for which forces on the section are in equilibrium, then finds the moment needed for moment equilibrium. This moment is then returned to the calling program.

Strainbalance - Finds an ϵ_1, ϵ_2 pair which satisfy force and moment equilibrium. The routine uses mfind to ensure that force equilibrium is satisfied for each guess of ϵ_1.

Printnum1 - Stores the value of curvature at each time step, and outputs details about stresses and strains when required. This routine is used during Phase 2.

Printnum2 - Similar to Printnum1 but is called during Phase 4.

Printtitle - Prints a title found in the .ot1 file.

timemarch - This routine drives the other routines through the analysis. It starts by initialising values of ϕ^* for various times, as well as zeroing matrices which require it.

loaddata - Loads the data into the program.

printinput - Echoes the input data into an output file.

deflection - Calculates the moments existing at particular sections of the beam, then calls timemarch to let it do the work. After the values of curvature along the beam have been calculated this routine calculates the deflections with time.

The way that these procedures are linked together within the program can be seen in the following diagram. This is not a flow-chart as such, but it shows where procedures are called from.

A.6 Variable definitions

- Section data

  nc - Number of slices into which the section is to be divided. The number is the same as "slices", however both are provided so that the data files can be used with earlier versions of the program.

  slices - See nc.

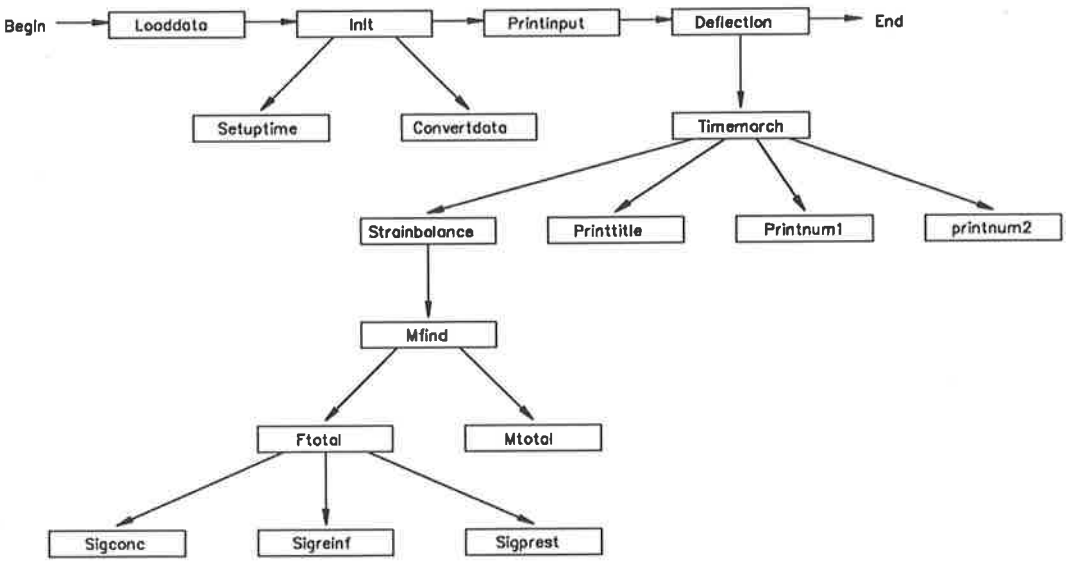

Figure A.1: Procedure chart

ns - Number of layers of reinforcing steel in the plank.

np - Number of layers of prestressing steel.

nt - Number of layers of reinforcing steel in the topping.

nr - Number of points in the section description entered by the user.

length - Length of the plank between the supports.

topdep - Depth to the first layer of topping concrete.

d - Total depth of the section.

tc - Thickness of the i^{th} layer of concrete.

bc - Width of the i^{th} layer of plank concrete.

bt - Width of the i^{th} layer of topping concrete.

dc - Depth to the centroid of the i^{th} layer of concrete.

erefc - Strain in the i^{th} layer of concrete, immediately after the topping has been added. This is the strain which must be subtracted from the linear strain diagram to obtain the actual strain in the topping concrete.

aas - Area of the j^{th} layer of reinforcing steel in the plank.

ds - Depth to the j^{th} layer of reinforcing steel.

ap - Area of the k^{th} layer of prestressing steel.

dp - Depth to the k^{th} layer of prestressing steel.

sigp - Value of prestress in the k^{th} layer of prestressing steel.

aat - Area of the m^{th} layer of reinforcing steel in the topping.

dt - Depth to the m^{th} layer of reinforcing steel in the topping.

ereft - Strain in the m^{th} layer immediately after the topping has been added.

wpl - Width of the plank at depth dpl. wpl,wto,dpl and circ contain the section information input by the user. The program produces the information in tc,bc,bt and dc from this.

wto - Width of topping at depth dpl.

dpl - Depth to the location at which the widths are being measured.

circ - circ[1,1] is the depth to the centre of the circular void, while circ[2,1] is the radius of the void.

- Loadings

mplank - Midspan moment caused by the self weight of the plank.

mtopping - Midspan moment caused by the self weight of the topping.

mll - Maximum moment caused by the live loading.

- Material Properties

ec - Young's modulus in compression of plank and topping concretes.

et - Assumed Young's modulus in tension of plank and topping concretes.

etp - Strain at peak tensile stress.

etf - Final strain when tensile stress is reduced to zero.

ftp - Ultimate direct tensile stress.

fcp - Characteristic compressive strength of concrete.

esmax - Yield strain of reinforcing steel.

fsy - Yield stress of reinforcing steel.

es - Young's modulus of reinforcing steel.

epmax - Yield strain of prestressing steel.

fpy - Yield stress of prestressing steel.

ep - Young's modulus of prestressing steel.

alpha - Contains the α parameter for the ACI209 shrinkage equation.

ksi - Contains the ψ parameter for the ACI209 creep equation.

faci - Contains the f parameter for the ACI209 shrinkage equation.

daci - Contains the d parameter for the ACI209 creep equation.

gamma1 - Non-dimensional stiffness for the non-linear concrete stress-strain curve.

gamma2 - Strain at which the stress reduces to zero in the non-linear stress-strain curve for concrete.

fcmax - Peak stress for concrete stress-strain curve.

ecmax - Strain at which the peak stress occurs.

phistar - Ultimate value of creep function, where stress is added at time zero.

phistar2 - Stores estimates of the ultimate value of the creep coefficient, for stress increments at various times.

eshstar - Ultimate value of the shrinkage function.

- Time information

m - Current time step.

m2 - Time step at which the topping concrete is added.

time2 - Time at which the topping is added.

m4 - Time step at which the live load is added and the analysis finishes.

time4 - Time at which the live load is added.

tim - Times at which the time steps occur.

- Variables used directly in the analysis

epsj1 - Elastic strain in each layer during the previous time step.

sigma - Latest guess of the stress in each layer. The stresses are calculated and stored for later use in calculating the force and moment on the section.

phit - The value of the creep coefficient at the current time, for each of the strain increments.

failed - Records which layers have failed in tension.

chi - Curvature of the k^{th} section at the m^th time step.

epsj - Temporary storage for increments in elastic strain.

cycle - Current section begin evaluated along the plank.

kpoint - Pointer to the next location to be used in the chi matrix.

ipltop - Layer number of the highest layer to contain plank concrete.

- Other variables

numcycles - Number of sections which are to be analysed.

todaysdate - Today's date.

name - Prefix used for input and output files.

descrip - A short description of the run, which is printed at the head of each output file.

numout - True if the details of this cycle are to be output to a file.

filein - The input data file.

file1out - File for data output.

file2out - File for output of section analysis.

file3out - File for output of deflections.

A.7 Camber - Source Code

```
program camber(input,output,filein,file1out,file2out,file3out);

var   alpha,ksi,faci,daci        : array [1..4] of real;
      gamma1,gamma2,fcmax,ecmax  : array [1..2] of real;
      tv,phivstar,alfad          : array [1..2] of real;
```

```
      phistar,eshstar,eshrink   : array [1..2] of real;
      epsj1,sigma,phit          : array [1..2,0..200] of real;
      failed                    : array [1..2,0..200] of real;
      tc,bc,bt,dc,erefc         : array [1..100] of real;
      aas,ds                    : array [1..20] of real;
      ap,dp,sigp                : array [1..20] of real;
      aat,dt,ereft              : array [1..20] of real;
      wpl,dpl,wto               : array [0..100] of real;
      circ                      : array [1..2,1..5] of real;
tim                       : array [1..2,0..201] of real;
chi                       : array [1..200,0..205] of real;
epsj                      : array [1..2,0..200,0..200] of real;
      phistar2                  : array [1..2,0..200] of real;
      gua,wei                   : array [1..3] of real;
      ec,et,etp,etf,ftp,fcp     : array [1..2] of real;
      esmax,fsy,es              : real;
      epmax,fpy,ep              : real;
      m,m2,m4,cycle             : integer;
      kpoint,ipltop,numcycles   : integer;
      nc,ns,np,nt,nr,slices     : integer;
      length,topdep,d,lengthdeb : real;
      mplank,mtopping,mll       : real;
      time2,time4               : real;
      todaysdate                : alfa;
      name                      : packed array [1..10] of char;
      descrip                   : packed array [1..60] of char;
      numout                    : boolean;
      filein,file1out,file2out  : text;
      file3out                  : text;
```

```
{                                                              }
{ The data file only contains the values of TIME2, TIME4       }
{ and the number of steps between each of them. The length     }
{ of each time step is calculated in the procedure, so         }
{ each time step produces an equal increment of the creep      }
{ function.                                                    }
{                                                              }

procedure setuptime;

var   k2,k4,ki,rt  : real;

begin
  k2:=(exp(ksi[1]*ln(time2))/(exp(ksi[1]*ln(time2))+daci[1]));
  k4:=(exp(ksi[1]*ln(time4))/(exp(ksi[1]*ln(time4))+daci[1]));
  tim[1,0]:=0;
  tim[2,0]:=0;
  for m:=1 to m2 do
  begin
    ki:=k2*m/m2;
    rt:=(exp(ln((ki*daci[1])/(1-ki))/ksi[1]))/time2;
    tim[1,m]:=rt*time2;
    tim[2,m]:=0;
  end;
  for m:=m2+1 to m4 do
  begin
    ki:=k4*(m-m2)/(m4-m2);
    rt:=(exp(ln((ki*daci[1])/(1-ki))/ksi[1]))/time4;
    tim[1,m]:=time2+(time4-time2)*rt;
```

```
    tim[2,m]:=(time4-time2)*rt;
  end;
  tim[1,m4+1]:=tim[1,m4];
  tim[2,m4+1]:=tim[2,m4];
end;

{                                                              }
{ This converts the section data the user inputs into something}
{ that the program finds more digestible.                      }
{                                                              }


procedure convertdata;

var  wx,wy,x,h1,h2,alpha,beta,b1,b2  : real;
     area,topdepth,botdepth          : real;
     area1,area2,dx,w1t,w1,w2t,w2    : real;
     i,j,kk  : integer;

    procedure wget;       {18200}
      begin
        wx:=(wpl[j-1]*(dpl[j]-dx)+wpl[j]*(dx-dpl[j-1]))/
                                          (dpl[j]-dpl[j-1]);
        wy:=(wto[j-1]*(dpl[j]-dx)+wto[j]*(dx-dpl[j-1]))/
                                          (dpl[j]-dpl[j-1]);
      end;

    procedure circles;    {18300}
      begin
        x:=(h1/circ[2,1]);
```

```
      alpha:=arctan(x/sqrt(1-x*x));
      x:=(h2/circ[2,1]);
      beta:=arctan(x/sqrt(1-x*x));
      b1:=circ[2,1]*cos(alpha);
      b2:=circ[2,1]*cos(beta);
      area:=circ[2,1]*circ[2,1]*(-alpha+beta)-b1*h1+b2*h2;
    end;

  begin
    dpl[0]:=0;
    wpl[0]:=0;
    wto[0]:=0;
    kk:=1;
    while wpl[kk]=0 do kk:=kk+1;
    topdep:=dpl[kk];
    d:=dpl[nr];
    for i:=1 to slices do
    begin
      topdepth:=d*(i-1)/slices;
      botdepth:=d*i/slices;
      area1:=0;
      area2:=0;
      j:=1;
      while ((dpl[j]<botdepth) and (j<9)) do
      begin
        if ((topdepth>dpl[j-1]) and (topdepth<dpl[j])) then
        begin
          dx:=topdepth;
          wget;
          area1:=(wx+wpl[j])*(dpl[j]-topdepth)/2;
```

```
      area2:=(wy+wto[j])*(dpl[j]-topdepth)/2;
    end
    else
      if topdepth<dpl[j] then
      begin
       area1:=area1+(wpl[j-1]+wpl[j])*(dpl[j]-dpl[j-1])/2;
       area2:=area2+(wto[j-1]+wto[j])*(dpl[j]-dpl[j-1])/2;
      end;
    j:=j+1;
  end;
  if dpl[j-1]<topdepth then
  begin
    dx:=topdepth;
    wget;
    w1:=wx;
    w1t:=wy;
    dx:=botdepth;
    wget;
    w2:=wx;
    w2t:=wy;
    area1:=(w1+w2)*(botdepth-topdepth)/2;
    area2:=(w1t+w2t)*(botdepth-topdepth)/2;
  end
  else
  begin
    dx:=botdepth;
    wget;
    area1:=area1+(wpl[j-1]+wx)*(botdepth-dpl[j-1])/2;
    area2:=area2+(wto[j-1]+wy)*(botdepth-dpl[j-1])/2;
  end;
```

```
        if ((topdepth<circ[1,1]+circ[2,1]) and
            (botdepth>circ[1,1]-circ[2,1])) then
        begin
          h1:=topdepth;
          h2:=botdepth;
          if h1<=(circ[1,1]-circ[2,1]) then
                    h1:=circ[1,1]-circ[2,1]+0.1;
          if h2>=(circ[1,1]+circ[2,1]) then
                    h2:=circ[1,1]+circ[2,1]-0.1;
          h1:=h1-circ[1,1];
          h2:=h2-circ[1,1];
          circles;
          area1:=area1-area;
        end;
        tc[i]:=botdepth-topdepth;
        bc[i]:=area1/tc[i];
        bt[i]:=area2/tc[i];
        dc[i]:=topdepth+tc[i]/2;
      end;
      nc:=slices;
    end;

{                                                    }
{ This procedure is called after the data is loaded and  }
{ it completes the initialisation process.           }
{                                                    }

procedure init;

var  i : integer;
```

```
  begin
    setuptime;
    convertdata;
{    for i:=1 to 2 do
    begin
      ftp[i]:=-0.6*sqrt(fcp[i]);
      et[i]:=(-0.48265*ec[i])/(0.393015+ftp[i]);
      etp[i]:=ftp[i]/ec[i];
      etf[i]:=etp[i]+ftp[i]/et[i];
    end; }
    ftp[1]:=0;
    etp[1]:=0;
    etf[1]:=0;
    ftp[2]:=0;
    etp[2]:=0;
    etf[2]:=0;
    date(todaysdate);
  end;


{ Stress-strain curve for reinforcing steel. }

function sigreinf(eps : real): real;

  begin
    if (eps<-esmax) then sigreinf:=-fsy
    else if eps<esmax then sigreinf:=es*eps
    else sigreinf:=fsy;
  end;
```

```
{ Stress-strain curve for prestressing steel. }

function sigprest(eps : real): real;

   begin
     if eps<-epmax then sigprest:=-fpy
     else if eps<epmax then sigprest:=ep*eps
     else sigprest:=fpy;
   end;


{ Stress-strain curve for concrete. }

function sigconc(eps:real; nn,i :integer): real;

var  sig,epsx : real;

   begin
     if ((eps<0) and (failed[nn,i]=1)) then sigconc:=0
     else if eps<etf[nn] then sigconc:=0
     else if eps<etp[nn] then
        sigconc:=ftp[nn]-(eps-etp[nn])*(et[nn])
     else if eps<0 then sigconc:=ec[nn]*eps
     else
     begin
       epsx:=eps/ecmax[nn];
       if epsx<1 then sig:=gamma1[nn]*epsx+
      (3-2*gamma1[nn])*epsx*epsx+(gamma1[nn]-2)*epsx*epsx*epsx
```

```
        else if epsx<gamma2[nn] then sig:=1-(1-2*epsx+epsx*epsx)/
       (1-2*gamma2[nn]+gamma2[nn]*gamma2[nn])
        else sig:=0;
        sigconc:=sig*fcmax[nn];
      end;
    end;


{ This routine sums the forces on a section for a given value }
{ of eps1,eps2.                                               }

function ftotal(eps1,eps2 : real): real;

var  i,j        : integer;
     eps,ftot   : real;

   begin
     for i:=1 to nc do
     begin
       eps:=(eps1*(d-dc[i])+eps2*dc[i])/d+epsj[1,i,m];
       sigma[1,i]:=sigconc(eps,1,i);
     end;
     if m>m2 then
       for i:=1 to nc do
       begin
         eps:=(eps1*(d-dc[i])+eps2*dc[i])/d+epsj[2,i,m];
         sigma[2,i]:=sigconc(eps,2,i);
       end;
     ftot:=0;
     for i:=1 to nc do ftot:=ftot+sigma[1,i]*tc[i]*bc[i];
```

```
    for i:=1 to ns do
    begin
      eps:=(eps1*(d-ds[i])+eps2*ds[i])/d;
      ftot:=ftot+sigreinf(eps)*aas[i];
    end;
    for i:=1 to np do
    begin
      eps:=(eps1*(d-dp[i])+eps2*dp[i])/d-sigp[i]/ep;
      ftot:=ftot+sigprest(eps)*ap[i];
    end;
    if m>m2 then
    begin
      for i:=1 to nc do ftot:=ftot+sigma[2,i]*tc[i]*bt[i];
      for i:=1 to nt do
      begin
        eps:=(eps1*(d-dt[i])+eps2*dt[i])/d-ereft[i];
        ftot:=ftot+sigreinf(eps)*aat[i];
      end;
    end;
    ftotal:=ftot;
  end;


{ Routine to calculate the moment needed for a given strain }
{ distribution.                                             }

function mtotal(var eps1,eps2 : real): real;

var  i          : integer;
     eps,mtot   : real;
```

```
  begin
    mtot:=0;
    for i:=1 to nc do mtot:=mtot+sigma[1,i]*tc[i]*bc[i]*dc[i];
    for i:=1 to ns do
    begin
      eps:=(eps1*(d-ds[i])+eps2*ds[i])/d;
      mtot:=mtot+sigreinf(eps)*aas[i]*ds[i];
    end;
    for i:=1 to np do
    begin
      eps:=(eps1*(d-dp[i])+eps2*dp[i])/d-sigp[i]/ep;
      mtot:=mtot+sigprest(eps)*ap[i]*dp[i];
    end;
    if m>m2 then
    begin
     for i:=1 to nc do mtot:=mtot+sigma[2,i]*tc[i]*bt[i]*dc[i];
      for i:=1 to nt do
      begin
        eps:=(eps1*(d-dt[i])+eps2*dt[i])/d-ereft[i];
        mtot:=mtot+sigreinf(eps)*aat[i]*dt[i];
      end;
    end;
    mtotal:=mtot;
  end;


{                                                              }
{ Given a value of eps1, this routine finds a value of eps2 }
{ which satisfies force equilibrium and returns the moment  }
```

```
{ needed to satisfy moment equilibrium.                    }
{                                                          }

function mfind(var eps1,eps2 : real): real;

var  ftot,fplus,fminus    : real;
     eps2plus,eps2minus   : real;
     steps                : integer;

      begin
        steps:=0;
        fplus:=0;
        fminus:=0;
        ftot:=ftotal(eps1,eps2);
        while (((fplus=0) or (fminus=0)) and (steps<40)) do
        begin
          steps:=steps+1;
          if ftot>=0 then
          begin
            fplus:=ftot;
            eps2plus:=eps2;
            eps2:=eps2-0.0001;
          end
          else
          begin
            fminus:=ftot;
            eps2minus:=eps2;
            eps2:=eps2+0.0001;
          end;
          ftot:=ftotal(eps1,eps2);
```

```
        end;
        while ((abs((eps2plus-eps2minus)/eps2plus)>0.00001)
           and (steps<40)) do
        begin
          steps:=steps+1;
          eps2:=(eps2plus+eps2minus)/2;
          ftot:=ftotal(eps1,eps2);
          if ftot>=0 then
          begin
            fplus:=ftot;
            eps2plus:=eps2;
          end
          else
          begin
            fminus:=ftot;
            eps2minus:=eps2;
          end;
        end;
        if (steps>39) then
        writeln('Warning: Convergence error in mfind');
        mfind:=mtotal(eps1,eps2)
      end;


{                                                    }
{ Uses mfind to find the stress distribution which   }
{ corresponds to the moment being applied to the     }
{ section.                                           }
{                                                    }
```

```
procedure strainbalance(mserv : real; var eps1,eps2 : real);

var i,j,steps                  : integer;
    mplus,mminus,mtot          : real;
    eps1plus,eps1minus,eps1old : real;

    begin
      if tim[1,m]=0 then eshrink[1]:=0 else
        eshrink[1]:=eshstar[1]*((exp(alpha[1]*ln(tim[1,m])))/
          (faci[1]+(exp(alpha[1]*ln(tim[1,m])))));
      if tim[2,m]<=0 then eshrink[2]:=0 else
        eshrink[2]:=eshstar[2]*((exp(alpha[2]*ln(tim[2,m])))/
          (faci[2]+(exp(alpha[2]*ln(tim[2,m])))));
      for i:=0 to m do
      begin
        if ((tim[1,m]-tim[1,i])<=0) then phit[1,i]:=0 else
phit[1,i]:=phistar2[1,i]*((exp(ksi[1]*ln(tim[1,m]-tim[1,i])))/
      (daci[1]+(exp(ksi[1]*ln(tim[1,m]-tim[1,i])))));
        if ((tim[2,m]-tim[2,i])<=0) then phit[2,i]:=0 else
phit[2,i]:=phistar2[2,i]*((exp(ksi[2]*ln(tim[2,m]-tim[2,i])))/
      (daci[2]+(exp(ksi[2]*ln(tim[2,m]-tim[2,i])))));
      end;
      for i:=1 to nc do
      begin
        epsj[1,i,m]:=-eshrink[1]+epsj1[1,i];
        for j:=0 to m-1 do
          epsj[1,i,m]:=epsj[1,i,m]-epsj[1,i,j]*(1+phit[1,j]);
      end;
      if m>m2 then
        for i:=1 to nc do
```

```
begin
  epsj[2,i,m]:=-eshrink[2]-erefc[i]+epsj1[2,i];
  for j:=m2 to m-1 do
    epsj[2,i,m]:=epsj[2,i,m]-epsj[2,i,j]*(1+phit[2,j]);
end;

     { The main search routine starts here. }

steps:=0;
mplus:=0;
mminus:=0;
mserv:=-mserv;
while (((mplus=0) or (mminus=0)) and (steps<40)) do
begin
  steps:=steps+1;
  mtot:=mfind(eps1,eps2);
  if mtot-mserv>=0 then
  begin
    mplus:=mtot;
    eps1plus:=eps1;
    eps1:=eps1+0.0001;
  end
  else
  begin
    mminus:=mtot;
    eps1minus:=eps1;
    eps1:=eps1-0.0001;
  end;
end;
while ((abs((eps1plus-eps1minus)/eps1plus)>0.00001)
```

```
    and (steps<40)) do
  begin
    steps:=steps+1;
    eps1old:=eps1;
    eps1:=(eps1plus+eps1minus)/2;
    eps2:=eps2-(eps1-eps1old);
    mtot:=mfind(eps1,eps2);
    if mtot-mserv>=0 then
    begin
      mplus:=mtot;
      eps1plus:=eps1;
    end
    else
    begin
      mminus:=mtot;
      eps1minus:=eps1;
    end;
  end;
  if steps>39 then
   writeln('Warning: Convergence error in strainbalance');
  for i:=1 to nc do
  begin
    epsj[1,i,m]:=epsj[1,i,m]+(eps1*(d-dc[i])+eps2*dc[i])/d
     -epsj1[1,i];
    epsj1[1,i]:=epsj1[1,i]+epsj[1,i,m];
    if (epsj1[1,i]<etf[1]) then failed[1,i]:=1;
    if (m>m2) then
    begin
      epsj[2,i,m]:=epsj[2,i,m]+
(eps1*(d-dc[i])+eps2*dc[i])/d-epsj1[2,i];
```

```
            epsj1[2,i]:=epsj1[2,i]+epsj[2,i,m];
            if (epsj1[2,i]<etf[2]) then failed[2,i]:=1;
          end;
        end;
      end;

procedure printnum1(eh,el : real);

var em : real;

begin
  em:=(eh*(d-topdep)+el*topdep)/d;
  chi[cycle,kpoint]:=(eh-el)/d;
  kpoint:=kpoint+1;
  if numout then
  begin
    write(file2out,tim[1,m]:5:2);
    write(file2out,'  ---------  ');
    write(file2out,em:2:6,'    ',el:2:6);
    writeln(file2out,'   ------    ',sigma[1,ipltop]:3:2,'    ',
    sigma[1,nc]:3:2);
  end;
end;


procedure printnum2(eh,el : real);

var em : real;

begin
```

```
  em:=(eh*(d-topdep)+el*topdep)/d;
  chi[cycle,kpoint]:=(eh-el)/d;
  kpoint:=kpoint+1;
  if numout then
  begin
    write(file2out,tim[1,m]:5:2,'  ');
    write(file2out,(eh-erefc[1]):2:6,'   ',em:2:6,'    ',el:2:6,
    ' ');
    writeln(file2out,'  ',sigma[2,1]:3:2,'    ',
    sigma[1,ipltop]:3:2,'    ',sigma[1,nc]:3:2);
  end;
end;



procedure printtitle;

begin
  writeln(file2out,'   Time   Strain in top fibre of    Strain',
  ' in   Stress in top fibre  Stress in');
  writeln(file2out,'            topping     plank      bottom',
  ' fibre   topping   plank  bottom fibre');
end;

{   The bit which actually drives the bits which do things, as }
{   opposed to the gnudge which surrounds it.                  }

procedure timemarch;
```

```
var  i,nn        : integer;
     eh,el,mt    : real;
     out2        : packed array [1..20] of char;

    begin
      eh:=0;
      el:=0;
      phistar2[1,0]:=phistar[1];
      phistar2[2,0]:=0;
      for m:=1 to m2 do
      begin
      phistar2[1,m]:=1.13*(exp(-0.094*ln(tim[1,m])))*phistar[1];
        phistar2[2,m]:=0;
      end;
      for m:=m2+1 to m4 do
      begin
      phistar2[1,m]:=1.13*(exp(-0.094*ln(tim[1,m])))*phistar[1];
        if tim[2,m]=0 then
          phistar2[2,m]:=phistar[2]
        else
      phistar2[2,m]:=1.25*(exp(-0.118*ln(tim[2,m])))*phistar[2];
      end;
      for i:=1 to nc do
        for nn:=1 to 2 do
        begin
          failed[nn,i]:=0;
          epsj1[nn,i]:=0;
          sigma[nn,i]:=0;
          for m:=0 to m4 do epsj[nn,i,m]:=0;
```

```
      end;
    kpoint:=0;
    i:=1;
    while bc[i]=0 do i:=i+1 ; ipltop:=i;

{                                                              }
{          Phase 0                                             }
{                                                              }
{   The stresses would be produced by the prestress acting     }
{   alone are calculated.                                      }
{                                                              }

    m:=0;                       { Time = 0   }
    mt:=0;                      { Moment = 0 }
    strainbalance(mt,eh,el);    { Inelastic analysis }
    if numout then
    begin
      i:=1;
      while (ord(name[i])>32) do
      begin
        out2[i]:=name[i];
        i:=i+1;
      end;
      out2[i]:='.';
      out2[i+1]:='o';
      out2[i+2]:='t';
      out2[i+3]:='1';
      i:=i+4;
      while i<=20 do
      begin
```

```
          out2[i]:=' ';
          i:=i+1;
        end;
        rewrite(file2out,out2);
        writeln(file2out,descrip);
        writeln(file2out,'Date: ',todaysdate);
        writeln(file2out,'File: ',name);
        writeln(file2out);
   writeln(file2out,'Phase 0 - Strains due to prestress only.');
        printtitle;
      end;
      printnum1(eh,el);

{                                                              }
{           Stage 1 - Just after transfer                      }
{                                                              }
{     The stresses immediately after transfer due to the       }
{   prestress and the self weight of the plank are then        }
{   calculated.                                                }
{                                                              }

      for i:=1 to nc do
        for nn:=1 to 2 do
        begin
          epsj1[nn,i]:=0;
          sigma[nn,i]:=0;
          epsj[nn,i,0]:=0;
        end;
      m:=0;
      mt:=mplank;
```

```
      strainbalance(mt,eh,el);
      if numout then
      begin
        writeln(file2out);
        writeln(file2out,'Stage 1 - Strains due to prestress',
        ' and plank self weight.');
      writeln(file2out,'  Plank moment= ',(mplank/1000000):4:1);
        printtitle;
      end;
      printnum1(eh,el);

{                                                              }
{     Phase 1 - Creep and shrinkage under plank self-weight    }
{                                                              }

      if numout then
      begin
        writeln(file2out);
        writeln(file2out,'Phase 1 - Time march during phase 1',
        ' commences here.');
        printtitle;
      end;
      for m:=1 to m2 do
      begin
        strainbalance(mt,eh,el);
        printnum1(eh,el);
      end;

{                                                              }
{ Stage 2 - The plank immediately prior to the application of  }
```

```
{           the topping.                                          }
{                                                                 }

      if numout then
      begin
        writeln(file2out);
        writeln(file2out,'Stage 2 - End of phase 1');
      end;

{                                                                 }
{           Phase 2 - The topping is added to the plank           }
{                                                                 }

      if numout then
      begin
        writeln(file2out);
        writeln(file2out,'Phase 2 - Application of topping');
        writeln(file2out,'   Topping moment= ',
       (mtopping/1000000):4:1);
      end;
      m:=m2;
      mt:=mplank+mtopping;
      strainbalance(mt,eh,el);
      if numout then printtitle;
      for i:=1 to nc do erefc[i]:=(eh*(d-dc[i])+el*dc[i])/d;
      for i:=1 to nt do ereft[i]:=(eh*(d-dt[i])+el*dt[i])/d;
      printnum2(eh,el);

{                                                                 }
{  Stage 3 - Composite beam, just after application of the        }
```

```
{  topping                                                    }
{                                                             }

      if numout then
      begin
        writeln(file2out);
        writeln(file2out,'Stage 3 - End of phase 2');
      end;

{                                                             }
{           Phase 3                                           }
{                                                             }

      if numout then
      begin
        writeln(file2out);
    writeln(file2out,'Phase 3 - Time march with topping added');
        printtitle;
      end;
      for m:=m2+1 to m4 do
      begin
        strainbalance(mt,eh,el);
        printnum2(eh,el);
      end;

{                                                             }
{ Stage 4 - Composite girder, after creep and shrinkage       }
{           have occurred, but prior to the live loading.     }
{                                                             }
```

```
{                                                                    }
{ Phase 4 - The live load increment is applied to the beam.          }
{                                                                    }

      m:=m4+1;
      mt:=mplank+mtopping+mll;
      strainbalance(mt,eh,el);
      if numout then
      begin
        writeln(file2out);
        writeln(file2out,'Phase 4 - Live loading of beam');
        printtitle;
      end;
      printnum2(eh,el);
    end;

{                                                                    }
{    Load data file from disk                                        }
{                                                                    }

procedure loaddata;

var  i    : integer;
     in1 : packed array [1..20] of char;

    begin
      readln(descrip);
      readln(name);
      i:=1;
```

```
while (ord(name[i])>32) do
begin
  in1[i]:=name[i];
  i:=i+1;
end;
in1[i]:='.';
in1[i+1]:='d';
in1[i+2]:='a';
in1[i+3]:='t';
i:=i+4;
while i<=20 do
begin
  in1[i]:=' ';
  i:=i+1;
end;
reset(filein,in1);
readln(filein,length,numcycles);
readln(filein,fcp[1],fcp[2]);
readln(filein,nc,ns,np,nt,nr,topdep,slices);
for i:=1 to nr do readln(filein,dpl[i],wpl[i],wto[i]);
readln(filein,circ[1,1],circ[2,1]);
for i:=1 to ns do readln(filein,aas[i],ds[i]);
for i:=1 to np do readln(filein,ap[i],dp[i],sigp[i]);
for i:=1 to nt do readln(filein,aat[i],dt[i]);
readln(filein,ec[1],es,ep,ec[2]);
readln(filein,mplank,mtopping,mll);
readln(filein,phistar[1],eshstar[1],tv[1],alfad[1]);
readln(filein,phistar[2],eshstar[2],tv[2],alfad[2]);
readln(filein,m2,time2);
readln(filein,m4,time4);
```

```
      readln(filein,gamma1[1],gamma2[1],fcmax[1],ecmax[1]);
      readln(filein,gamma1[2],gamma2[2],fcmax[2],ecmax[2]);
      readln(filein,fsy,fpy);
      esmax:=fsy/es;
      epmax:=fpy/ep;
for i:=1 to 2 do readln(filein,ksi[i],daci[i],alpha[i],faci[i]);
    end;


procedure printinput;

var  i,j : integer;
     out1 : packed array [1..20] of char;

    begin
      i:=1;
      while (ord(name[i])>32) do
      begin
        out1[i]:=name[i];
        i:=i+1;
      end;
      out1[i]:='.';
      out1[i+1]:='d';
      out1[i+2]:='t';
      out1[i+3]:='o';
      i:=i+4;
      while i<=20 do
      begin
        out1[i]:=' ';
        i:=i+1;
```

```
    end;
    rewrite(file1out,out1);
    writeln(file1out,descrip);
    writeln(file1out,'Date: ',todaysdate);
    writeln(file1out,'File: ',name);
    writeln(file1out);
    write(file1out,'Section details-',' ':24,
    'Number of slices= ');
    writeln(file1out,slices:3);
    writeln(file1out);
    writeln(file1out,' ':13,'#',' ':5,'Depth    Plank width',
    '    Topping width');
    for i:=1 to nr do
      writeln(file1out,' ':13,i:2,' ':4,dpl[i]:4:1,' ':6,
    wpl[i]:4:1,' ':12,wto[i]:4:1);
    if circ[2,1]<>0 then
       writeln(file1out,'         Circular void at depth ',
    circ[1,1]:5:1,
  ' with radius ',circ[2,1]:5:1)
    else
       writeln(file1out,'         No void in section');
    writeln(file1out);
  writeln(file1out,' ':24,'Plank concrete    Topping concrete');
    writeln(file1out);
    writeln(file1out,'    Youngs modulus',' ':7,ec[1]:8:0,
    ' ':13,ec[2]:8:0);
    writeln(file1out);
    writeln(file1out,'     Phistar',' ':17,phistar[1]:2:2,
    ' ':14,phistar[2]:2:2);
    writeln(file1out,'     Eshstar',' ':17,eshstar[1]:2:6,
```

```
' ':10,eshstar[2]:2:6);
writeln(file1out,'       Tv   ',' ':16,tv[1]:3:1,
' ':14,tv[2]:3:1);
writeln(file1out,'     Alphad ',' ':17,alfad[1]:2:2,
' ':14,alfad[2]:2:2);
writeln(file1out);
writeln(file1out,'     alpha  ',' ':17,alpha[1]:2:2,
' ':14,alpha[2]:2:2);
writeln(file1out,'     daci   ',' ':16,daci[1]:4:1,
' ':14,daci[2]:4:1);
writeln(file1out,'     ksi    ',' ':17,ksi[1]:2:1,
' ':15,ksi[2]:2:1);
writeln(file1out,'     faci   ',' ':16,faci[1]:4:0,
' ':16,faci[2]:4:0);
writeln(file1out);
writeln(file1out,'    gamma1  ',' ':17,gamma1[1]:2:2,
' ':14,gamma1[2]:2:2);
writeln(file1out,'    gamma2  ',' ':17,gamma2[1]:2:2,
' ':14,gamma2[2]:2:2);
writeln(file1out,'    fcmax   ',' ':16,fcmax[1]:3:1,
' ':14,fcmax[2]:3:1);
writeln(file1out,'    ecmax   ',' ':17,ecmax[1]:2:6,
' ':10,ecmax[2]:2:6);
writeln(file1out);
if ((ns<>0) and (nt<>0)) then
begin
  writeln(file1out,'Non-prestressed reinforcement-');
  writeln(file1out,'Youngs modulus ',es:8:0);
  writeln(file1out,'Yield stress    ',fsy:5:0);
  if ns<>0 then
```

```
  begin
    writeln(file1out,'     Plank     Layer #    Depth',
    '   Cross sectional area');
    for j:=1 to ns do
      writeln(file1out,' ':17,j:2,' ':9,ds[j]:4:1,' ':8,
     aas[j]:5:1);
    writeln(file1out);
  end;
  if nt<>0 then
  begin
    writeln(file1out,'     Topping   Layer #    Depth',
    '   Cross sectional area');
    for j:=1 to nt do
      writeln(file1out,' ':17,j:2,' ':9,dt[j]:4:1,' ':8,
      aas[j]:5:1);
    writeln(file1out);
  end;
end;
writeln(file1out,'Prestressing tendons-');
writeln(file1out,'Youngs modulus ',ep:8:0);
writeln(file1out,'Yield stress ',fpy:4:0);
writeln(file1out,' ':15,'Layer #     Depth   Cross',
' sectional area   Initial prestress');
for j:=1 to np do
  writeln(file1out,' ':17,j:2,' ':9,dp[j]:4:1,' ':11,
  ap[j]:5:1,' ':16,sigp[j]:5:1);
writeln(file1out);
writeln(file1out,'Loading details-');
writeln(file1out,'         Plank self-weight moment ',
(mplank/1000000):5:1);
```

```
      writeln(file1out,'       Topping self-weight moment ',
      (mtopping/1000000):5:1);
      writeln(file1out,'                  Live load moment ',
      (mll/1000000):5:1);
      writeln(file1out);
      writeln(file1out,'        Topping is added at t= ',
      time2:4:1,' days');
      writeln(file1out,'              Final time is t= ',
      time4:4:1,' days');
      writeln(file1out);
      writeln(file1out,'   Number of intervals in the',
      ' first time period= ',m2:3);
      writeln(file1out,'  Number of intervals in the',
      ' second time period= ',(m4-m2):3);
    end;


{           '                                                    }
{           ' Calculates the deflection along the beam           }
{           '                                                    }

procedure deflection;

var   mfact,xloc,l2,defl,delx  : real;
      xx,jj,kk,i               : integer;
      wplank,wtopping,wll,xbit : real;
      out3  : packed array [1..20] of char;

    begin
      numout:=false;
```

```
wplank:=8*mplank/(length*length);
wtopping:=8*mtopping/(length*length);
wll:=8*mll/(length*length);
delx:=length/(2*(numcycles-1));
for cycle:=1 to numcycles do
begin
  if (cycle=numcycles) then numout:=true;
  xloc:=delx*(cycle-1);
  mfact:=length*xloc/2-xloc*xloc/2;
  mplank:=mfact*wplank;
  mtopping:=mfact*wtopping;
  mll:=mfact*wll;
  timemarch;
end;
l2:=length*length;
mplank:=wplank*l2/8;
mtopping:=wtopping*l2/8;
mll:=wll*l2/8;
xx:=1;
i:=1;
while (ord(name[i])>32) do
begin
  out3[i]:=name[i];
  i:=i+1;
end;
out3[i]:='.';
out3[i+1]:='o';
out3[i+2]:='t';
out3[i+3]:='2';
i:=i+4;
```

```
      while i<=20 do
      begin
        out3[i]:=' ';
        i:=i+1;
      end;
      rewrite(file3out,out3);
      writeln(file3out,descrip);
      writeln(file3out,'Date: ',todaysdate);
      writeln(file3out,'File: ',name);
      writeln(file3out);
      writeln(file3out,'    Time  Deflection');
      writeln(file3out,'   (days)   (mm)');
      writeln(file3out);
      for jj:=1 to m4+3 do
      begin
        defl:=0;
        for kk:=1 to numcycles-1 do
        begin
          xbit:=delx*(chi[kk,jj]+2*chi[kk+1,jj])/
           (3*(chi[kk,jj]+chi[kk+1,jj]));
          defl:=defl+(chi[kk,jj]+chi[kk+1,jj])*
           ((kk-1)*delx+xbit)*delx/2;
        end;
        writeln(file3out,jj:2,'  ',tim[1,jj-xx]:4:1,'  ',
        defl:4:2);
        if jj=m2+1 then xx:=2;
      end;
    end;

begin
```

```
  loaddata;
  init;
  printinput;
  deflection;
end.
```

Appendix B

Experimental data

B.1 Leong's data

B.1.1 Input data for CAMBER

For all the beams, the effective length of the span was taken to be 9600mm. Also, the characteristic compressive strength (f'_c) was taken to be 30 MPa and 40 MPa for the topping and plank concrete respectively. As this was only used to estimate the tension characteristics of the concrete, its accuracy was not terribly important.

Only the input data for beams PA10NT1 and PR10NT1 are shown, as the data for beams 2 and 3 in each series differ only in the time at which the topping concrete is poured. The concrete is poured at 28 days for beams 2 and 3 and 146 days for the first beam in each series.

Beam PA10NT1

Section details- Number of slices= 20

No.	Depth	Plank width	Topping width
1	0.0	0.00	600.00
2	125.0	0.00	600.00
3	125.0	530.00	0.00
4	175.0	530.00	0.00
5	200.0	480.00	0.00
6	250.0	480.00	0.00
7	310.0	600.00	0.00
8	425.0	600.00	0.00

No void in section

		Plank concrete	Topping concrete
Young's modulus		23700	21530
Creep Parameters	Phistar	0.880	1.860
	Eshstar	0.000360	0.000532
	Tv	60.0	60.0
	Alphad	0.850	0.700
ACI creep curve data	alpha	0.97	2.04
	d	54	89
shrinkage curve data	ksi	1.27	1.42
	f	20	148
Non-linear	gamma1	2.00	2.00

stress-strain	gamma2	3.00	3.00
curve	fc.max	47.0	35.0
	ec.max	0.002000	0.002000

Prestressing tendons-

Young's modulus 191000

Yield stress 1770

Layer No.	Depth	Cross sectional area	Initial prestress
1	380.0	800	600.0
2	335.0	200	600.0

Loading details-

Plank self-weight moment 47.4

Topping self-weight moment 21.6

Live load moment 77.5

Topping is added at t= 146 days

Final time is t= 182 days

Number of intervals in the first time period= 20

Number of intervals in the second time period= 20

Beam PR10NT1

Section details- Number of slices= 20

No.	Depth	Plank width	Topping width

1	0.0	0.00	600.00
2	125.0	0.00	600.00
3	125.0	530.00	0.00
4	175.0	530.00	0.00
5	200.0	480.00	0.00
6	250.0	480.00	0.00
7	310.0	600.00	0.00
8	425.0	600.00	0.00

No void in section

		Plank concrete	Topping concrete
	Young's modulus	33250	21500
Creep Parameters	Phistar	0.900	1.860
	Eshstar	0.000340	0.000532
	Tv	60.0	60.0
	Alphad	0.850	0.700
ACI creep curve data	alpha	0.97	2.04
	d	54	89
shrinkage curve data	ksi	1.27	1.42
	f	20	148
Non-linear stress-strain curve	gamma1	2.00	2.00
	gamma2	3.00	3.00
	fc.max	47.0	35.0
	ec.max	0.002000	0.002000

Non-prestressed reinforcement-

```
                Young's modulus 207900
                Yield stress      410
     Plank   Layer No.   Depth   Cross sectional area
                1          380.0        1257.0

Prestressing tendons-
                Young's modulus 188000
                Yield stress 1770
Layer No.    Depth   Cross sectional area   Initial prestress
   1          380.0        400                   1150.0
   2          335.0        200                   1150.0

Loading details-
          Plank self-weight moment   47.4
       Topping self-weight moment    21.6
                Live load moment     77.5

          Topping is added at t=  146 days
                Final time is t=  182 days

      Number of intervals in the first time period=  20
     Number of intervals in the second time period=  20
```

B.1.2 Live load graphs

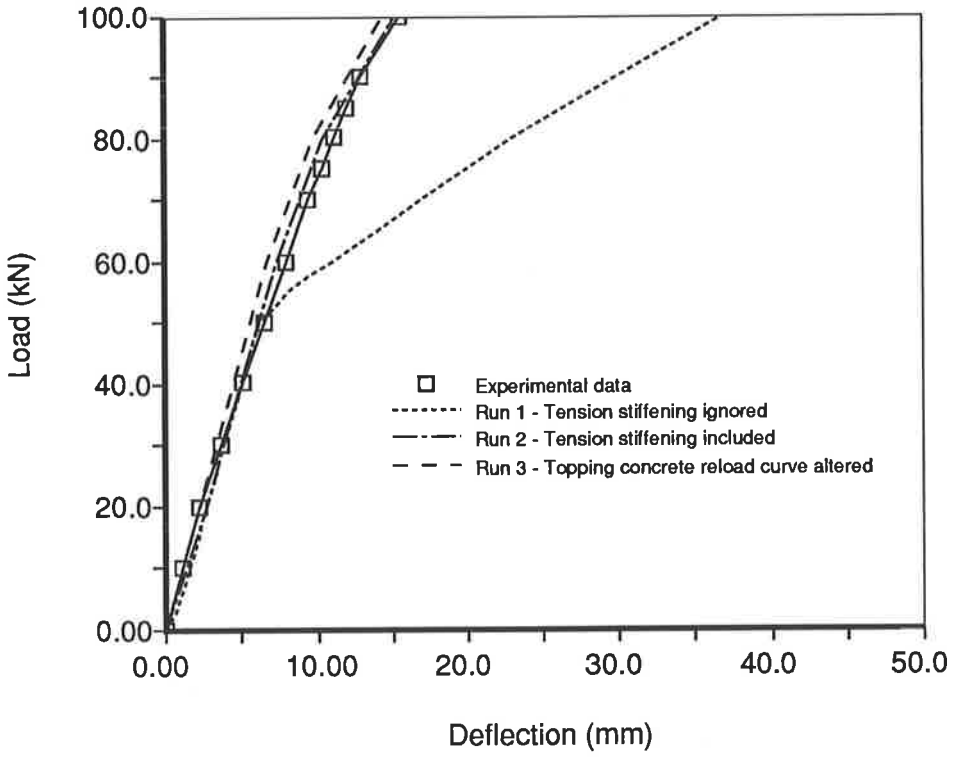

Figure B.1: Live loading of beam PA10NT2 - Load 0-120kN

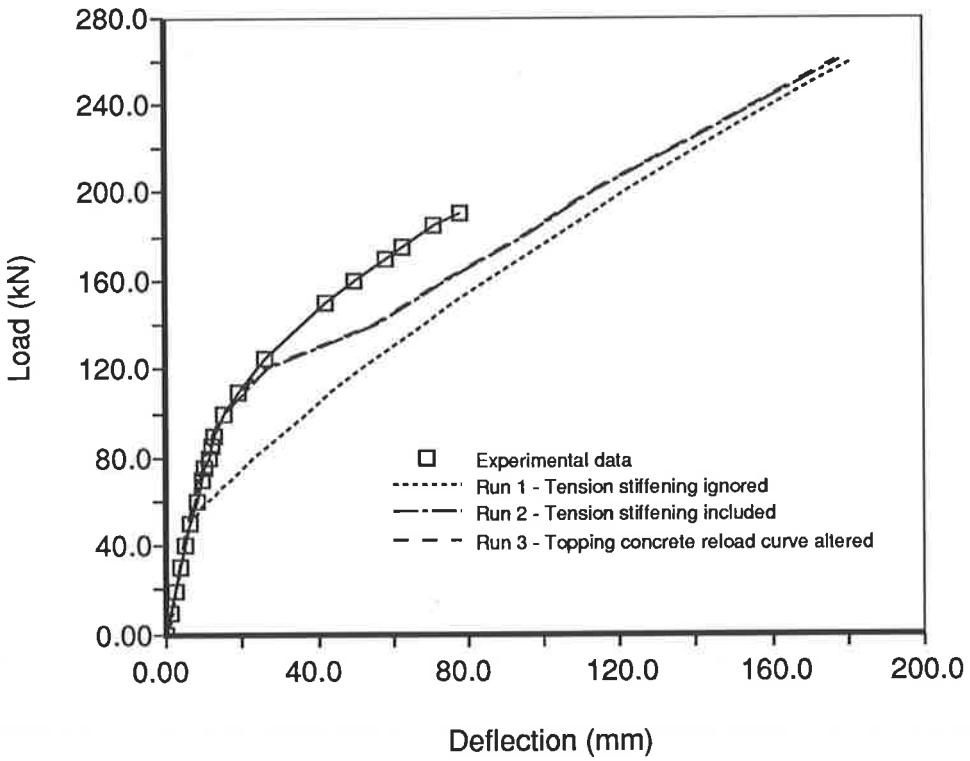

Figure B.2: Live loading of beam PA10NT2 - Load 0-260kN

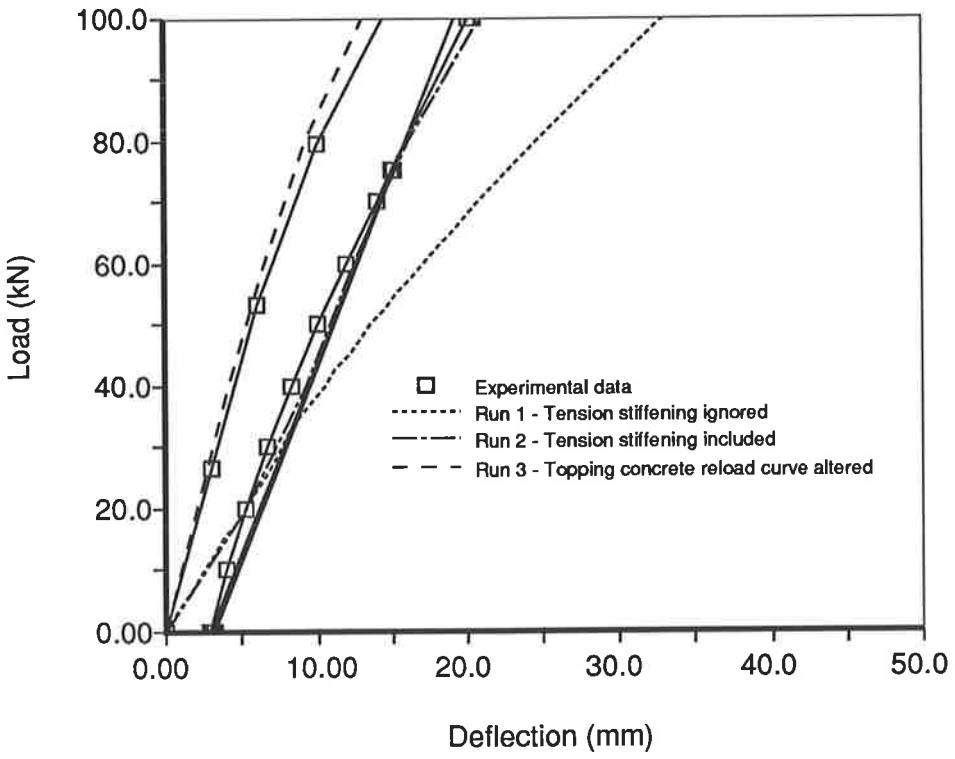

Figure B.3: Live loading of beam PR10NT1 - Load 0-120kN

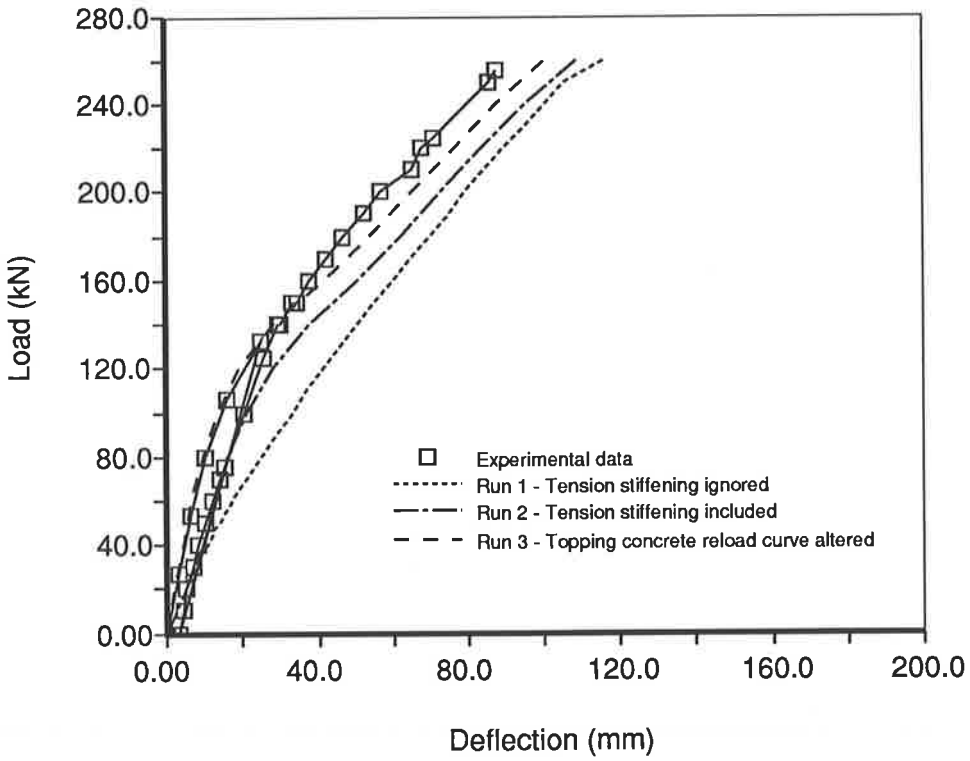

Figure B.4: Live loading of beam PR10NT1 - Load 0-260kN

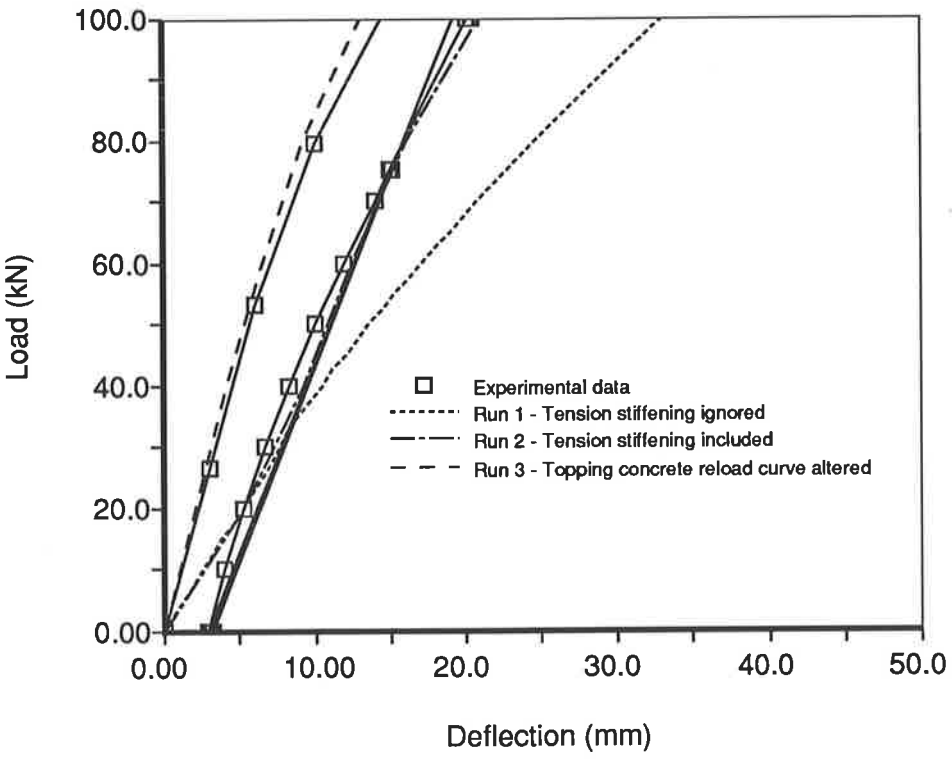

Figure B.3: Live loading of beam PR10NT1 - Load 0-120kN

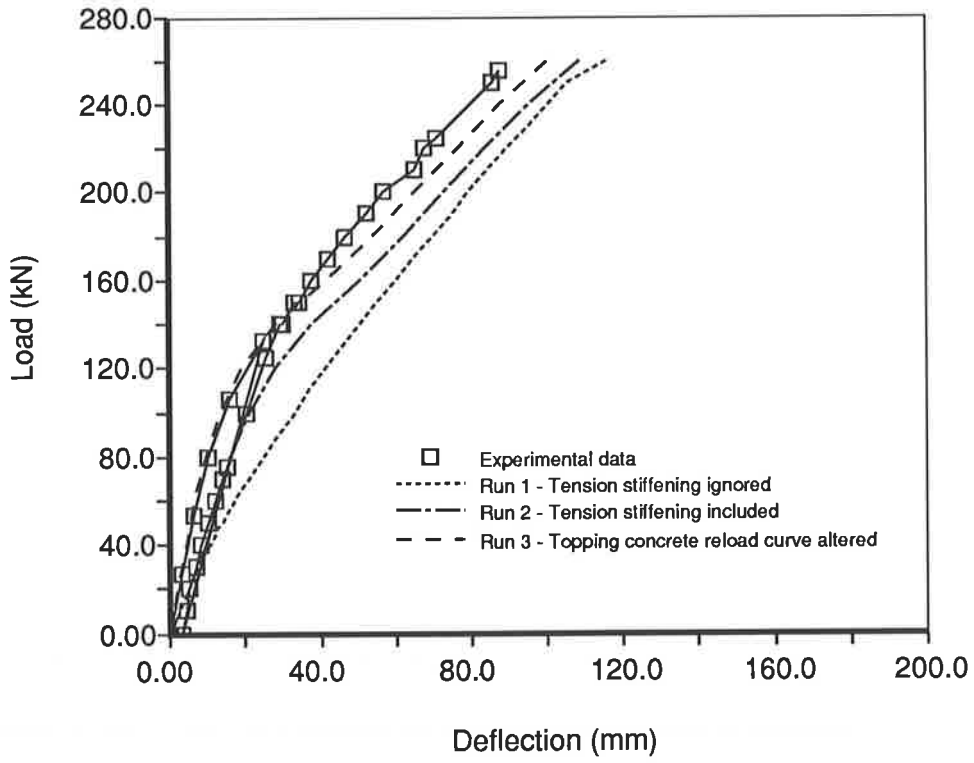

Figure B.4: Live loading of beam PR10NT1 - Load 0-260kN

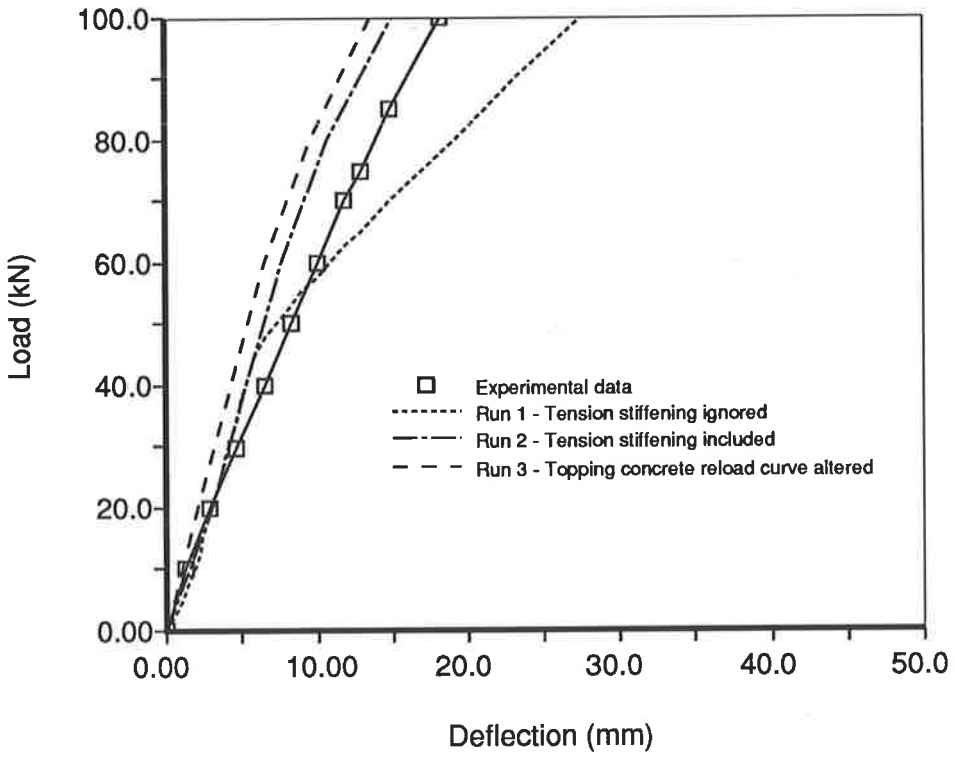

Figure B.5: Live loading of beam PR10NT2 - Load 0-120kN

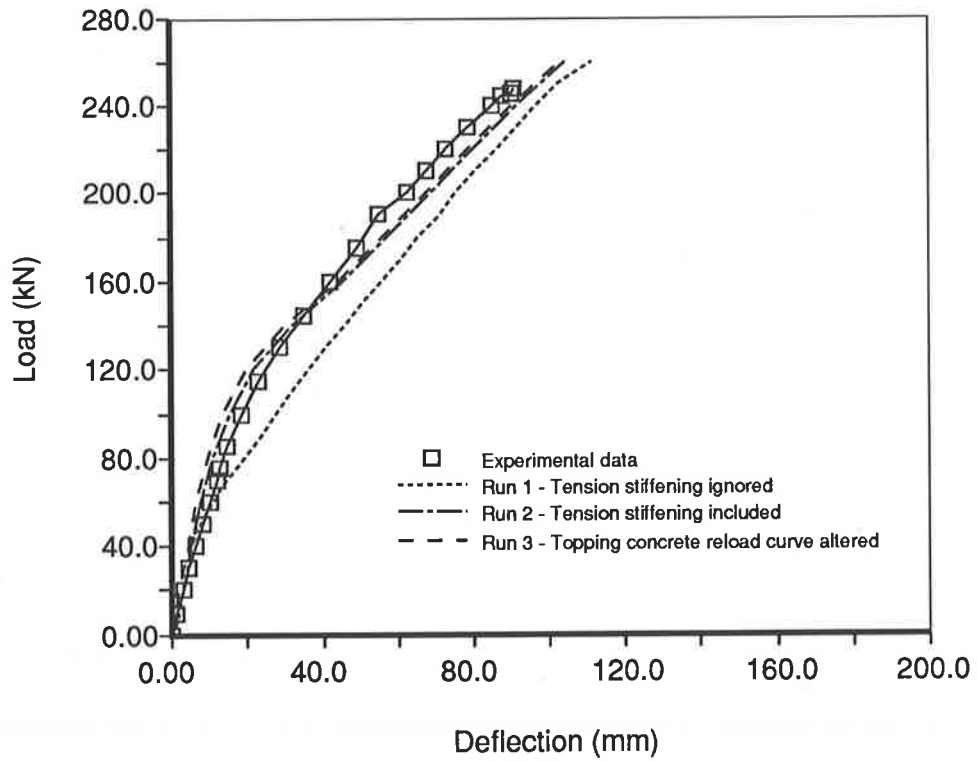

Figure B.6: Live loading of beam PR10NT2 - Load 0-260kN

B.2 Gawler data

B.2.1 Input data for CAMBER

Gawler bridge beams

Date: 28 Dec 88

File: gawler

Section details- Number of slices= 20

#	Depth	Plank width	Topping width
1	0.0	0.0	600.0
2	124.9	0.0	600.0
3	125.0	550.0	50.0
4	230.0	520.0	80.0
5	250.0	600.0	0.0
6	355.0	600.0	0.0
7	375.0	560.0	0.0

No void in section

	Plank concrete	Topping concrete
Youngs modulus	34000	30000
Phistar	1.98	2.69
Eshstar	0.000525	0.000525
Tv	60.0	60.0
Alphad	0.85	0.70
alpha	1.00	1.00

daci	20.0	20.0
ksi	0.6	0.6
faci	55	35
gamma1	2.00	2.00
gamma2	3.00	3.00
fcmax	40.0	30.0
ecmax	0.002000	0.002000

Prestressing tendons-

Youngs modulus 188000

Yield stress 1770

Layer #	Depth	Cross sectional area	Initial prestress
1	175.0	200.0	1323.0
2	275.0	400.0	1323.0
3	325.0	800.0	1323.0

Loading details-

Plank self-weight moment 25.8

Topping self-weight moment 26.0

Live load moment 20.0

Topping is added at t= 139.0 days

Final time is t= 500.0 days

Number of intervals in the first time period= 30

Number of intervals in the second time period= 10

B.2.2 Experimental Deflection Results

Date	Time	Nett Hog of Beam #				Notes
		65	66	67	68	
28-7-88	7:30am	0	0	0	0	Before transfer
	7:50am	8.0	5.5	6.0	6.0	After transfer
	8:10am	14.0	7.0	10.5	9.0	After removal from bed
	9:10am	16.5	9.5	12.5	11.0	
	10:00am	16.0	12.0	16.5	13.5	
	2:00pm	17.0	13.5	16.5	10.5	After moving to storage
29-7-88	8:25am	15.0	13.5	14.5	10.5	
2-8-88	8:40am	17.0	13.5	15.0	12.0	
4-8-88	9:50am	20.0	15.0	17.0	13.5	
8-8-88	9:45am	23.0	16.0	16.5	15.0	
10-8-88	10:00am	19.5	18.0	16.0	14.0	
12-8-88	9:30am	19.5	17.0	17.0	13.5	
15-8-88	9:20am	15.5	17.0	16.5	14.0	
	10:20am	17.0	8.0	12.5	10.5	After preloading
17-8-88	9:40am	14.0	6.5	11.0	10.5	
22-8-88	9:40am	14.5	6.0	10.0	7.5	
29-8-88	9:20am	13.0	3.0	9.0	7.0	
6-9-88	9:10am	11.0	4.0	8.0	5.5	
12-9-88	9:00am	13.0	2.5	7.0	6.5	
4-10-88	9:10am	11.0	2.5	6.0	6.0	
22-11-88	1:30pm	23.50	18.0	20.0	16.5	Preload removed and beams
2-12-88	10:30am	21.0	18.8	12.0	26.5	transferred to Gawler
23-12-88	11:00am	21.5	15.0	10.5	9.0	Topping added
30-12-88	10:30am	22.3	13.5	9.0	9.0	

B.3 Moama data

B.3.1 Strains under base load

South Top - Base Loads					
Strain gauge Number	Strains measured at				
	7:40am	9:40am	11:45am	2:05pm	3:25pm
1	0	-25	-30	30	45
3	0	-10	10	15	25
5	0	-40	-25	-25	-30
7	0	-20	-10	5	5
8	0	-10	-20	-10	5
9	0	-5	10	5	0
10	0	-10	-5	0	15
11	0	-5	-25	15	30

Middle Top - Base Loads					
Strain gauge Number	Strains measured at				
	7:40am	9:40am	11:45am	2:05pm	3:25pm
1	0	15	20	25	50
2	0	-5	0	5	5
3	0	10	25	30	30
5	0	5	10	20	20
6	0	5	15	20	25
7	0	5	15	15	30
8	0	-10	-15	-10	5
9	0	-5	25	35	45
10	0	-5	5	20	15
11	0	0	15	25	30

Middle Bottom - Base Loads					
Strain gauge Number	Strains measured at				
	7:40am	9:40am	11:45am	2:05pm	3:25pm
1	0	-5	0	15	-15
2	0	-10	0	15	-10
3	0	15	35	55	60
4	0	0	10	0	0
5	0	-10	0	10	0
6	0	-10	-10	10	0
7	0	0	0	0	0
8	0	-10	-10	0	10
9	0	0	-10	10	10
10	0	0	0	0	20
11	0	0	-10	0	10

North Top - Base Loads					
Strain gauge Number	Strains measured at				
	7:40am	9:40am	11:45am	2:05pm	3:25pm
1	0	15	40	70	65
3	0	-5	15	35	30
5	0	-10	-5	20	25
7	0	-35	-30	-5	5
8	0	-20	55	80	95
9	0	0	5	30	35
10	0	-15	0	40	55
11	0	-5	-5	15	15

B.3.2 Strains under Live Loads

South Top - Live Loads				
Strain gauge Number	Strains measured at			
	Pattern 1	Pattern 2	Pattern 3	Pattern 4
1	-30	50	-30	15
3	55	30	10	20
5	70	25	20	15
7	70	40	15	50
8	60	30	5	30
9	85	35	0	35
10	65	30	5	15
11	35	50	0	10

Middle Top - Live Loads				
Strain gauge Number	Strains measured at			
	10:50am	12:10pm	1:30pm	2:55pm
	Pattern 1	Pattern 2	Pattern 3	Pattern 4
1	-20	-35	-20	-20
2	-30	-40	-20	-10
3	-45	-45	-50	-15
5	-55	-45	-40	-30
6	-55	-40	-30	-25
7	-45	-55	-30	-25
8	-60	-30	-10	-35
9	-25	-50	0	-25
10	-35	-35	-10	-30
11	-20	-30	0	-15

Middle Bottom - Live Loads				
Strain gauge Number	Strains measured at			
	10:50am	12:10pm	1:30pm	2:55pm
	Pattern 1	Pattern 2	Pattern 3	Pattern 4
1	60	45	10	5
2	70	35	30	-10
3	65	15	15	25
4	60	30	30	-10
5	50	40	20	20
6	40	50	20	30
7	40	50	10	30
8	50	40	20	30
9	40	30	-10	40
10	40	50	10	30
11	40	40	10	20

North Top - Live Loading				
Strain gauge Number	Strains measured at			
	10:50am	12:10pm	1:30pm	2:55pm
	Pattern 1	Pattern 2	Pattern 3	Pattern 4
1	45	10	20	-5
3	70	55	20	15
5	75	70	40	15
7	80	95	20	40
8	115	80	20	50
9	70	80	5	30
10	65	75	0	25
11	40	50	0	5

Appendix C

Creep and shrinkage - Introduction

This appendix aims to provide a brief introduction to those parts of creep and shrinkage theory which are relevant to this work. It is not a comprehensive review, but rather it aims to provide the background needed for a reader who is unfamiliar with the subject.

More detail about this subject may be found in Gilbert (In press), Bažant and Wittmann (1982), or other texts on creep and shrinkage.

C.1 Creep and shrinkage - definitions

If a concrete specimen is placed under a sustained load, then a slow increase in strain will be observed. It is the increase which is caused by the sustained load which is termed creep. The change is often defined in terms of the creep

coefficient, $\phi(t,\tau)$:

$$\phi(t,\tau) = \frac{\epsilon_c(t,\tau)}{\epsilon_e(\tau)} \tag{C.1}$$

where $\epsilon_c(t,\tau) =$ the creep strain in a specimen under a constant load,

$\epsilon_e(\tau) =$ the size of the elastic strain increment,

$t =$ the time since the load was applied (usually in days), and

$\tau =$ the age of the concrete when the load was applied.

τ is required as concrete is an ageing material and the amount of creep produced by a given load will decrease as the age at loading increases.

Creep is sometimes defined using the compliance function (also known as the creep function) which can be written in terms of the creep coefficient as:

$$J(t,\tau) = \frac{1+\phi(t,\tau)}{E(\tau)} \tag{C.2}$$

The main advantage of this approach is that it avoids the need to ensure that compatible values of $\phi(t,\tau)$ and $E(\tau)$ are being used. As it is impossible to load a specimen instantaneously, some creep will occur during the determination of $E(\tau)$, so a predictive formula or test will only give the value of $E(\tau)$ for a loading which took a certain amount of time. A creep formula will give inaccurate answers unless the appropriate value is used. By using the compliance function, this problem can be avoided.

Creep in concrete is approximately proportional to stress, within the range of service stresses (stress less than about 0.4 of the ultimate strength). This allows the strain due to a stress increment to be written as:

$$\epsilon(t) = \frac{\sigma(\tau)}{E(\tau)} + \frac{\sigma(\tau)\phi(t,\tau)}{E(\tau)} + \frac{\sigma(\tau)}{E(\tau)}(1+\phi(t,\tau)) \tag{C.3}$$

omit this term

where $\sigma(\tau)$ is a stress increment applied at time τ, and

$E(\tau)$ is the Young's modulus of the concrete at that time.

Strains also develop in unloaded specimens, principally because of water loss during drying, although carbonation also contributes to this effect. These are termed shrinkage strains and are defined as strains which occur in the absence of load in specimens held at a constant temperature.

The shrinkage strain, ϵ_{sh}, is normally assumed to be the average shrinkage strain across a section, rather than shrinkage at a point. This is done because the moisture loss from a section is greater near the edges leading to larger shrinkage strains at the edges. As a result of this, self equilibrating, elastic strains form in the section to ensure that plane sections remain plane. As there are, at present, no accurate ways for predicting shrinkage strains through a section, it is both simpler and more accurate to use the average strain across the section.

Having defined the creep and shrinkage components of the total strain, we can write the total strain on a concrete section, under a uniaxial stress and at a constant temperature as:

$$\epsilon(t) = \epsilon_e(t) + \epsilon_c(t) + \epsilon_{sh}(t) \tag{C.4}$$

It should be noted that this equation treats creep and shrinkage as being independent. In reality they are interdependent, as the rate of creep increases in a drying environment. This is, however, mostly important in the formulation of the creep and shrinkage functions and should not affect the validity of the analysis.

C.2 Predictive methods

Various creep and shrinkage functions are available, which aim to match the curves obtained experimentally. The parameters in these curves can be found by various means, possibly the most accurate being to fit the curve to test data. Even if only a fairly short series of data is available, this can be relatively accurate.

Various types of relation have been used to fit these curves, including exponential, hyperbolic, logarithmic and power expressions. Hyperbolic functions [Ross (1937)] are used quite often and have the form:

$$\phi(t,\tau) = \frac{(t-\tau)}{\alpha + \beta(t-\tau)} \tag{C.5}$$

This type of function tends to underestimate the long term values of creep. A better fit is often obtained by using a hyperbolic-power relation [ACI-209 (1978)] instead:

$$\phi(t,\tau) = \frac{\alpha(t-\tau)^{\gamma}}{\beta + (t-\tau)^{\gamma}} \tag{C.6}$$

Long time values are still often underestimated with this formula.

Bažant and Osman (1976) presented a double power law for creep of concrete, which they claim provides a good fit for concrete which is not drying (Basic creep only). Reasonable results are claimed for comparisons with drying specimens. The formula is:

$$\phi(t,\tau) = \phi_1 \tau^{-m}(t-\tau)^{n} \tag{C.7}$$

In order to obtain good results with this formula, it is necessary to use the asymptotic Young's modulus for the concrete when calculating the instantaneous strain. The asymptotic modulus corresponds to extrapolation of the creep curve to very short durations and is much higher than the conventional modulus. If the conventional Young's modulus is used then much of the ad-

vantage of this formula is lost. One final advantage in using this formula is that it provides a simple way of accounting for the ageing of the concrete.

When test data is not available, some method is needed to predict the creep and shrinkage curves from the factors which are known. Some of these factors include concrete strength, aggregate type, temperature, humidity, age at loading and the size and shape of the specimen.

However there is, at best, an incomplete understanding of the processes involved in the creep and shrinkage of concrete, meaning that there is no definitive method of predicting creep and shrinkage curves. The method which probably has the best theoretical base is that of Bažant and Panula (1978), however the method is extremely complex, and not significantly more accurate than other, simpler methods. Some of the other methods are given in CEB-FIP (1978), ACI-209 (1978) and AS3600 (SAA, 1988). Reviews of the various methods are presented by Gilbert (In press), Bažant and Panula (1980) and Diamantidis et. al. (1984).

The method given in AS3600 was used for the calculation of final creep and shrinkage values in this work. Unfortunately, AS3600 does not give an equation for the shape of these curves. For this reason, the equation given by ACI-209 was used to define the curve shape. Both of these methods make no pretense of any great accuracy, however they are simple and give reasonable answers.

Appendix D

Beam Designs

D.1 14m. Plank - Pattern 1

1. **Deflections**

- At transfer	2.81 mm.
- Topping added at 28 days	
Before addition of topping	3.55 mm.
After addition of topping	-1.65 mm.
At 500 days	-4.91 mm.
Under live load	-19.53 mm.

Live load increment / span = $\frac{\Delta}{L} = \frac{1}{956}$

- Topping added at 300 days	
Before addition of topping	2.35 mm.
After addition of topping	-2.52 mm.
At 500 days	-8.35 mm.

Under live load -25.46 mm.

Live load increment / span $= \frac{\Delta}{L} = \frac{1}{818}$

2. **Stress Increment after decompression**

   Stress increment = 33.9 MPa.

3. **Ultimate Strength**

   - $M_u = 1342$ kNm
   - $\frac{\phi M_u}{M^*} = 1.13$

4. **Shear Details** Yet to be designed

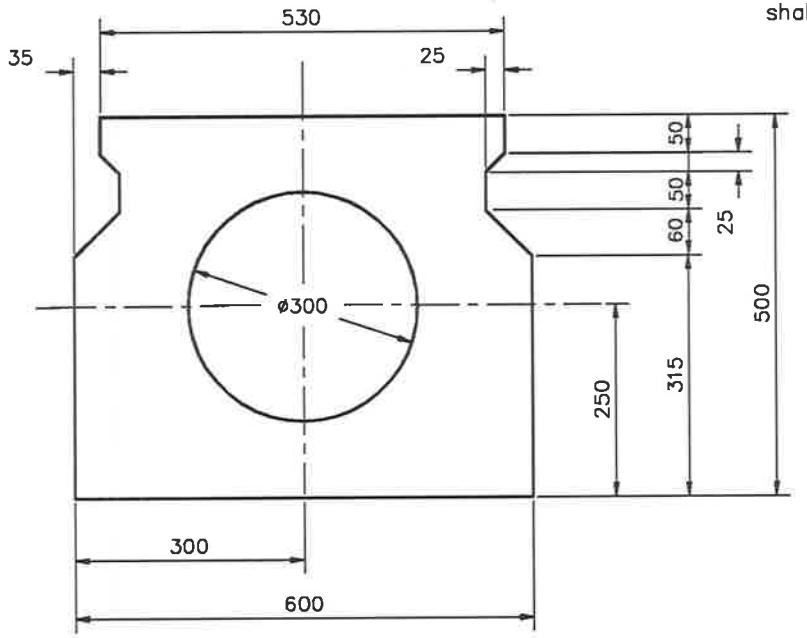

END ELEVATION
SCALE 1:10

The force at the midspan of each of these strands, immediately after the release of the tensioning jacks shall be 139kN.

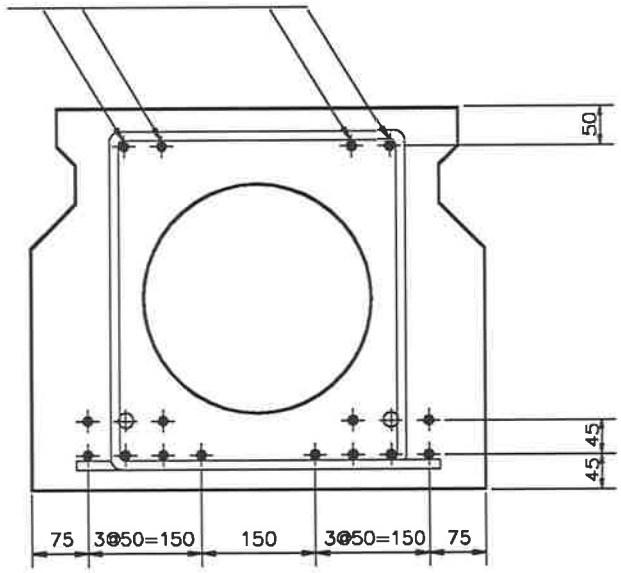

18/ 12.7mm LOW RELAXATION SUPER GRADE STRANDS

REINFORCEMENT AND STRAND DETAIL
2/ 20 Y bars 14000 long ⊕
16/φ12.7mm LOW RELAXATION SUPER GRADE STRANDS ✦
STRANDS SHALL BE STRAIGHT
SCALE 1:10

General Notes

Minimum 28 day compressive strength of concrete shall be 40MPa. Minimum compressive strength of concrete at transfer of prestress shall be 32MPa. Debonding may be used to reduce this.

The force in each 12.7mm strand at the mid-span of the plank immediately after the release of the pretensioning jack shall be 128kN or as shown on the drawing.

PRELIMINARY DESIGN	
14m. SPAN PARTIAL PSC PLANK	
DESIGN DRAWN	Sheet No. 1
DATE 24-11-88	No. of sheets 1

D.2 14m. Plank - Pattern 2

1. **Deflections**

   - At transfer 2.82 mm.
   - Topping added at 28 days
     - Before addition of topping 4.47 mm.
     - After addition of topping -0.81 mm.
     - At 500 days -3.60 mm.
     - Under live load -17.84 mm.

   Live load increment / span = $\frac{\Delta}{L} = \frac{1}{983}$

   - Topping added at 300 days
     - Before addition of topping 3.88 mm.
     - After addition of topping -1.15 mm.
     - At 500 days -7.02 mm.
     - Under live load -23.58 mm.

   Live load increment / span = $\frac{\Delta}{L} = \frac{1}{845}$

2. **Stress Increment after Decompression** Stress increment = 26.2 MPa.

3. **Ultimate Strength**

   - $M_u = 1288$ kNm
   - $\frac{\phi M_u}{M^*} = 1.08$

4. **Shear Details** Yet to be designed

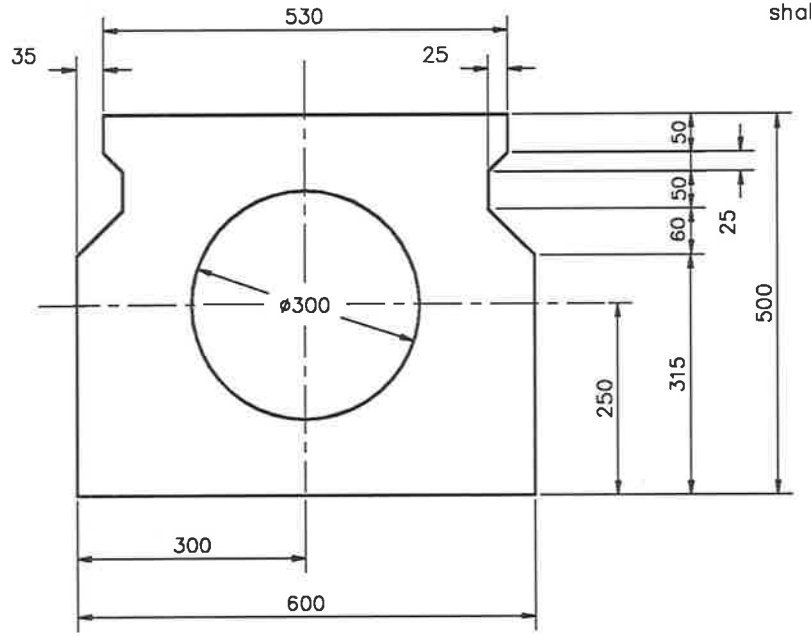

END ELEVATION
SCALE 1:10

The force at the midspan of each of these strands, immediately after the release of the tensioning jacks shall be 139kN.

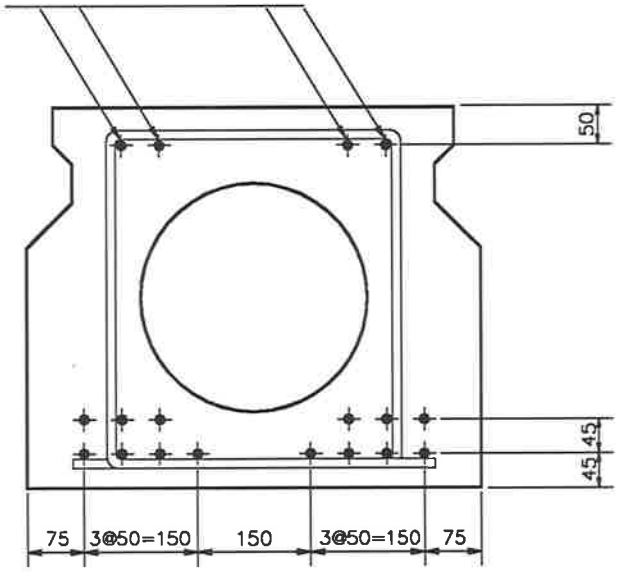

REINFORCEMENT AND STRAND DETAIL
18/φ12.7mm LOW RELAXATION SUPER GRADE STRANDS ✦
STRANDS SHALL BE STRAIGHT
SCALE 1:10

General Notes

Minimum 28 day compressive strength of concrete shall be 40MPa. Minimum compressive strength of concrete at transfer of prestress shall be 35 MPa. Debonding may be used to reduce this.

The force in each 12.7mm strand at the mid-span of the plank immediately after the release of the pretensioning jack shall be 111kN or as shown on the drawing.

PRELIMINARY DESIGN	
14m. SPAN PARTIAL PSC PLANK	
DESIGN DRAWN	Sheet No. 1
DATE 24-11-88	No. of sheets 1

D.3 16m. Plank - Pattern 1

1. **Deflections**

- At transfer	3.91 mm.
- Topping added at 28 days	
Before addition of topping	4.37 mm.
After addition of topping	-1.02 mm.
At 500 days	-5.73 mm.
Under live load	-21.30 mm.

Live load increment / span = $\frac{\Delta}{L} = \frac{1}{1028}$

- Topping added at 300 days	
Before addition of topping	2.52 mm.
After addition of topping	-2.40 mm.
At 500 days	-8.41 mm.
Under live load	-26.64 mm.

Live load increment / span = $\frac{\Delta}{L} = \frac{1}{878}$

2. **Stress Increment after Decompression** Stress increment = 30.7 MPa.

3. **Ultimate Strength**

   - $M_u = 1698$ kNm
   - $\frac{\phi M_u}{M^*} = 1.04$

4. **Shear Details** Yet to be designed

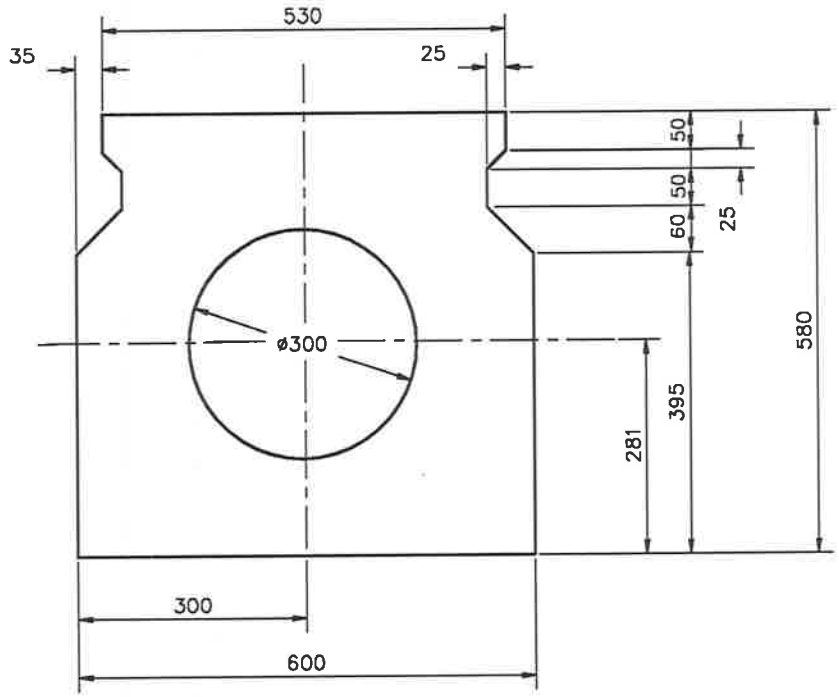

END ELEVATION
SCALE 1:10

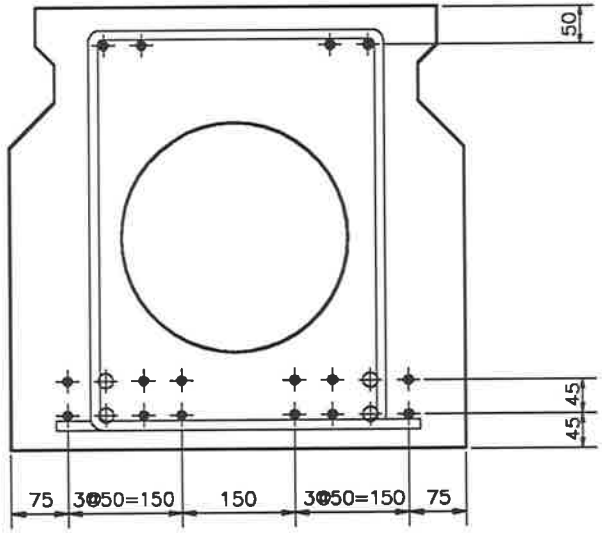

REINFORCEMENT AND STRAND DETAIL
4/20 Y bars 16000 LONG ⊕
16/φ12.7mm LOW RELAXATION SUPER GRADE STRANDS ✦
STRANDS SHALL BE STRAIGHT
SCALE 1:10

General Notes

Minimum 28 day compressive strength of concrete shall be 40MPa. Minimum compressive strength of concrete at transfer of prestress shall be 35MPa. Debonding could be used to reduce this.

The force in each 12.7mm strand at the mid-span of the plank immediately after the release of the pretensioning jack shall be 139kN.

PRELIMINARY DESIGN	
16m. SPAN PARTIAL PSC PLANK	
DESIGN DRAWN	Sheet No. 1
DATE 24-11-88	No. of sheets 1

D.4 16m. Plank - Pattern 2

1. **Deflections**

- At transfer	4.84 mm.
- Topping added at 28 days	
Before addition of topping	8.80 mm.
After addition of topping	3.22 mm.
At 500 days	-0.37 mm.
Under live load	-15.65 mm.

Live load increment / span = $\frac{\Delta}{L} = \frac{1}{1047}$

- Topping added at 300 days	
Before addition of topping	8.79 mm.
After addition of topping	3.50 mm.
At 500 days	-2.61 mm.
Under live load	-20.32 mm.

Live load increment / span = $\frac{\Delta}{L} = \frac{1}{903}$

2. **Stress Increment after Decompression** Stress increment = 21.0 MPa.

3. **Ultimate Strength**

   - $M_u = 1650$ kNm
   - $\frac{\phi M_u}{M^*} = 1.01$

4. **Shear Details** Yet to be designed

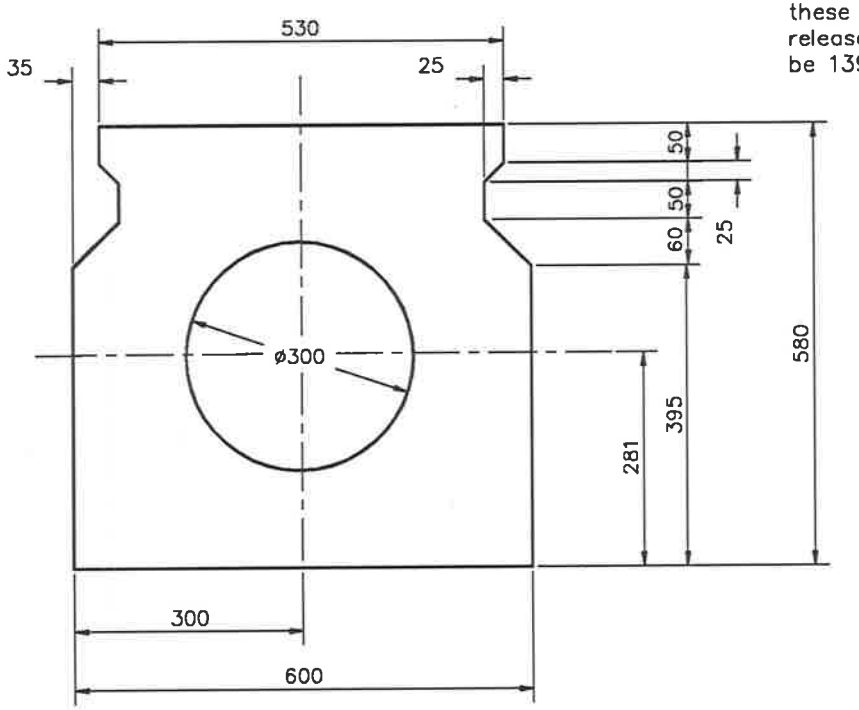

END ELEVATION
SCALE 1:10

The force in the midspan of each of these strands, immediately after the release of the tensioning jacks shall be 139kN.

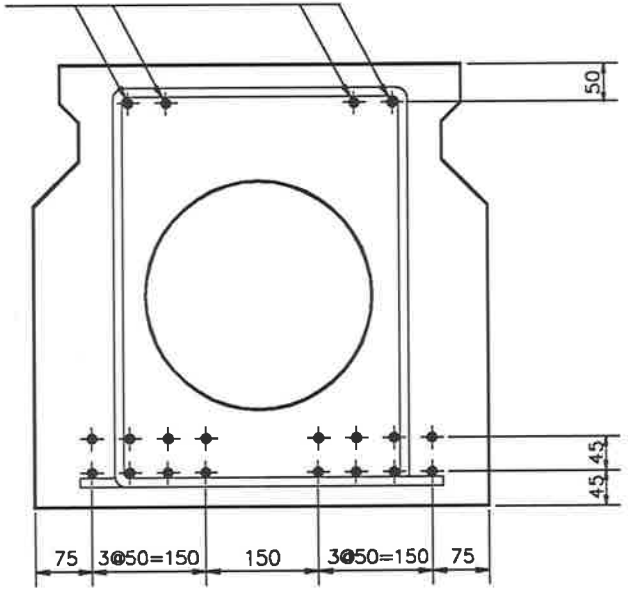

REINFORCEMENT AND STRAND DETAIL
20/φ12.7mm LOW RELAXATION SUPER GRADE STRANDS ✦
STRANDS SHALL BE STRAIGHT
SCALE 1:10

General Notes

Minimum 28 day compressive strength of concrete shall be 40MPa. Minimum compressive strength of concrete at transfer of prestress shall be 32MPa. Debonding could be used to reduce this.

The force in each 12.7mm strand at the mid-span of the plank immediately after the release of the pretensioning jack shall be 117kN.

PRELIMINARY DESIGN	
16m. SPAN PARTIAL PSC PLANK	
DESIGN DRAWN	Sheet No. 1
DATE 24-11-88	No. of sheets 1

D.5 18m. Plank - Pattern 1

1. **Deflections**

   - At transfer 6.71 mm.
   - Topping added at 28 days
     - Before addition of topping 10.31 mm.
     - After addition of topping 3.99 mm.
     - At 500 days -1.39 mm.
     - Under live load -19.01 mm.

   Live load increment / span = $\frac{\Delta}{L} = \frac{1}{1022}$

   - Topping added at 300 days
     - Before addition of topping 9.11 mm.
     - After addition of topping 3.33 mm.
     - At 500 days -3.74 mm.
     - Under live load -23.92 mm.

   Live load increment / span = $\frac{\Delta}{L} = \frac{1}{892}$

2. **Stress Increment after Decompression** Stress increment = 25.8 MPa.

3. **Ultimate Strength**

   - $M_u = 2209$ kNm
   - $\frac{\phi M_u}{M^*} = 1.05$

4. **Shear Details** Yet to be designed

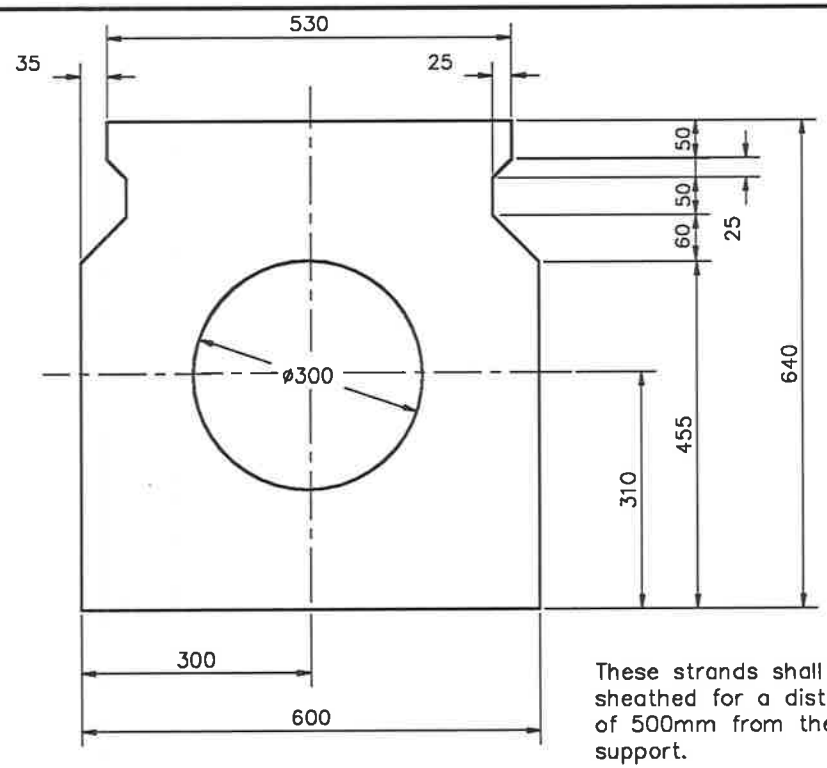

END ELEVATION
SCALE 1:10

These strands shall be sheathed for a distance of 500mm from the support.

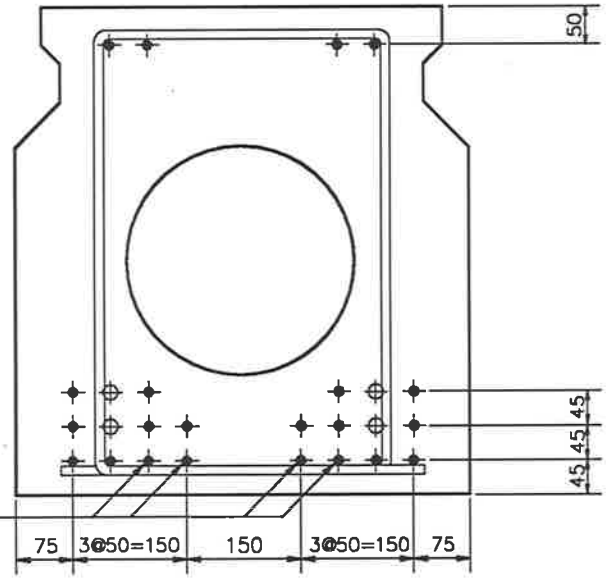

REINFORCEMENT AND STRAND DETAIL
4/20 Y bars 18000 LONG ⊕
22/φ12.7mm LOW RELAXATION SUPER GRADE STRANDS ✦
STRANDS SHALL BE STRAIGHT
SCALE 1:10

General Notes

Minimum 28 day compressive strength of concrete shall be 40MPa. Minimum compressive strength of concrete at transfer of prestress shall be 35MPa.

The force in each 12.7mm strand at the mid-span of the plank immediately after the release of the tensioning jack shall be 128kN unless otherwise shown.

PRELIMINARY DESIGN	
18m. SPAN PARTIAL PSC PLANK	
DESIGN DRAWN	Sheet No. 1
DATE 24-11-88	No. of sheets 1

D.6 18m. Plank - Pattern 2

1. **Deflections**

- At transfer	6.15 mm.
- Topping added at 28 days	
Before addition of topping	10.88 mm.
After addition of topping	4.36 mm.
At 500 days	-0.17 mm.
Under live load	-17.59 mm.

Live load increment / span = $\frac{\Delta}{L} = \frac{1}{1033}$

- Topping added at 300 days	
Before addition of topping	10.72 mm.
After addition of topping	4.58 mm.
At 500 days	-2.60 mm.
Under live load	-22.34 mm.

Live load increment / span = $\frac{\Delta}{L} = \frac{1}{912}$

2. **Stress Increment after Decompression** Stress increment = 18.1 MPa.

3. **Ultimate Strength**

   - $M_u = 2147$ kNm
   - $\frac{\phi M_u}{M^*} = 1.02$

4. **Shear Details** Yet to be designed

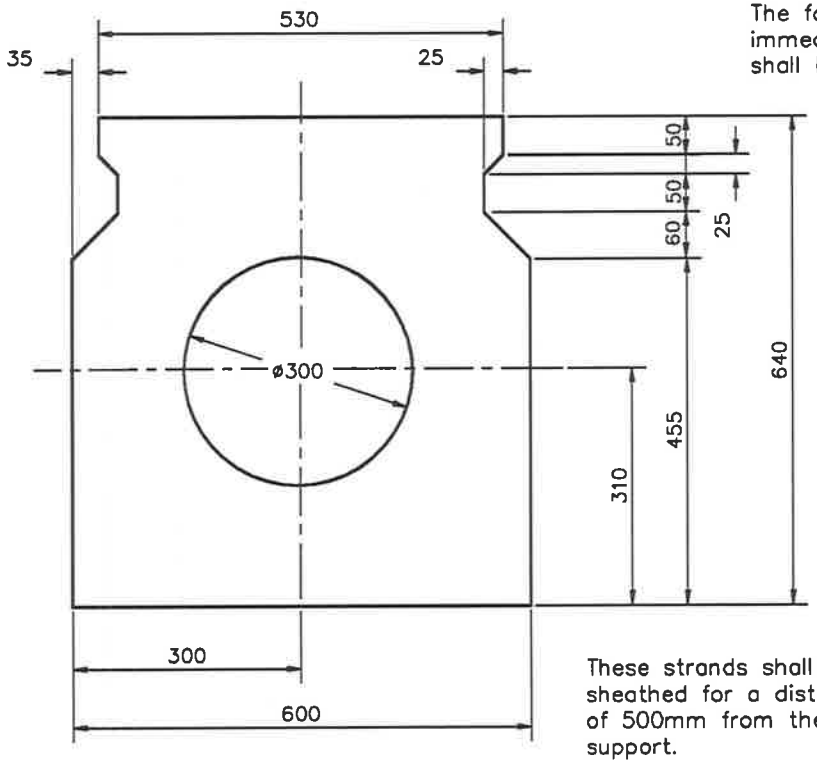

END ELEVATION
SCALE 1:10

The force at the midspan of each of these strands, immediately after the release of the tensioning jacks shall be 139kN.

These strands shall be sheathed for a distance of 500mm from the support.

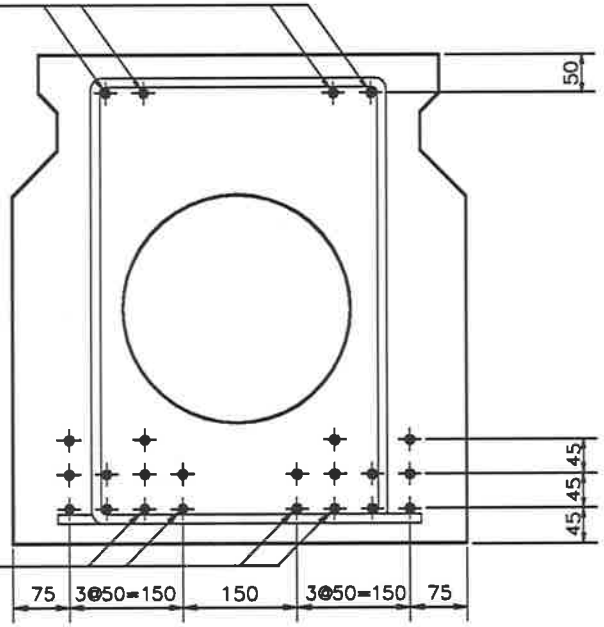

REINFORCEMENT AND STRAND DETAIL
24/φ12.7mm LOW RELAXATION SUPER GRADE STRANDS ✦
STRANDS SHALL BE STRAIGHT
SCALE 1:10

General Notes

Minimum 28 day compressive strength of concrete shall be 40MPa. Minimum compressive strength of concrete at transfer of prestress shall be 35MPa.

The force in each 12.7mm strand at the mid-span of the plank immediately after the release of the tensioning jack shall be 115kN unless otherwise shown.

PRELIMINARY DESIGN	
18m. SPAN PARTIAL PSC PLANK	
DESIGN DRAWN	Sheet No. 1
DATE 24-11-88	No. of sheets 1

D.7 20m. Plank - Pattern 1

1. **Deflections**

   - At transfer 5.81 mm.
   - Topping added at 28 days
     - Before addition of topping 6.01 mm.
     - After addition of topping -1.22 mm.
     - At 500 days -8.73 mm.
     - Under live load -28.51 mm.

   Live load increment / span $= \frac{\Delta}{L} = \frac{1}{1011}$

   - Topping added at 300 days
     - Before addition of topping 3.13 mm.
     - After addition of topping -3.38 mm.
     - At 500 days -11.41 mm.
     - Under live load -33.90 mm.

   Live load increment / span $= \frac{\Delta}{L} = \frac{1}{889}$

2. **Stress Increment after Decompression** Stress increment = 26.6 MPa.

3. **Ultimate Strength**

   - $M_u = 2709$ kNm
   - $\frac{\phi M_u}{M^*} = 1.02$

4. **Shear Details** Yet to be designed

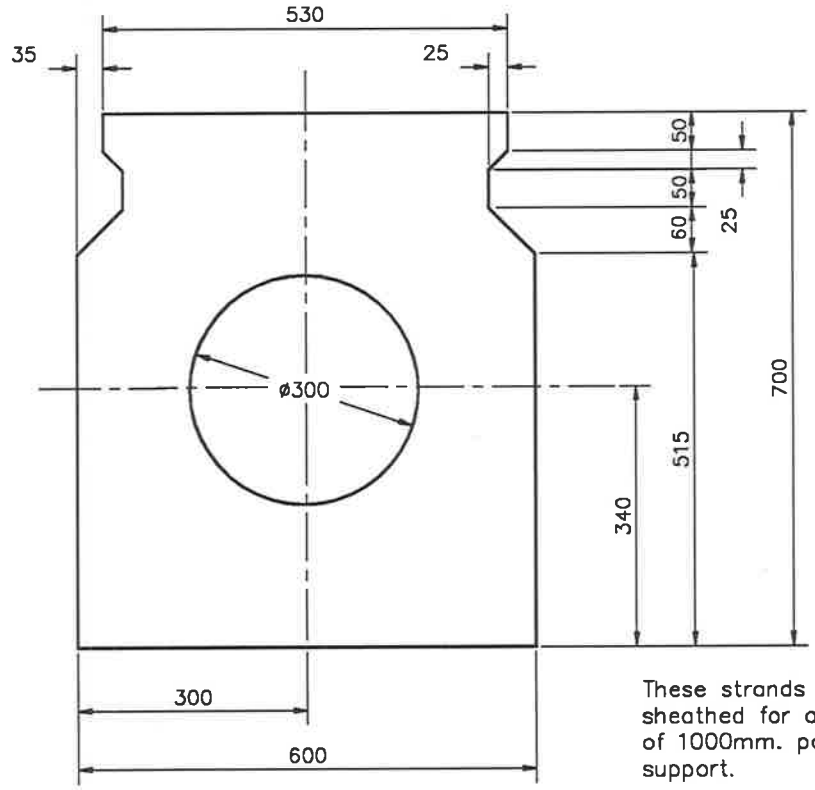

END ELEVATION
SCALE 1:10

These strands shall be sheathed for a distance of 1000mm. past the support.

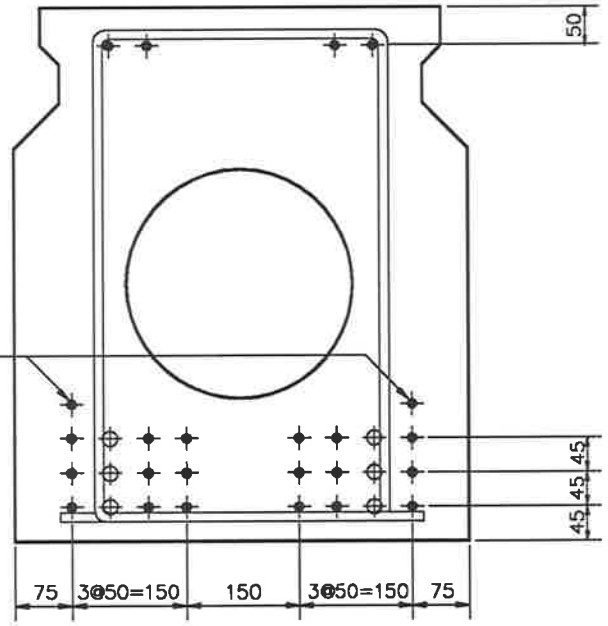

REINFORCEMENT AND STRAND DETAIL
6/20 Y bars 20000 LONG ⊕
24/φ12.7mm LOW RELAXATION SUPER GRADE STRANDS ✦
STRANDS SHALL BE STRAIGHT
SCALE 1:10

General Notes

Minimum 28 day compressive strength of concrete shall be 40MPa. Minimum compressive strength of concrete at transfer of prestress is 35MPa.

The force in each 12.7mm strand at the mid-span of the plank immediately after the release of the tensioning jack shall be 139kN unless otherwise shown.

PRELIMINARY DESIGN	
20m. SPAN PARTIAL PSC PLANK	
DESIGN DRAWN	Sheet No. 1
DATE 24-11-88	No. of sheets 1

D.8 20m. Plank - Pattern 2

1. **Deflections**

   - At transfer 6.79 mm.
   - Topping added at 28 days
     - Before addition of topping 11.27 mm.
     - After addition of topping 3.78 mm.
     - At 500 days -2.23 mm.
     - Under live load -21.89 mm.

   Live load increment / span = $\frac{\Delta}{L} = \frac{1}{1017}$

   - Topping added at 300 days
     - Before addition of topping 10.71 mm.
     - After addition of topping 3.69 mm.
     - At 500 days -4.49 mm.
     - Under live load -26.66 mm.

   Live load increment / span = $\frac{\Delta}{L} = \frac{1}{902}$

2. **Stress Increment after Decompression** Stress increment = 18.7 MPa.

3. **Ultimate Strength**

   - $M_u = 2699$ kNm
   - $\frac{\phi M_u}{M^*} = 1.03$

4. **Shear Details** Yet to be designed

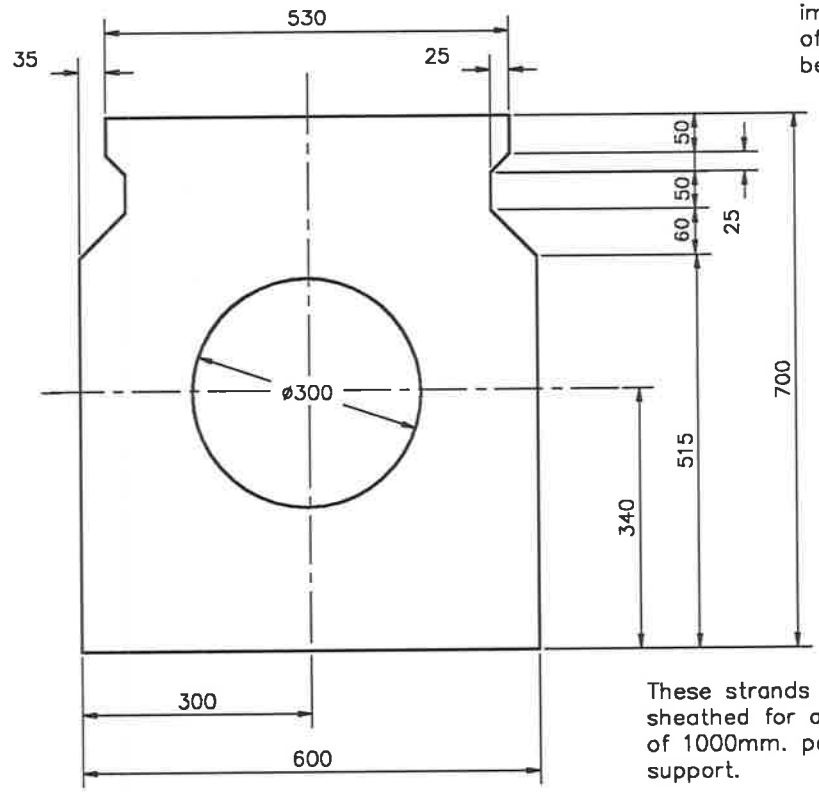

END ELEVATION
SCALE 1:10

The force in these strands, immediately after the release of the tensioning jacks, shall be 139kN.

These strands shall be sheathed for a distance of 1000mm. past the support.

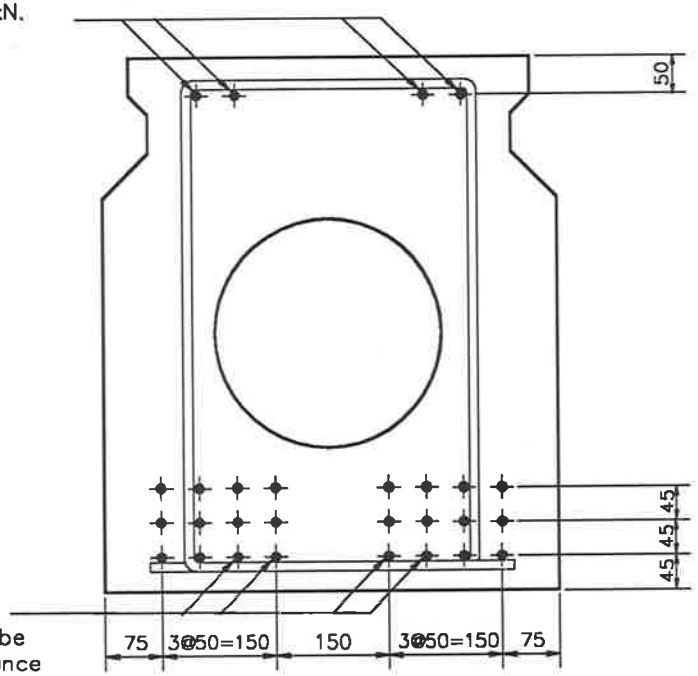

REINFORCEMENT AND STRAND DETAIL
28/φ12.7mm LOW RELAXATION SUPER GRADE STRANDS ✦
STRANDS SHALL BE STRAIGHT
SCALE 1:10

General Notes

Minimum 28 day compressive strength of concrete shall be 40MPa. Minimum compressive strength of concrete at transfer of prestress is 35MPa.

The force in each 12.7mm strand at the mid-span of the plank immediately after the release of the tensioning jack shall be 111kN unless otherwise shown.

PRELIMINARY DESIGN	
20m. SPAN PARTIAL PSC PLANK	
DESIGN DRAWN	Sheet No. 1
DATE 24-11-88	No. of sheets 1

Appendix E

Linear Analysis - Equations

Two sets of equations are given, the first set applies prior to the topping being added, the second apply after the topping is added.

The basic array, which applies all of the time is-

$$\begin{bmatrix} A11 & A12 \\ A21 & A22 \end{bmatrix} \begin{bmatrix} \epsilon_0[t] \\ \epsilon_b[t] \end{bmatrix} = \begin{bmatrix} A13 \\ A23 \end{bmatrix} \tag{E.1}$$

Before the topping is added, the following equations are used to evaluate the terms in the array-

$$A11 = \sum_{i=1}^{N_c} b_{pl}[i]t[i]E_{pl}\left(\frac{D - d_c[i]}{D}\right) + \sum_{j=1}^{N_s} E_s A_s[j]\left(\frac{D - d_s[j]}{D}\right) + \sum_{k=1}^{N_p} E_p A_p[k]\left(\frac{D - d_p[k]}{D}\right) \tag{E.2}$$

$$A12 = \sum_{i=1}^{N_c} b_{pl}[i]t[i]E_{pl}\left(\frac{d_c[i]}{D}\right) + \sum_{j=1}^{N_s} E_s A_s[j]\left(\frac{d_s[j]}{D}\right) + \sum_{k=1}^{N_p} E_p A_p[k]\left(\frac{d_p[k]}{D}\right) \tag{E.3}$$

$$A21 = \sum_{i=1}^{N_c} b_{pl}[i]t[i]E_{pl}\left(\frac{D-d_c[i]}{D}\right)d_c[i] + \sum_{j=1}^{N_s} E_sA_s[j]\left(\frac{D-d_s[j]}{D}\right)d_s[j] + \sum_{k=1}^{N_p} E_pA_p[k]\left(\frac{D-d_p[k]}{D}\right)d_p[k] \quad \text{(E.4)}$$

$$A22 = \sum_{i=1}^{N_c} b_{pl}[i]t[i]E_{pl}\left(\frac{d_c[i]}{D}\right)d_c[i] + \sum_{j=1}^{N_s} E_sA_s[j]\left(\frac{d_s[j]}{D}\right)d_s[j] + \sum_{k=1}^{N_p} E_pA_p[k]\left(\frac{d_p[k]}{D}\right)d_p[k] \quad \text{(E.5)}$$

$$A13 = \sum_{i=1}^{N_c}\left[E_{pl}b_{pl}[i]t[i]\left(\epsilon(0)\phi(t,\tau_0) + \sum_{j=1}^{i-1}\epsilon(\tau_j)\phi(\tau_i,\tau_j) + \epsilon_{sh}(\tau_i)\right)\right] + \sum_{k=1}^{N_p}\sigma_p[k,0]A_p[k] \quad \text{(E.6)}$$

$$A23 = \sum_{i=1}^{N_c}\left[E_{pl}b_{pl}[i]t[i]\left(\epsilon(0)\phi(t,\tau_0) + \sum_{j=1}^{i-1}\epsilon(\tau_j)\phi(\tau_i,\tau_j) + \epsilon_{sh}(\tau_i)\right)d_c[i]\right] + \sum_{k=1}^{N_p}\sigma_p[k,0]A_p[k]d_p[i] - M_{applied} \quad \text{(E.7)}$$

The total strain in the cross-section at time t_n, as defined by $\epsilon_0[t_n]$ and $\epsilon_b[t_n]$ is then found by solving the equation E.1.

After the addition of the topping concrete, the equations become-

$$A11 = \sum_{i=1}^{N_c} b_{pl}[i]t[i]E_{pl}\left(\frac{D-d_c[i]}{D}\right) + \sum_{j=1}^{N_s} E_sA_s[j]\left(\frac{D-d_s[j]}{D}\right) + \sum_{k=1}^{N_p} E_pA_p[k]\left(\frac{D-d_p[k]}{D}\right) + \sum_{i=1}^{N_c} b_{top}[i]t[i]E_{top}\left(\frac{D-d_c[i]}{D}\right) + \sum_{m=1}^{N_t} E_sA_{st}[m]\left(\frac{D-d_{st}[m]}{D}\right) \quad \text{(E.8)}$$

$$A12 = \sum_{i=1}^{N_c} b_{pl}[i]t[i]E_{pl}\left(\frac{d_c[i]}{D}\right) + \sum_{j=1}^{N_s} E_s A_s[j]\left(\frac{d_s[j]}{D}\right) + \sum_{k=1}^{N_p} E_p A_p[k]\left(\frac{d_p[k]}{D}\right) + \sum_{i=1}^{N_c} b_{top}[i]t[i]E_{top}\left(\frac{d_c[i]}{D}\right) + \sum_{m=1}^{N_t} E_s A_{st}[m]\left(\frac{d_{st}[m]}{D}\right) \quad \text{(E.9)}$$

$$A21 = \sum_{i=1}^{N_c} b_{pl}[i]t[i]E_{pl}\left(\frac{D-d_c[i]}{D}\right)d_c[i] + \sum_{j=1}^{N_s} E_s A_s[j]\left(\frac{D-d_s[j]}{D}\right)d_s[j] + \sum_{k=1}^{N_p} E_p A_p[k]\left(\frac{D-d_p[k]}{D}\right)d_p[k] + b_{top}[i]t[i]E_{top}d_c[i]\left(\frac{D-d_c[i]}{D}\right) + \sum_{m=1}^{N_t} E_s A_{st}[m]d_{st}[m]\left(\frac{D-d_{st}[m]}{D}\right) \quad \text{(E.10)}$$

$$A22 = \sum_{i=1}^{N_c} b_{pl}[i]t[i]E_{pl}\left(\frac{d_c[i]}{D}\right)d_c[i] + \sum_{j=1}^{N_s} E_s A_s[j]\left(\frac{d_s[j]}{D}\right)d_s[j] + \sum_{k=1}^{N_p} E_p A_p[k]\left(\frac{d_p[k]}{D}\right)d_p[k] + \sum_{i=1}^{N_c} b_{top}[i]t[i]E_{top}d_c[i]\left(\frac{d_c[i]}{D}\right) + \sum_{m=1}^{N_t} E_s A_{st}[m]d_{st}[m]\left(\frac{d_{st}[m]}{D}\right) \quad \text{(E.11)}$$

$$A13 = \sum_{i=1}^{N_c}\left[E_{pl}b_{pl}[i]t[i]\left(\epsilon(0)\phi(t,\tau_0) + \sum_{j=1}^{i-1}\epsilon(\tau_j)\phi(\tau_i,\tau_j) + \epsilon_{sh}(\tau_i)\right)\right] + \sum_{i=1}^{N_c}\left[E_{top}b_{top}[i]t[i]\left(\epsilon(0)\phi(t,\tau_0) + \sum_{j=1}^{i-1}\epsilon(\tau_j)\phi(\tau_i,\tau_j) + \epsilon_{sh}(\tau_i) + \epsilon_{ref}[i]\right)\right] + \sum_{k=1}^{N_p}\sigma_p[k,0]A_p[k] + \sum_{m=1}^{N_t} E_s A_{st}[m]\epsilon_{ref}[m] \quad \text{(E.12)}$$

$$A23 = \sum_{i=1}^{N_c}\left[E_{pl}b_{pl}[i]t[i]\left(\epsilon(0)\phi(t,\tau_0) + \sum_{j=1}^{i-1}\epsilon(\tau_j)\phi(\tau_i,\tau_j) + \epsilon_{sh}(\tau_i)\right)d_c[i]\right] +$$

$$\sum_{i=1}^{N_c}\left[E_{top}b_{top}[i]t[i]\left(\epsilon(0)\phi(t,\tau_0)+\sum_{j=1}^{i-1}\epsilon(\tau_j)\phi(\tau_i,\tau_j)+\epsilon_{sh}(\tau_i)+\epsilon_{ref}[i]\right)d_c[i]\right]+$$
$$\sum_{k=1}^{N_p}\sigma_p[k,0]A_p[k]d_p[i]+\sum_{m=1}^{N_t}E_sA_{st}[m]\epsilon_{ref}[m]d_{st}[m]-M_{applied} \qquad \text{(E.13)}$$

Bibliography

[1] Abeles, P.W. (1945), *Fully and Partially Prestressed Reinforced Concrete,* ACI Journal, Proceedings, Vol. 41, No. 3, January, 1945, pp.181-216.

[2] Abeles, P.W. (1948), *The economy of prestressed concrete,* Final Report of the Third Congress of the IABSE, Liège, 1948. Paper IIb-4, pp. 379-385.

[3] Abeles, P.W. (1952), *The use of high-strength steel in ordinary reinforced and prestressed concrete beams,* IABSE. Preliminary Publication for the Fourth Congress held at Cambridge and London, 1952. Paper CII-2, pp.871-891.

[4] Abeles, P.W. (1967), *Design of Partially Prestressed Concrete Beams,* ACI Journal / October 1967, Vol. 64, No. 10, pp. 669-677.

[5] ACI Committee 209 (1978), *Prediction of Creep, Shrinkage and Temperature Effects in Concrete Structures,* ACI Symposium for Creep and Shrinkage, Nov. 2, 1978. Fall Convention of the ACI, Houston, Texas.

[6] Al-Zaid, R.Z. ; Naaman, A.E. (1986), *Analysis of Partially Prestressed Composite Beams,* Journal of the Structural Division of the ASCE, Vol. 112, No. 4, April, 1986, pp.709-725.

[7] Al-Zaid, R.Z. ; Naaman, A.E. (1988a), *Closure to "Analysis of Prestressed Composite Beams",* Journal of the Structural Division of the ASCE, Vol. 114, No. 1, Jan., 1988, pp.243-246.

[8] Al-Zaid, R.Z. ; Naaman, A.E. ; Nowak, A.S. (1988b), *Partially Prestressed Composite Beams Under Sustained and Cyclic Loads,* Journal of Structural Engineering, Vol. 114, No. 2, Feb., 1988, pp.269-291.

[9] Arutyunyan, N. Kh. (1966), *Some Problems in the Theory of Creep in Concrete Structures,* Pergammon Press, 290pp.

[10] Bachmann, H. (1984), *Design of Partially Prestressed Concrete Structures Based on Swiss Experiences,* PCI Journal / July-Aug. 1984, pp.84-105.

[11] Baurs, R.; Depauw, V. (1966), *Investigation of Partial Prestressing,* "Annales Des Travaux Publics De Belgique," No. 2, April 1966, pp.34-73.

[12] Bay, H. (1962), *General Report - Economics of prestressed concrete in relation to regulations, safety, partial prestressing, lightweight concrete, etc.,* Fourth FIP Congress, Rome-Naples, 1962, Vol. 2, Theme III.

[13] Bažant, Z.P. (1972), *Prediction of Concrete Creep Effects Using Age Adjusted Effective Modulus Method,* ACI Journal, April 1972, pp.212-217.

[14] Bažant, Z.P. ; Najjar, L.J. (1973), *Comparisons of Approximate Linear Methods for Concrete Creep,* Journal of the Structural Division, Proceedings of the ASCE, Vol. 99, No. ST9, Sept., 1973, pp.1851-1874.

[15] Bažant, Z.P. ; Osman, E. (1976a), *Double Power Law for Basic Creep of Concrete,* Matériaux et Constructions, Vol. 9, No. 49, pp.3-11.

[16] Bažant, Z.P. ; Osman. E. ; Thonguthai, W. (1976b), *Practical Formulation of Shrinkage and Creep of Concrete,* Matériaux et Constructions, Vol. 9, No. 54, pp.395-406.

[17] Bažant, Z.P. ; Panula, L. (1978), *Practical Prediction of time-dependent deformations of concrete. Part 1: Shrinkage. Part 2: Basic creep,* Matériaux et Constructions, Vol. 11, No. 65, pp.307-328. *Part 3: Drying Creep. Part 4: Temperature Effect on Basic Creep,* Matériaux et Constructions, Vol. 11, No. 66, pp.415-435. *Part 5: Temperature Effect on*

drying creep. Part 6: Cyclic creep, nonlinearity and statistical scatter, Matériaux et Constructions, Vol. 12, No. 69, pp.169-183.

[18] Bažant, Z.P. ; Panula, L. (1979), *A note on the limitations of a certain creep function used in practice,* Matériaux et Constructions, Vol. 12, No. 67, pp.29-31.

[19] Bažant, Z.P. ; Panula, L. (1980), *Creep and Shrinkage Characterisation for Analysing Prestressed Concrete Structures,* PCI Journal, May-June, 1980, pp.86-122.

[20] Bažant, Z.P. ; Wittmann, F.H. (1982), *Creep and Shrinkage in Concrete Structures,* John Wiley and Sons, Ltd.

[21] Bažant, Z.P. ; Oh, B.H. (1983a), *Deformation of Cracked Net-Reinforced Concrete Walls,* Journal of the Structural Division of the ASCE, Vol. 109, No. 1, January 1983, pp.93-108.

[22] Bažant, Z.P. ; Oh, B.H (1983b)., *Crack Bond Theory for Fracture of Concrete,* Matériaux et Constructions , Vol. 16, No. 93, July, 1983, pp.155-177.

[23] Bažant, Z.P. ; Oh, B.H. (1984), *Deformation of Progressively Cracking Reinforced Concrete Beams,* ACI Journal / May-June, 1984, No. 3, pp.268-278.

[24] Bažant, Z.P. ; Chern, J.C. (1985a), *Concrete Creep at variable humidity: Constitutive Law and Mechanism,* Matériaux et Constructions, Vol. 18, No. 103, pp.1-20.

[25] Bažant, Z.P. ; Wang, T.S. (1985b), *Practical Prediction of cyclic humidity effect in creep and shrinkage of concrete,* Matériaux et Constructions, Vol. 18, No. 106, pp.247-252.

[26] Bažant, Z.P. ; Kwang, L.L. (1985c), *Random Creep and Shrinkage in Structures: Sampling,* Journal of the Structural Division of the ASCE, Vol. 111, No. 5, May, 1985, pp.1113-1134.

[27] Beasley, A.J. (1987a), *A Numerical Solution for the Prediction of Elastic, Creep, Shrinkage and Thermal Deformations in the Columns and Cores of Tall Concrete Buildings,* Research Report CM - 87/2, Civil and Mechanical Engineering Department, University of Tasmania.

[28] Beasley, A.J. (1987b), *COLECS - A Computer Program for the Analysis of Elastic, Creep, Shrinkage and Thermal Deformations in the Columns and Cores of Tall Concrete Buildings,* Research Report CM - 87/3, Civil and Mechanical Engineering Department, University of Tasmania.

[29] Bennett, E.W.; Veerasubramanian, N. (1972), *Behaviour of Non-Rectangular Beams with Limited Prestress after Flexural Cracking,* ACI Journal / September 1972, pp. 533-542, Vol. 69, No. 9.

[30] Bennett, E.W. (1984), *Partial Prestressing - A Historical Overview,* PCI Journal / Sept.-Oct. 1984, Vol. 29, No. 5, pp. 104-117.

[31] Branson, D.E. ; Ozell, A.M. (1961), *Camber in Prestressed Concrete Beams,* Journal of the American Concrete Institute, Vol. 32, No. 12, June 1961, (Proceedings Vol. 57), pp.1549-1574.

[32] Branson, D.E. (1964), *Time Dependent Effects in Composite Concrete Beams,* ACI Journal, Proceedings Vol. 61, No. 2, Feb. 1964, pp.213-230.

[33] Branson, D.E. (1968), *Design Procedures for Computing Deflections,* ACI Journal, Proceedings Vol. 65, No. 9, Sept. 1968, pp.730-742.

[34] Branson, D.E.; Meyers, B.L.; Kripanarayanan, K.M. (1970), *Time Dependent Deformation of Non-Composite and Composite Prestressed Concrete Structures,* National Academy of Sciences – National Academy of En-

gineering, Highway Research Record, No. 324, Symposium on Concrete Deformation, Fall 1970, pp.15-43.

[35] Branson, D.E.; Kripanarayanan, K.M. (1971a), *Loss of Prestress, Camber and Deflection of Non-Composite and Composite Prestressed Concrete Structures,* PCI Journal, Vol. 16, No. 5, Sept-Oct. 1971, pp.22-52.

[36] Branson, D.E. (1971b), *Discussion of "Flexural Cracking of Pretensioned I- and T- Beams",* ACI Journal / Vol. 68, No. 11, November 1971, pp. 875 - 876.

[37] Branson, D.E. (1974), *The Deformation of Non-Composite and Composite Prestressed Members,* ACI Publication SP-43, "Deflections of Concrete Structures", Symposium held on April 5, 1974, San Francisco, California, pp.83-127.

[38] Branson, D.E. ; Trost, H. (1982a), *Unified Procedures for Predicting the Deflection and Centroidal Axis Location of Partially Cracked Nonprestressed and Prestressed Concrete Members,* ACI Journal / March-April, 1982, pp.119-130.

[39] Branson, D.E. ; Trost, H. (1982b), *Application of the I-Effective Method in Calculating Deflections of Partially Prestressed Members,* PCI Journal / Sept.-October, 1982, pp.62-77.

[40] Branson, D.E. ; Shaikh, A.F. (1986), *Deflection of Partially Prestressed Members,* Ch.7 "Partial Prestressing, From Theory to Practice," Vol II: Prepared Discussion, Martinus Nijhoff Publishers.

[41] Bresler, B. ; Selna, L. (1964), *Analysis of Time-Dependent Behaviour of Reinforced Concrete Structures,* Paper No. 5 , ACI Symposium on Creep of Concrete, March 4, 1964, SP-9.

[42] Brigginshaw, G.F., *A new era for structural frames,* Concrete, Vol. 21, No. 10, pp.6-9.

[43] Brøndum-Nielsen, T., *Partial Prestressing,* Concrete Institute of Australia, FIP, 24p.

[44] Bruggeling, A.S.G. (1985), *Partially Prestressed Concrete Structures - A design challenge,* PCI Journal / Mar.-Apr., 1985, pp.140-171.

[45] Comite Euro-International Du Beton (1978), *Bulletin D'Information N.124/125-E-CEB-FIP, CEB-FIP Model Code for Concrete Structures, English Translations,* April, 1978.

[46] Chaikes, S. (1966), *Partially Prestressed Concrete - Technical Studies, Tests and Achievements,* "Annales Des Travaux Publics De Belgique," No. 2, April 1966, pp.2-24.

[47] Cohn, M.Z. ; MacRae, A.J. (1984a), *Optimisation of Structural Concrete Beams,* Journal of the Structural Division of the ASCE, Vol. 110, No. 7, July, 1984, pp.1573-1588.

[48] Cohn, M.Z. ; MacRae, A.J. (1984b), *Prestressing Optimisation and its implications for design,* PCI Journal / July-August, 1984, pp.68-83.

[49] Connolly, W.H. (1960), *Design of Prestressed Concrete Beams,* F.W. Dodge Corporation (USA).

[50] Corley, W.G. ; Sozen, M.A. ; Siess, C.P. (1961), *Time Dependent Deflections of Prestressed Concrete Beams,* Highway Research Board Bulletin 307, 1961.

[51] Darby, S.G. ; Warner, R.F. (1988a), *Long Term Behaviour of Composite, Partially Prestressed Concrete Planks,* Report No. DMR5, The University of Adelaide, April 1988.

[52] Darby, S.G. ; Warner. R.F. (1988b), *Prediction of Long Term Deflections of Composite, Partially Prestressed Beams : Comparison with Test Results,* Report No. DMR6, The University of Adelaide, November, 1988.

[53] Diamantidis, D. ; Madsen, H.O. ; Rackwitz, R. (1984), *On the variability of the creep coefficient of structural concrete,* Matériaux et Constructions, Vol. 17, No. 100, pp.321-328.

[54] Dilger, W.H. ; Neville, A.M. (1969), *Effects of Creep and Shrinkage in Composite Members,* Paper No. 23, Proceedings of the Second Australasian Conference on the Mechanics of Structures and Materials, Adelaide, South Australia, August, 1969.

[55] Dilger, W.H. (1982), *Creep Analysis of Prestressed Concrete Structures Using Creep Transformed Section Properties,* PCI Journal / Jan.-Feb. 1982, pp.98-118, Vol. 27, No. 1.

[56] Domone, P.L. (1974), *Unixial tensile creep and failure of concrete,* Magazine of Concrete Research, Vol. 26, No. 88, Sept. 1974, pp. 144-152, Cement and Concrete Association.

[57] D'Orazio, R.E. (1984), *Introduction to Structured Program Design,* D.C.R. Computers, Perth, Western Australia, 218pp.

[58] England, G.L. ; Illston, J.M. (1965), *Methods of Computing Stress in Concrete from a History of Measured Strain,* Civil Engineering and Public Works Review, April 1965, pp.513-517 (Part 1), May 1965, pp.692-694 (Part 2), June 1965, pp.846-847 (Part 3).

[59] Faber, O. (1927), *Plastic Yield, Shrinkage and Other Problems of Concrete, and their Effect on Design,* Minutes of the Proceedings of the Institution of Civil Engineers. Vol. 255, pp.27-73. 15^{th} November, 1927.

[60] Foo, M.H. (1986), *Behaviour of Partially Prestressed Concrete Structures Under Fatigue Loading,* Thesis presented to the University of Adelaide for the degree of Doctor of Philosophy, May 1986.

[61] Flügge, W. (1967), *Viscoelasticity,* Blaisdell Publishing Company (1967), USA.

[62] Freyermuth, C.L. (1969), *Design of Continuous Highway Bridges with precast, prestressed concrete girders,* PCI Journal / April 1969, pp.14-39, Vol. 14, No. 2.

[63] Ghali, A. ; Neville, A.M. ; Jha, P.C. (1967), *Effect of Elastic and Creep Recoveries of Concrete on Loss of Prestress,* ACI Journal, 64, 1967, pp.802-810.

[64] Ghali, A. ; Dilger, W.H. (1973), *Rapid Accurate Evaluation of Prestress Losses,* ACI Journal / November, 1973, pp.759-763.

[65] Ghali, A. ; Tadros, M.K. ; Dilger, W.H. (1974), *Accurate Evaluation of Time-Dependent Deflections of Prestressed Concrete Frames,* ACI Publication SP-43,"Deflections of Concrete Structures," Symposium on Deflections of Structures held on April 5, 1974, San Francisco, California, pp.357-375.

[66] Ghali, A. ; Tadros, M.K. (1985), *Partially Prestressed Concrete Structures,* Journal of the Structural Division of the ASCE, Vol. 111, No. 8, August, 1985, pp.1846-1865.

[67] Ghali, A. (1986), *A Unified Approach fo Serviceability Design of Prestressed and Non-Prestressed Reinforced Concrete Structures,* PCI Journal/ March-April 1986, pp.118-137.

[68] Gilbert, R.I. ; Warner, R.F. (1977), *Time-Dependent Behaviour of Reinforced Concrete Slabs,* UNICIV Report No. R-173, The University of New South Wales.

[69] Gilbert, R.I. ; Warner, R.F. (1978), *Tension Stiffening in Reinforced Concrete Slabs,* Journal of the Structural Division, ASCE, Vol. 104 No. ST12, Dec.1978, pp.1885-1899.

[70] Gilbert, R.I. (1986), *Methods for the Time-Dependent Analysis of Concrete Structures – The State of the Art,* UNICIV Report No. R-235, The University of New South Wales, September, 1986.

[71] Gilbert, R.I. (To be published), *Time Effects in Concrete Structures,* To be published by Elsevier Science Publishers, Holland.

[72] Goldberg, J.E. ; Richard, R.M. (1963), *Analysis of Non-Linear Structures,* Journal of the Structural Division, Proceedings ASCE, Vol. 89, No. ST4, August, 1963, pp. 333-351.

[73] Gopalaratnam, V.S. ; Shah, S.P. (1985), *Softening Response of Plain Concrete in Direct Tension,* ACI Journal / May-June, 1985, pp.310-323.

[74] Hanson, N.W. (1960), *Precast - Prestressed Concrete Bridges: 2. Horizontal Shear Connectors,* Portland Cement Association, Research and Development Laboratories, Development Department, Bulletin D35, May 1960.

[75] Haralji, M.H. ; Naaman, A.E. (1985), *Static and Fatigue Tests on Partially Prestressed Beams,* Journal of the Structural Division of the ASCE, ASCE, Vol. 111, No. 7, July 1985, pp.1602-1618.

[76] Hill, A.W. (1962), *Some recent developments in the design and construction of prestressed concrete structures in Great Britain,* Fourth FIP Congress, Rome-Naples 1962, Volume 1, Theme III, Paper No. 2.

[77] Hognestad, E. ; Hanson, N.W. ; McHenry, D. (1955), *Concrete Stress Distribution in Ultimate Strength Design,* ACI Journal, Proceedings Vol. 52, No. 4, Dec. 1955, pp.455-479.

[78] Illston, J.M. (1968), *Components of Creep in Mature Concrete,* ACI Journal, March 1968, pp.219-227.

[79] Inomata, S. (1982), *A Design Procedure for Partially Prestressed Concrete Beams Based on Strength and Serviceability,* PCI Journal / Sept.-Oct. 1982, pp.100-116, Vol. 27, No. 5.

[80] Inomata, S. (1987), *Creep Analysis of Cracked Partially Prestressed Concrete Members,* PCI Journal / Jan.-Feb., 1987, pp.104-123.

[81] Janko, L. (1982), *Elastic Stresses in Cracked Prestressed Pretensioned Concrete Composite Beams with Bonded Tendons,* Acta Technica, Scientiarum Hungaricae, 95(1-4), pp.63-82 (1982).

[82] Jones, H.L. (1985), *Minimum Cost Prestressed Concrete Beam Design,* Journal of the Structural Division of the ASCE, Vol. 111, No. 11, November, 1985.

[83] Jordaan, I.J. ; England, G.L. ; Khalifa, M.A. (1977), *Creep of Concrete: A consistent engineering approach,* Journal of the Structural Division of the ASCE, Vol. 103, No. ST3, March, 1977, pp.475-491.

[84] Jordaan, I.J. (1980), *Models for creep of concrete, with special emphasis on probabilistic aspects,* Matériaux et Constructions, Vol. 13, No. 73, pp.29-40.

[85] Kaar, P.H.; Kriz, B.K.; Hognestad, E. (1959), *Precast-Prestressed Concrete Bridges: 1. Pilot Tests of Continuous Bridges,* Portland Cement Association, Research and Development Laboratories, Development Department. Bulletin D34, 1959.

[86] Kang, Young-Jin ; Scordelis, A.C. (1980), *Non-Linear Analysis of Prestressed Concrete Frames,* Journal of the Structural Division of the ASCE, Vol. 106, No. ST2, February 1980, pp.445-462.

[87] Kent, D.C. ; Park, R. (1971), *Flexural Members with Confined Concrete,* Journal of the Structural Division of the ASCE, Vol. 97, No. ST7, July, 1971, pp.1969-1990.

[88] Kgoboko, K. (1987), *Collapse Behaviour of Non-Ductile Partially Prestressed Concrete Bridge Girders,* Thesis submitted for the degree of Master of Engineering Science at the University of Adelaide, Australia.

[89] Kirsch, U. (1973), *Optimized Prestressing by Linear Programming,* International Journal for Numerical Methods in Engineering, Vol. 7, pp.125-136.

[90] Koretsky, A.V.; Pritchard, R.W. (1982), *Assessment of Relaxation Loss Estimates for Strands,* ASCE Journal of the Structural Division, Vol. 108, No. ST12, December 1982.

[91] Kulicki, J.M. ; Kostem, C.N. (1975), *Inelastic Response of Prestressed Concrete Beams,* IABSE Publications, Vol. 35-II, pp.101-112, (Zürich, 1975).

[92] Lai, R.K.L. ; Warner, R.F. (1973), *Non-Linear Time-Varying Behaviour of Reinforced Concrete Structures,* 4^{th} Australian Conference on the Mechanics of Structures and Materials, Queensland, 20-22 August, 1973.

[93] Lai, K.L. ; Warner, R.F. (1975), *Non-Linear Behaviour of Indeterminate Concrete Structures Under Sustained Loading,* UNICIV Report No. R-149, The University of New South Wales.

[94] Leong, T.W. ; Crawley, D.B. ; Warner, R.F. (1987), *Tests on Composite, Partially Prestressed Concrete Bridge Planks,* Report No. DMR2, The University of Adelaide, October 1987.

[95] Lin, T.Y. (1963), *Load-Balancing Method for Design and Analysis of Prestressed Concrete Structures,* Proceedings of the ACI, Vol. 60, No. 6, June 1963, pp.719-742.

[96] Lin, C.S. ; Scordelis, A.C. (1975), *Non-Linear Analysis of RC shells of general form,* Journal of the Structural Division of the ASCE, Vol. 101, No. ST3, Mar., 1975, pp.523-538.

[97] Liu, T.C.Y. ; Nilson, A.H. ; Slate, F.O. (1972), *Stress-Strain Response and Fracture of Concrete in Uniaxial and Biaxial Compression,* ACI Journal, Proceedings, Vol. 69, No. 5, May, 1972, pp.291-295.

[98] Magnel,G. (1947), *A Comparison of Partially and Fully Prestressed Concrete Beams,* Concrete and Constructional Engineering, Vol. 42, No. 1, January 1947, pp.11-15.

[99] Martin, L.D. (1977), *A Rational Method for Estimating Camber and Deflection of Precast Prestressed Members,* PCI Journal / January-February 1977, pp.100-108.

[100] Mattock, A.H.; Kaar, P.H. (1960), *Precast-Prestressed Concrete Bridges: 3. Further Tests of Continuous Girders,* Portland Cement Association, Research and Development Laboratories, Sept. 1960, pp.51-78, Development Department, Bulletin D43.

[101] Mattock, A.H.; Kaar, P.H. (1961), *Precast-Prestressed Concrete Bridges: 4. Shear Tests of Continuous Girders,* Portland Cement Association, Research and Development Laboratories, Development Department, Bulletin D45, 1961.

[102] Mattock, A.H. (1961), *Precast-Prestressed Concrete Bridges: 5. Creep and Shrinkage Studies,* Portland Cement Association, Research and Development Laboratories, Development Department. Bulletin D46, 1961.

[103] Mattock, A.H.; Kaar, P.H. (1961), *Precast-Prestressed Concrete Bridges: 6. Test of Half-Scale Highway Bridge Continuous over Two Spans,* Portland Cement Association, Research and Development Laboratories, Development Department. Bulletin D51, 1961.

[104] McHenry, D. (1943), *A New Aspect of Creep and its Application to Design,* Proceedings of the American Society for Testing and Materials, Vol. 43, 1943, pp.1069-1084.

[105] Menegotto, M. ; Pinto, P.E. (1973), *Method of Analysis for Cyclically Loaded R.C. Plane Frames Including Changes in Geometry and Non-Elastic Behaviour of Elements under Combined Normal Force and Bending,* IABSE Symposium on "Resistance and Ultimate Deformability of Structures acted on by Well Defined Repeated Loads," Lisbon, 1973. Preliminary Report.

[106] Moosecker, W.; Grasser, E. (1981), *Evaluation of Tension Stiffening Effects in Reinforced Concrete Linear Members,* IABSE Congress, Reports of the Working Commission BD34, 1981.

[107] Moustafa, S.E. (1977), *Design of Partially Prestressed Concrete Flexural Members,* PCI Journal / May-June 1977, pp.12-29.

[108] Naaman, A.E. ; Siriaksorn, A. (1979a), *Serviceability Based Design of Partially Prestressed Beams - Part 1 : Analytic Formulation,* PCI Journal / March-April, 1979, pp.64-89.

[109] Naaman, A.E. ; Siriaksorn, A. (1979b), *Serviceability Based Design of Partially Prestressed Beams - Part 2 : Computerised Design and Evaluation of Major Parameters,* PCI Journal / May-June, 1979, pp.40-60.

[110] Naaman, A.E. (1983a), *Time Dependent Deflection of Prestressed Beams by the Pressure Line Method,* PCI Journal / Mar.-Apr., 1983.

[111] Naaman, A.E. (1983b), *An approximate nonlinear design procedure for Partially Prestressed Concrete Beams,* Computers and Structures, Vol. 17, No. 2, pp. 287-299, 1983.

[112] Naaman, A.E. ; Haralji, M.H. (1985), *Evaluation of the Ultimate Steel Stress in Partially Prestressed Flexural Members,* PCI Journal / Sept-Oct., 1985, pp.54-81.

[113] Naaman, A.E. (1985), *Partially Prestressed Concrete : Review and Recommendations,* PCI Journal, Nov-Dec., 1985, pp.31-71.

[114] Naaman, A.E.; Haralji, M.H.; Wight, J.K. (1986), *Analysis of Ductility in Partially Prestressed Concrete Flexural Members,* PCI Journal, Vol. 31, No. 3, May/June 1986.

[115] National Association of State Road Authorities (NAASRA), (1987), *Draft Bridge Design Specification and Commentary (in Limit State Format),* September, 1987.

[116] Nawy, E.G.; Huang, P.T. (1977), *Crack and Deflection Control of Prestressed Beams,* PCI Journal / May-June, 1977, pp.30-47.

[117] Nielsen, L.F. (1978), *The Improved Dischinger Method as related to other Methods and Practical Applicability,* Paper presented at the symposium on "Design for Creep and Shrinkage in Concrete Structures," ACI Fall Convention in Houston, Texas, Oct.29-Nov.3, 1978.

[118] Paduart, A. (1966), *Safety Against Rupture of a Partially Prestressed Concrete Section Under Deflection,* "Annales Des Travaux Publics De Belgique," No. 2, April 1966, pp. 25-33.

[119] Pauw, A.; Breen, J.E. (1961), *Field Testing of Two Prestressed Concrete Girders,* Highway Research Board Bulletin 307, 1961, pp.42-63.

[120] Pauw, A. (1969), *Static modulus of Elasticity of Concrete as Affected by Density,* ACI Journal, Dec. 1969, pp.679-687.

[121] Parameswaran, V.S.; Annamalai, G.; Ramaswamy, G.S. (1974), *Theoretical and Experimental Investigations on the Flexural Behaviour of Class 3 Beams,* Paper presented at the Seventh Congress of the Federation Internationale de la Precontainte, New York, 28-30 May, 1974.

[122] PCI Committee on Prestress Losses (1975), *Recommendations for estimating Prestress Loss,* PCI Journal, Vol. 20, No. 4, Jul-Aug. 1975, pp.43-76.

[123] Peterson, D.N. ; Tadros, M.K. (1985), *Simplified Flexural Design of Partially Prestressed Concrete Members,* PCI Journal / May-June, 1985, pp.50-67.

[124] Priestley, M.J.N. ; Park, R. ; Lu, F.P.S. (1971), *Moment- Curvature Relationships for prestressed concrete in constant moment zones,* Magazine of Concrete Research: Vol. 23, No.75-76, June-Sept., 1971, pp.69-78.

[125] Rabotnov, Yu. N. (1969), *Creep Problems in Structural Members,* North-Holland Publishing Company, Amsterdam, 822pp.

[126] Rao, V.J.; Dilger, W.H. (1974a), *Time Dependent Deflections of Composite Prestressed Concrete Beams,* ACI Publication SP-43,"Deflections of Concrete Structures," Symposium on Deflections of Structures held on April 5, 1974, San Francisco, California, pp.421-442.

[127] Rao, V.J. ; Dilger, W.H. (1974b), *Analysis of Composite Prestressed Concrete Beams,* Journal of the Structural Division, ASCE, Vol. 100, No. ST10, October, 1974, pp.2109-2121.

[128] Raphael, J.M. (1953), *The Development of Stresses in Shasta Dam,* Transactions of the ASCE, Vol. 118, 1953, pp.289-321.

[129] Ross, A.D. (1943), *Creep and Shrinkage in Plain, Reinforced and Prestressed Concrete. A general method of calculation,* Journal of the Institution of Civil Engineers, November, 1943, No. 1, pp.38-57.

[130] Ross, A.D. (1958), *Creep of Concrete under Variable Stress,* Journal of the American Concrete Institute, Vol. 29, No. 9, March 1958, Proceedings Vol. 54, pp.739-758.

[131] Saito, M.; Imai, S. (1983), *Direct Tensile Fatigue of Concrete by the use of Friction Grips,* ACI Journal / Sept-Oct 1983, pp.431-438.

[132] Sanchez-Galvez, V. ; Elices, M. ; Astiz, M.A. (1976), *A new formula for relaxation of stress-relieved steels,* Matériaux et Constructions, Vol. 9, No. 54, pp.411-417.

[133] Scordelis, A.C. (1984), *Computer Models for Nonlinear analysis of Reinforced and Prestressed Concrete Structures,* PCI Journal / Nov-Dec. 1984, pp.116-135.

[134] Shaikh, A.F. and Branson, D.E. (1970), *Non-Tensioned Steel in Prestressed Concrete Beams,* PCI Journal, Vol. 15, No. 1, Feb. 1970, pp. 14-36.

[135] Shushkewich, K.W. (1988), *Analysis of Partially Prestressed Beams (Discussion),* Journal of the Structural Division of the ASCE, Vol. 114, No. 1, Jan, 1988, pp.243-246.

[136] Standards Association of Australia (SAA), (1988), *Australian Standard for Concrete Structures*

[137] Tadros, M.K. ; Ghali, A. ; Dilger, W.H. (1977a), *Effect of Non-Prestressed Steel on Prestress Loss and Deflection,* PCI Journal / Mar-Apr. 1977, Vol. 22, No. 22, pp.50-63.

[138] Tadros, M.K. ; Ghali, A. ; Dilger, W.H. (1977b), *Time-Dependent Analysis of Composite Frames,* Journal of the Structural Division, Proceedings ASCE, Vol. 103, No. ST4, April, 1977, pp.871-884.

[139] Tadros, M.K. (1983), *Author's closure to "Expedient Service Load Analysis of Cracked Prestressed Concrete Sections,* PCI Journal / November-December 1983, pp.151-158.

[140] Tadros, M.K. ; Ghali, A. ; Meyer, A.W. (1985), *Prestressed Loss and Deflection of Precast Concrete Members,* PCI Journal / Jan-Feb. 1985, pp.114-141.

[141] Thürlimann, B. (1971), *A Case for Partial Prestressing,* Institut für Baustatik ETH Zürich, May 1971. Reprinted from Proceedings Structural Concrete Symposium, Toronto May 13 and 14 1971.

[142] Vecchio, F.J. (1987), *Non-Linear Analysis of Reinforced Concrete Frames Subjected to Thermal and Mechanical Loads,* ACI Structural Journal, Nov-Dec. 1987, pp.492-501.

[143] Verna, P.J. (1962), *Economics of Prestressed Concrete in relation to regulations, safety, partial prestressing, lightweight concrete, etc., in the USA,* Fourth FIP Congress, Rome-Naples, 1962, Volume 1, Theme III, Paper No. 1.

[144] Walley, F. (1984), *The Childhood of Prestressing - An Introduction,* The Structural Engineer, Vol. 62A, No. 1, January 1984, pp.5-9.

[145] Warner, R.F. (1969), *Biaxial Moment-Thrust Curvature Relations,* Journal of the Structural Division of the ASCE, Vol. 95, No. 5.

[146] Warner, R.F. (1970), *Non-linear creep in Concrete Columns,* Madrid Creep Symposium 1970, IABSE.

[147] Warner, R.F. ; Lambert, J.H. (1974), *Moment-Curvature-Time Relations for Reinforced Concrete Beams,* International Association for Bridge and Structural Engineering, Volume 34-I of the Publications, Zürich, 1974.

[148] Warner, R.F. ; Faulkes, K.A. (1979), *Prestressed Concrete,* Pitman Publishing Pty. Ltd. (Victoria).

[149] Warner, R.F. (1986), *Partially Prestressed Composite Bridge Planks,* Report No. DMR1, The University of Adelaide, 1986.

[150] Warner, R.F. (1987), *Computer Analysis of Long-Term Effects in DMR PPC Plank, Moama,* Report No. DMR4, The University of Adelaide, November 1987.

[151] Warner, R.F.; Faulkes, K.A. (1988), *Prestressed Concrete,* Second Edition, Longman Cheshire Pty. Ltd.

[152] Whitney, C.S. (1932), *Plain and Reinforced Concrete Arches,* Journal of the American Concrete Institute, Proceedings, Vol.28 - 1932, pp.479-510.

[153] Wium, D.J.W. ; Buyukozturk, O. (1985), *Variability in Long-Term Concrete Deformations,* Journal of the Structural Division of the ASCE, Vol. 111, No. 8, August, 1985, pp.1792-1809.

[154] Wyche, P.J. (1987), *Deflection Controlled Precast Prestressed Concrete Beams,* 13^{th} Biennial CIA Conference, 1987.

[155] Wyche, P.J.; Uren, J.G. (1988), *Deflection Controlled Prestressed Concrete Beams,* Proceedings 14th ARRB Conference, Part 6, pp. 144-157.